

**Towards identifying potential drug and vaccine targets for human malaria
parasite using rodent *Plasmodium berghei* model**

&

**Investigation of host long non coding RNA profiles during *Plasmodium
berghei* and *Toxoplasma gondii* infections**

*Thesis submitted to University of Hyderabad
for the award of Ph.D. degree in
Department of Animal Biology*



By

Segireddy Rameswara Reddy

11LAPH07

Department of Animal Biology
School of Life Sciences
University of Hyderabad
Hyderabad - 500 046
India

August 2017



CERTIFICATE

This is to certify that the thesis entitled **“Towards identifying potential drug and vaccine targets for human malaria parasite using rodent *Plasmodium berghei* model & Investigation of host long non coding RNA profiles during *Plasmodium berghei* and *Toxoplasma gondii* infections”** submitted by **Segireddy Rameswara Reddy** bearing registration number **11LAPH07** in partial fulfilment of the requirements for award of Doctor of philosophy in the **School of Life Sciences** is a bonafide work carried out by him under my supervision and guidance.

This thesis is free from plagiarism and has not been submitted previously in part or in full to this or any other University or Institution for award of any degree or diploma.

A. Published in the following publications:

1. Scientific Reports. 2017 Jan 9; 7:40407 (ISSN 2045-2322).
2. Cellular Microbiology. 2017 Jul; 19(7) (ISSN: 1462-5822).

B. Presented in the following conferences:

1. AS-UoH joint workshop on “Frontiers in Life Sciences” at University of Hyderabad, September, 2016 (International).
2. “Cell Biology of Infection” at NCBS, Bangalore, October, 2016 (International).

Further, the student has passed the following courses towards fulfillment of coursework requirement for Ph.D.

Course Code	Name	Credits	Pass/Fail
1. AS 801	Seminar 1	1	PASS
2. AS 802	Research Ethics & Management	2	PASS
3. AS 803	Biostatistics	2	PASS
4. AS 804	Analytical Techniques	3	PASS
5. AS 805	Lab Work	4	PASS

Supervisor

Head of Department

Dean of School



UNIVERSITY OF HYDERABAD

Central University (P.O.), Hyderabad-500046, INDIA

DECLARATION

I hereby declare that the results of the study incorporated in the thesis entitled “**Towards identifying potential drug and vaccine targets for human malaria parasite using rodent *Plasmodium berghei* model & Investigation of host long non coding RNA profiles during *Plasmodium berghei* and *Toxoplasma gondii* infections**” has been carried out by me under the supervision of **Dr. Kota Arun Kumar** and this work has not been submitted for any degree or diploma of any other university earlier.

Dated

Segireddy Rameswara Reddy

(Research Scholar)



Acknowledgements



*I would like to express my deepest sense of gratitude to my supervisor **Dr. Kota Arun Kumar**, for giving me an opportunity to work under his guidance, constant cooperation, and encouragement throughout my work. I am highly grateful to him for all the efforts he has put in for the successful completion of this thesis.*

I thank Head, Dept of Animal Biology, Prof. Jagan Pongubala, and previous HOD's Prof. Senthilkumaran, Prof. Manjula Sritharan and Prof. S Dayananda for the departmental facilities

I thank the Dean, School of Life Sciences, Prof. P Reddanna and former Dean Prof. A.S. Raghavendra, Prof Aparna Dutta Gupta, Prof. R.P. Sharma and Prof Ramanadham for providing the central facilities at the School of Life Sciences

I thank the doctoral committee members Prof. S Dayananda and Prof. Aparna Dutta Gupta for constructive criticism and guidance

I thank Dr. Suresh Yenugu and Dr. Arunasree for allowing me to use their laboratory equipment

I thank all my lab mates Dr. Maruthi, Dr. Jyothi, Dr. Surendra, Ravi, Mastan, Dr. Faizal, Sandeep and Dipti for their help and support during my stay in lab

I thank all my friends Dr. Papa Rao, Dr. Ravinder, Trinadh, Suman, Sravan and Dr. Suresh Ch.

I thank Narasimha and Yadagiri for assistance in the laboratory

*The financial support from DBT, DST, CSIR, ICMR, UGC, PURSE and DBT-CREBB is highly acknowledged
Financial support through CSIR JRF and SRF is highly acknowledged*

The support from Dr. Kota Arun Kumar's collaborators: Dr. Satish Mishra, CDRI, Lucknow; Dr. Puran

Singh, CCMB, Hyderabad is highly acknowledged

*I am extremely grateful to my **parents** and my sisters for their unwavering love, support and patience throughout my life.*

*Above the all, I owe my thanks to **Almighty**, for everything.*

Rameswar.....✍

*DEDICATED TO
MY
PARENTS*

Table of Contents

	Page No
Abbreviations	i
Chapter 1: Review of Literature	
1.1 Introduction	2
1.1.1 History of Malaria	2
1.1.2 Malaria epidemiology	2
1.2 Life cycle of <i>Plasmodium</i>	4
1.2.1 Asexual development in the vertebrate host	5
1.2.1.1 Exo-erythrocytic stages	5
1.2.1.2 Erythrocytic stages	9
1.2.2 Sexual development in the mosquito vector	12
1.2.3 Sporozoite	14
1.3 Clinical manifestations of Malaria	16
1.4 Diagnosis and treatment	17
1.5 Control measures and prophylaxis	17
1.6 Current challenges to control malaria	19
1.7 <i>Plasmodium berghei</i> as model	20
1.8 Objectives	21
Chapter 2: Functional characterization of <i>Plasmodium berghei</i> nicotinamidase by reverse genetics approach	
2.1 Introduction	24
2.2 Material and methods	32
2.3 Results	49
2.4 Discussion	63

Chapter 3: Functional characterization of *Plasmodium berghei* S10 by reverse genetics approach

3.1 Introduction	68
3.2 Material and methods	77
3.3 Results	84
3.4 Discussion	96

Chapter 4: Investigation of host long non coding RNA profiles during *Plasmodium berghei* and *Toxoplasma gondii* infections

4.1 Introduction	99
4.2 Material and methods	101
4.3 Results	104
4.4 Discussion	109

<i>Summary</i>	111
-----------------------	-----

<i>References</i>	114
--------------------------	-----

Publications

Anti-plagiarism certificate

Abbreviations

ACT	Artemisinin combination therapy
AMA	Apical membrane antigen
Bp	Base pairs
BSA	Bovine serum albumin
CD	Cluster of differentiation
CDK	Cyclin dependent kinase
cDNA	Complementary DNA
CDPK	Calcium dependent protein kinase
CELTOS	Cell traversal protein for ookinetes and sporozoites
CS	Circumsporozoite
DAPI	4', 6' diamidino-2 phenyl indole
DIC	Differential interference contrast
DMEM	Dulbecco's modified Eagle's medium
DNA	Deoxy ribonucleic acid
DOZI	Development of zygote inhibited
EBL	Erythrocyte binding like
EDTA	Ethylene diamine tetra acetic acid
EEF	Exo erythrocytic form
EMP	Erythrocyte Membrane Protein
FBS	Fetal bovine serum
FP	Forward primer
FLP	Flippase
FRT	Flippase recognition target site
GAP	Genetically attenuated parasite
GAPDH	Glyceraldehyde 3-phosphate dehydrogenase
GFP	Green fluorescent protein
HBV	Hepatitis B virus
HCV	Hepatitis C virus
hDHFR	Human Dihydrofolate reductase
HEPES	4-(2-hydroxyethyl)-1-piperazineethanesulfonic acid
HSPG	Heparin sulfate proteoglycan
IFN	Interferon
IFN-gamma	Interferon gamma

IFN- β	Interferon beta
iRBC	Infected red blood cell
ITN	Insecticide treated net
Kb	Kilobase pairs
KO	Knockout
LB broth	Luria-Bertani broth
LIISP	Liver specific protein
LncRNAs	Long non-coding RNAs
Lys	Lysine
MAP/MAPK	Mitogen activated protein kinase
miRNAs	MicroRNAs
mRNA	Messenger RNA
MSP	Merozoite surface protein
MTI	Myosin tail interacting protein
NEK	NIMA related kinase
ng	nanogram
NIMA	Never in mitosis <i>Aspergillus</i>
OD	Optical density
<i>P. falciparum</i>	<i>Plasmodium falciparum</i>
<i>P. malariae</i>	<i>Plasmodium malariae</i>
<i>P. knowlesii</i>	<i>Plasmodium knowlesii</i>
<i>P. ovale</i>	<i>Plasmodium ovale</i>
<i>P. vivax</i>	<i>Plasmodium vivax</i>
PBS	Phosphate buffer saline
PEXEL	<i>Plasmodium</i> export element
piRNAs	Piwi-interacting RNAs
PKG	cGMP dependent protein kinase/ protein kinase G
PL	Phospholipase
PUF	Pumilio and fem3 transcription binding factor
PV	Parasitophorous vacuole
PVM	Parasitophorous vacuolar membrane
RBC	Red blood cell
RH	Relative humidity
RNA	Ribonucleic acid

RP	Reverse primer
RPM	Revolutions per minute
RPMI	Roswel Park Memorial Institute medium
SAP	Sporozoite asparagine rich protein
SERA	Serine repeat antigen
SIAP	Sporozoite invasion associated protein
siRNAs	Short interfering RNAs
SncRNAs	Small non-coding RNAs
snoRNAs	Small nucleolar RNAs
SPECT	Sporozoite protein essential for cell traversal
SRPK	Serine arginine rich protein kinase
SSH	Suppression subtractive hybridization
SSP	Sporozoite surface protein
SUB1	Subtilisin like protease 1
<i>T. gondii</i>	<i>Toxoplasma gondii</i>
TAE	Tris acetate EDTA
TBS	Tris buffer saline
TE	Tris EDTA
TRAP	Thrombospondin related anonymous protein
TRSP	Thrombospondin related sporozoite protein
TSR	Thrombospondin related
UIS	Up regulated in infected salivary glands
UTR	Untranslated region
UV	Ultraviolet
VTs	Vacuolar translocation signal
WHO	World health organization
WT	Wild type
XA	Xanthurinic acid
°C	Degrees Celsius
µg	Microgram
µL	Microliter
µM	Micrometer

Review of Literature

1.1 Introduction

1.1.1 History of Malaria

Malaria is one of the most common infectious diseases known since 1600 B.C.E from Vedic writings in India and from 5th century B.C.E in Greece. Hippocrates, “The Father of Medicine” and probably first malariologist described characteristics of the disease relating to seasons. Malaria term originated from Italian word *mal' aria* means ‘bad air’, because people believed that the disease was caused by the bad air coming from swamps and rivers. A French army doctor, Charles Louis Alphonse Laveran was the first person to observe and identify *Plasmodium* parasites in malaria patient blood in 1880 and named it as *Oscillaria malariae*. An Italian neurophysiologist, Camillo Golgi explained about tertian periodicity and quartan periodicity (fever every alternative day or after every three days). He observed that fever concurred with the rupture and release merozoites from iRBC. In 1897, Sir Ronald Ross, a British doctor, demonstrated about malaria transmission through mosquitoes in avian species. Later in 1899, an Italian group including Giuseppe Bastianelli and Amico Bignami headed by Giovanni Batista Grassi used *Anopheles claviger* mosquitoes to feed on malaria patients and explained complete sporogonic life cycle [1]. Later in 1948, pre-erythrocytic development was demonstrated by two British scientists named Henry Edward Shortt and Percy Cyril Garnham [3]. Ross, Golgi and Laveran were awarded Nobel prizes in the years 1902, 1906 and 1907 respectively for their discoveries of malaria parasite life cycle stages.

1.1.2 Malaria epidemiology

In humans malaria caused by different *Plasmodium* species including *Plasmodium vivax* (*P. vivax*), *Plasmodium falciparum* (*P. falciparum*), *Plasmodium ovale* (*P. ovale*), *Plasmodium malariae* (*P. malariae*) and *Plasmodium knowlesi* (*P. knowlesi*). Among all the species *P. falciparum* is the most severe species responsible for the majority of the mortality in the world. In some cases, *P. falciparum* causes cerebral malaria characterized by sequestration of infected RBC in brain leading to death. Most malaria cases and deaths occur in sub-Saharan Africa [4]. However, there are reports of malaria related mortality in Asia, Latin America and to a lesser extent, in the Middle East. In 2015, 95 countries and territories had successful malaria transmission. There are 212 million clinical incidences yearly, predominantly in Sub Saharan Africa and approximately 4,20,000 malaria deaths were reported in 2016, worldwide (Fig 1) [5]. Clinical symptoms of malaria range from fever to severe complications including acidosis, organ failure, anemia and death if left untreated. For women and their newborn children, pregnancy associated malaria is

a major health concern. Malaria is a disease of socio-economic importance and can be held partially accountable for vicious circle of poverty in the developing countries [6].

Estimated malaria cases and deaths by region, 2015					
WHO region	Number of countries with ongoing transmission	Estimated cases*		Estimated deaths*	
		Number (in thousands, %)		Number (in thousands, %)	
Global total	96	214,000	100%	438	100%
Africa	44	188,000	88%	395	90%
Americas	21	660	<1%	0.5	<1%
E. Mediterranean	8	3,900	2%	6.8	2%
Europe	3	0	0%	0	0%
South-East Asia	10	20,000	9%	32	7%
Western Pacific	10	1,500	<1%	3.2	<1%

NOTES: * Represents WHO's "best estimate" for each indicator.

Table 1: Worldwide malaria incidence [7]

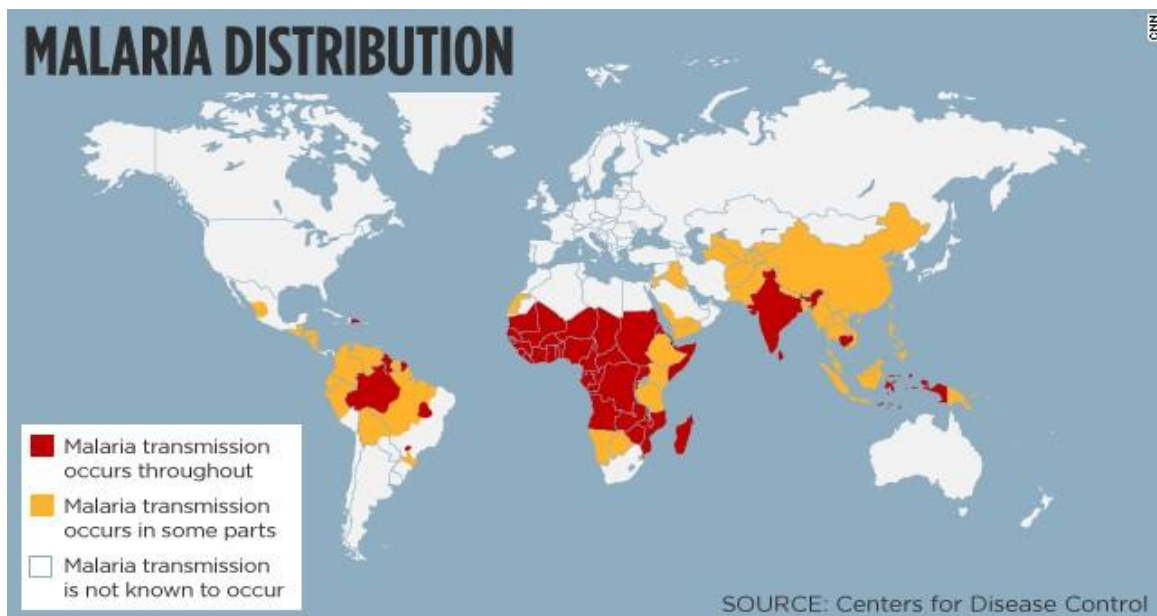


Fig 1: Global malaria distribution and countries at risk of transmission. Malaria transmission occurs mostly in tropical and sub-tropical regions. Most of the malaria cases are from Sub-Saharan Africa and India (Red). Countries like South America and China have succeeded in controlling malaria (yellow) where the disease transmission is low. In few countries, malaria transmission is not known to occur (white) due to high altitudes, low temperatures and public health measures but the reintroduction of the disease may occur if control measures are not followed.

1.2 *Plasmodium* life cycle

The life cycle of *Plasmodium* is very complex. The parasite is digenetic and completes its asexual life cycle in the vertebrate host and sexual life cycle in the female *Anopheles* mosquito (Fig 2). The life cycle starts with the deposition of sporozoites into the vertebrate host skin by the mosquito while probing for the blood [8]. These sporozoites forms glide through the dermis, penetrate blood vessels and enter the circulatory system through which they are selectively arrested in the liver.

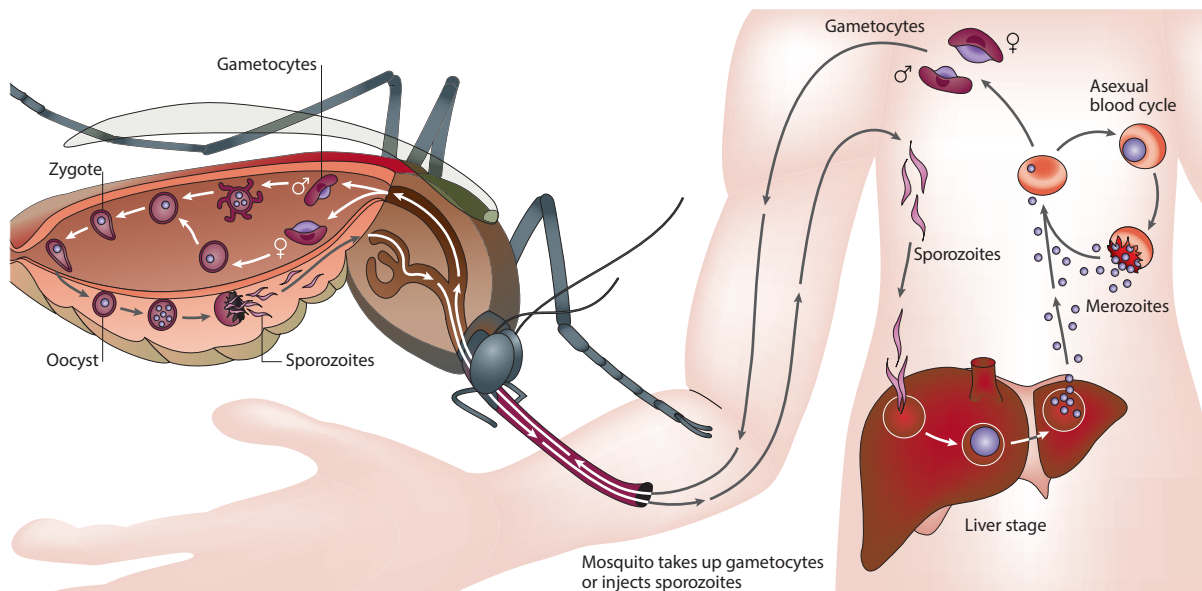


Fig 2: Life cycle of *Plasmodium*. The life cycle starts with the deposition of sporozoites into the vertebrate host skin, from where they make their way to the liver. In liver, they infect hepatocytes and develop into exoerythrocytic forms. After several rounds of asexual reproduction, the hepatic merozoites are packaged in membrane bound structures called merozoites that are released into liver sinusoids. In blood, merozoites infect RBC and transform into different stages like rings, trophozoites and schizonts. The mature schizonts rupture and release merozoites that either reinitiates a new erythrocytic cycle or transforms into male or female gametocytes. The gametocytes are the infective forms of the parasite to the mosquito vector. During blood meal, mosquito takes up gametocytes along with the blood. In the mosquito gut, male and female gametes emerge from male and female gametocytes respectively. These gametes fuse and form zygote that further develops into motile ookinete. Ookinete breaches the midgut epithelium and develops into oocyst on hemocoel side of the epithelium. In the oocyst, sporogony occurs resulting in the generation of thousands of sporozoites. Upon rupture, the sporozoites are released into the hemocoel. They migrate to salivary glands by a process of gliding motility. The sporozoites reside in the salivary glands until they are introduced into the vertebrate host during bite of mosquito (Image adapted from [9])

In liver, sporozoites invade hepatocytes by a process of productive invasion resulting in the formation of parasitophorous vacuole (PV). Within the PV, the parasite transforms into exo-erythrocytic form (EEF). After undergoing several rounds of replication, the mature EEFs release hepatic merozoites packaged in merosomes that are delivered into sinusoidal spaces. The rupture of merosome membrane releases merozoites into blood. In blood, merozoites infect RBCs and transform into different stages like rings, trophozoites and schizonts. Schizont contains 16-32 merozoites, which will be released into blood upon rupture of RBC [10]. In this process, some of the ring forms will be converted into gametocytes that are the transmissible forms of malaria to the mosquito vector [11]. During blood meal, mosquito takes up gametocytes along with the blood. In the mosquito gut, male and female gametes emerge from male and female gametocytes respectively. These gametes fuse and form zygote that further develops into motile ookinete within 18-24 h. Ookinete breaches the midgut epithelium and develops into oocyst on hemocoel side of the epithelium. In the oocyst, sporogony occurs resulting in the generation of thousands of sporozoites over a period of 8-15 days. Upon rupture, the sporozoites are released into the hemocoel. The sporozoites migrate to salivary glands by a process of gliding motility. The salivary gland sporozoites are introduced into the vertebrate host when the female *Anopheles* mosquito obtains the blood meal.

1.2.1 Asexual development in the vertebrate host

1.2.1.1 Exo-erythrocytic stages

On an average, 15 to 123 *Plasmodium* sporozoites are deposited in the vertebrate skin by the bite of infected *Anopheles* mosquito [12], [13]. They are highly motile and reside in the skin for less than 5 min. The shift in the change of environmental conditions may act as a cue to activate the sporozoite to start asexual cycle in mammalian host. From the site of injection, the route of sporozoite journey to the bloodstream is highly unknown. It is speculated that sporozoites enter through the capillaries which are damaged by mosquito proboscis or that sporozoites themselves possess the ability to migrate through capillary linings [14]. Most of the sporozoites traverse through many cells by specialized locomotion called gliding motility with the help of actin myosin motor complex present beneath the membrane [15], [16], [17]. Sporozoites enter into liver sinusoid, glide through Kupffer cell and traverse into hepatocytes [18], [19], [20]. Loss of function mutants of sporozoite protein essential for cell traversal like (SPECT)-1 and SPECT-2 were immobilized in the skin, thus reiterating the essentiality of these proteins in cell traversal activity [21], [22]. Apart from these, phospholipase (Pb PL), present on the sporozoite surface is also required for sporozoite cell traversal. Disruption of *Pb PL* impaired

the sporozoite ability to migrate through epithelial layers, thus resulted in 90% reduction in sporozoite infectivity in the liver and delayed prepatent period by 1 day [23]. Sporozoites specifically get arrested in the liver by the interaction between the highly sulfated heparan sulfate proteoglycans (HSPGs) present on the hepatocyte and circumsporozoite protein (CSP), a predominant secretory surface antigen of the sporozoite [24], [25]. Region II-plus, N- and C-terminal GAG-binding motifs of CSP are involved in attachment [26], [27]. Sporozoites are capable of migrating through hepatocytes without forming parasitophorous vacuolar membrane (PVM) [28].

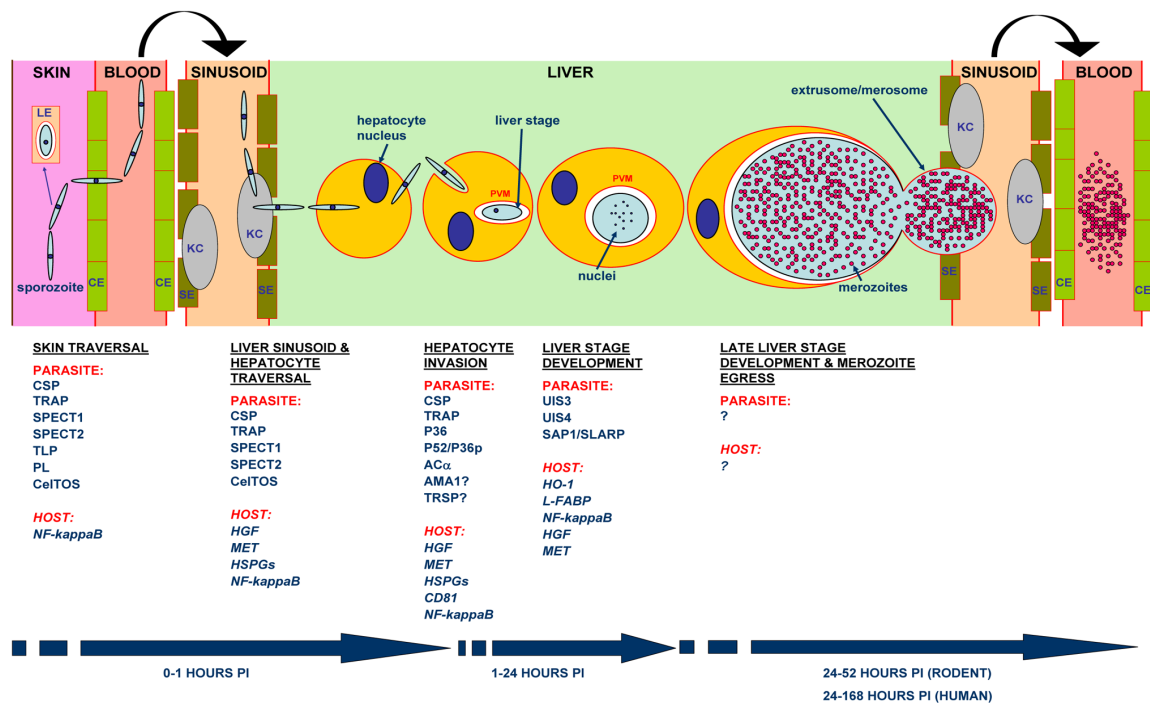


Fig3: Sporozoite journey to liver and liver stage development. Sporozoites deposited in the skin enter into the circulation by gliding motility and cell traversal activity from the capillary endothelial cell (CE). Through blood, they enter into liver sinusoids by a hepatic artery or portal vein. In the liver sinusoids, they migrate through resident Kupffer cells and traverses many hepatocytes before successful invasion. Once inside the hepatocyte the sporozoites transform into EEFs within the parasitophorous membrane (PVM). Inside PVM, massive replication takes place resulting in production of thousands of merozoites. Infected hepatocyte plasma membrane bulges out to form merosomes that harbor merozoites. The merozoites are released into the blood stream to initiate erythrocytic cycle. Proteins involved in these series of events are indicated below the image and time required for each event is mentioned as arrows. (Image adapted from [29])

In this process, they disrupt the host cell plasma membrane (PM), glide in the cytosol and egress from the cell again by membrane disruption.

During gliding motility in the hepatocyte, sporozoites release secretory antigens, especially CSP [30]. The CSP antigen shed in the host cytoplasm during process of migration or exported during early hours of EEF development was shown to be involved in modulation of host cellular machinery [31]. After migration through several cells, they establish successful infection by forming parasitophorous vacuolar membrane (PVM) in the host cell [32]. PVM separates parasite from the host environment, helps to escape from host immunity and provides access to nutrients from the host cell. Inside PVM, parasite develops into EEF. Till date the mechanism of PVM formation is obscure, but some reports demonstrate that PVM is formed by remodeling of the host membrane components by incorporation of parasite derived proteins and lipids [33]. Depletion of parasitic proteins P36 and P52 resulted in early liver stage arrest with the defect in PVM formation [34]. Other proteins like *upregulated in infected sporozoites 3* (UIS3), UIS4, exported protein1 (EXP1) and early transcribed membrane proteins (ETRAMPs) are PVM resident proteins and are essential for liver stage development. UIS3/UIS4 knockouts failed to initiate blood stage infection and confer sterile long lasting immunity [35], [36]. Through specialized machinery, parasite exports many proteins into host cell cytoplasm required for host cell takeover. These proteins contain specific canonical motif called host targeting motif (HT) or *Plasmodium* export element (PEXEL) with a conserved sequence RxLxE (x-any amino acid) [37], [38] and are conserved among all *Plasmodium* species [39]. However, not essentially all the proteins which are exported to the host cytosol contain PEXEL/HT motif. In fact, the PEXEL-negative exported proteins (PNEPs) also [40] traffic to host compartment. CSP, the immunodominant surface antigen of sporozoites [41] contain two PEXEL motifs that are required for export into hepatocyte cytosol [42]. CSP has inhibitory roles by binding to ribosomes and inhibiting NF- κ B nuclear translocation [30], [43], [42]. Proteins exported to the host cell compartment takeover the host cellular machinery thus benefiting the parasite.

For parasite stage specific propagation, a tight regulation of gene expression is a prerequisite. Till date, Apicomplexan Apetela2 (ApiAP2) DNA binding proteins are the only known transcription factors that are involved in regulation of gene expression and silencing [44]. Transcription factor AP2-L is necessary for parasite development in the hepatocytes. AP2-L depleted parasites showed normal development in the blood and mosquito but unable to develop in the liver [45]. Inside the hepatocyte, parasites are surrounded by parasitophorous vacuolar membrane (PVM) and undergo asymptomatic, clinically silent, enormous asexual replication and produce 10,000 to 30,000 merozoites after the completion of asexual reproduction [12]. These hepatic merozoites are released into the blood as merozoites - packets

of hundreds of daughter merozoites surrounded by host PM. Merosomes are of 12-18 microns in size and contain 100-200 merozoites, facilitate host immune evasion from surveillance by liver resident macrophages called Kupffer cells, which are highly phagocytic and are strategically positioned in the liver lining of sinusoids [46]. In the blood stream, daughter merozoites get released upon rupture of merosome membrane and infect erythrocytes to initiate blood stage infection [47]. Several parasitic proteins are involved in the egress of merozoites from merosomes. Most of them belong to the cysteine proteases of the serine repeat antigen (SERA) family. SERA3 is highly upregulated in late liver stages, localized to PVM and detected in host cell cytoplasm upon rupture of the PVM [48]. Subtilisin like protease (SUB1) was shown to be required for the egress of blood stage and liver stage merozoites. SUB1 mediated cleavage of SERA3 protease marks the initiation of merozoite egress [49]. Liver- specific protein 1 (LISP1) depleted parasites failed to degrade the PVM and release of merozoites from hepatocyte thus reiterating its essential role in egress [50]. By transcriptomic analysis, several genes were identified that are specifically upregulated in infectious sporozoites, referred to as UIS genes [51] and S genes [52]. UIS genes were identified in suppression subtractive hybridization (SSH) screen between salivary gland sporozoites versus midgut sporozoites [51]. Whereas S genes were identified in SSH screen between salivary gland sporozoites versus merozoites [52]. Recent evidences show that UIS3 and UIS4 genes (with a signal peptide) are essential for liver stage development as sporozoites lacking these proteins failed to initiate breakthrough infection. However, these mutants confer sterile protection when challenged with wild type sporozoites [35], [36]. In S gene cluster, there are 12 proteins with a signal peptide, which indicates their ability to enter into the secretory pathway. Among them, CSP, a dense coat protein of the sporozoite is essential for attachment and establishment of successful infection [43], [26]. TRAP (thrombospondin-related anonymous protein) [53] and S6 (TREP, TRAP related protein) are transmembrane secretory proteins which are essential for sporozoite motility and host cell entry [54], [55]. CelTOS (S4), is an essential protein for motility [56]. S22 (SAP1 [57], SLARP [58]) is required for hepatocyte infection. Several lines of evidence points to the role of the genes upregulated in sporozoites to be essential for establishing hepatocyte infection. By deleting the genes essential for liver stage development, parasites can be arrested in the liver to generate long lasting sterile pre-erythrocytic immunity that confers protection against challenge by wild type sporozoites [59]. An exciting possibility of using these genetically attenuated parasites (GAPs) as whole organism vaccines is currently underway [60].

1.2.1.2 Erythrocytic stages

Exo-erythrocytic stages are clinically silent, asymptomatic and release thousands of merozoites into the blood. These hepatic merozoites invade erythrocytes, undergo repeated asexual replication cycles to produce numerous daughter merozoites which eventually invade naive RBCs. Hepatic merozoites released from the liver, recognize, attach, reorient and infect RBC by multiple receptor ligand interactions in less than 60 seconds [61], [62]. Hepatic merozoites are there in the blood for very short span of time to ensure that they are not cleared by host immune response. Parasites have specialized secretory organelles at the apical end, called the micronemes, rhoptries and dense granules, which secrete surface proteins like adhesins and invasins that help the parasite for attachment, invasion and development in the host cell [63]. These surface proteins act as ligands to interact with RBC membrane receptors for invasion. *P. vivax* infects only reticulocytes in blood with the help of Duffy binding protein and reticulocyte homology protein receptors [64]. The virulent *P. falciparum* uses many redundant pathways for attachment and invasion. Surface antigens of parasite like erythrocyte binding like (EBL) proteins, Duffy binding-like (DBL) homologous proteins and reticulocyte binding like proteins are different kind of adhesins, involved in attachment of this parasite to the RBC [65]. Apical membrane antigen (AMA1) is a major vaccine candidate, as it translocates to the merozoite surface prior to invasion [66] and hence can be effectively neutralized by antibodies. AMA1 forms moving junction (MJ) by interacting with rhoptry neck proteins (RONs) [67], [68], [69]. In the invasion, the first step is the formation of parasite-host cell junction by a wavy deformation of RBC membrane that is stimulated by merozoite interaction with RBC [70]. The parasite reaches the RBC membrane with the help of acto-myosin motor complex present beneath the PM [71]. Motility in the invasion is mediated by the formation of an actin-myosin motor complex that comprises of thrombospondin-related anonymous protein in merozoite (mTRAP) linked to short actin filaments via aldolase [72].

These actin filaments further interacts with myosin A (Myo A) tail domain, where myosin is anchored to inner membrane complex (IMC) by the interaction between myosin tail domain interacting protein (MTIP) with two IMC proteins referred to as glideosome associated proteins (GAP) - GAP45 and GAP50, which acts as a grip and the parasite adhesins are pulled through fluidic lipid bilayer of PM and the end result is forward motion of the parasite [74], [72]. During this process, invagination of membranes from both host and parasite contribute to the formation of PVM surrounding the parasite, thus creating a favorable niche for its development in the RBC by allowing nutrients uptake from the host [75].

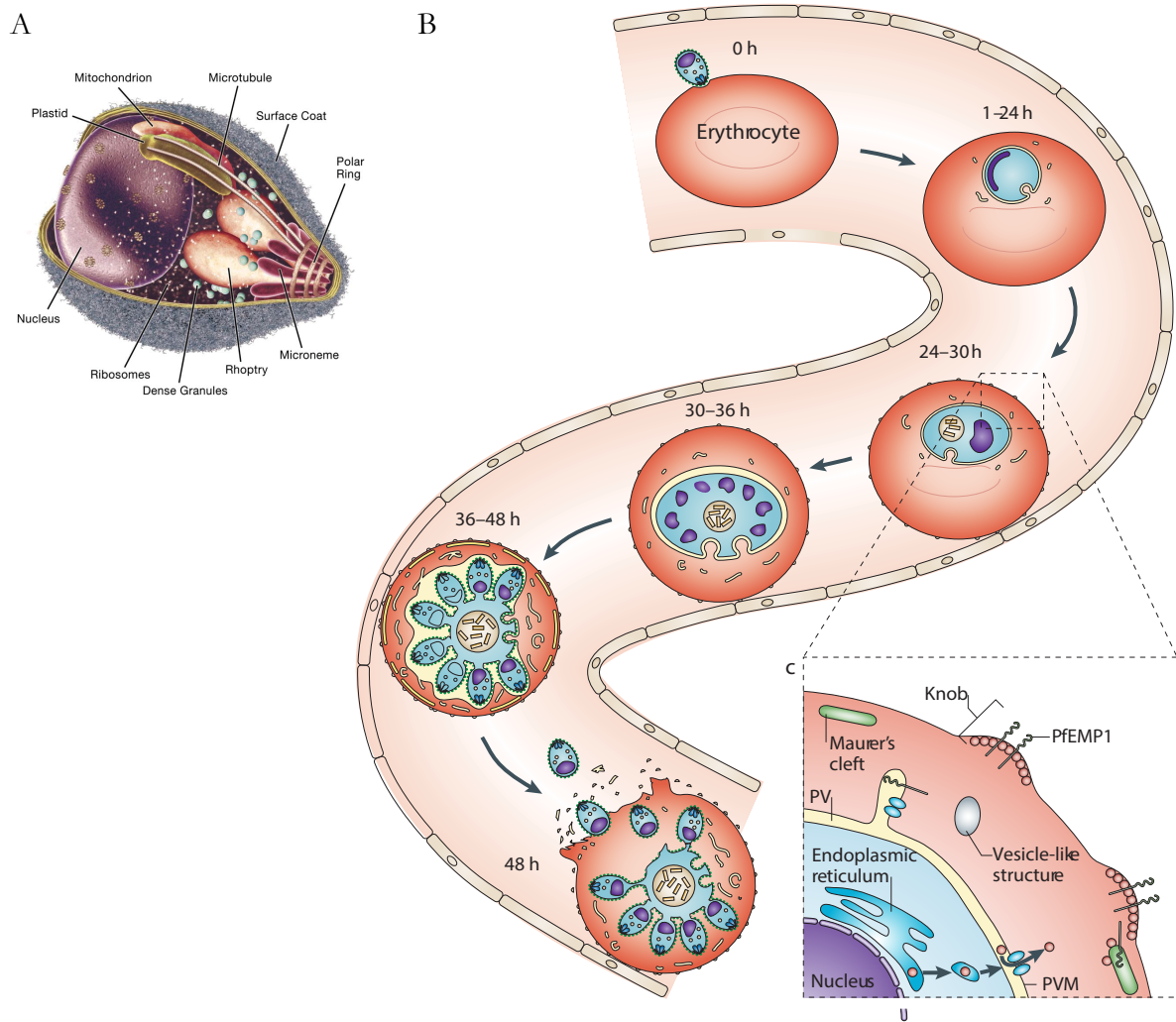


Fig 4: (A) Typical merozoite structure with a representation of major organelles. **(B)** Circulating hepatic merozoites attach to RBC in random orientation. Parasite reorients in such a way that apical complex comes in contact with RBC membrane. Then merozoite invades, form PVM and exports antigen for host remodeling that occur in duration of 1 – 24 h. The parasite then mature to become highly metabolic trophozoite, loses its apical complex organelles and grows substantially during 24 – 36 h. After this period the parasite develops into schizont where multiple DNA replications and asynchronous mitotic divisions occur. Upon rupture of schizont 16 – 32 merozoites are released into the blood after 36 – 48 h post invasion period. During early development, parasite exports PfEMP1 onto the surface of RBC membrane that acts as a ligand to adhere to receptors of the endothelium of microvasculature. (Image adapted from [73])

At the beginning of PVM formation, the junction between host and parasites appears like a ring and the parasite moves through the annulus forming complete PVM. Once the parasite is invaded successfully, it undergoes a trophic phase followed by a replicative phase. In RBC, the parasite becomes round shaped and forms a trophozoite. The trophozoite develops

by ingesting host cell cytoplasm. Intracellular parasites degrade hemoglobin as a source of amino acids and the end product heme is converted to malaria pigment hemozoin because heme is toxic to the parasite [76]. Many anti-malarial drugs like chloroquine and mefloquine inhibit the hemozoin formation and crystallization thus helping in parasite clearance [77]. Approximately after 18 h, trophozoites develop into schizonts. The persistence of parasite proliferation depends on its ability to escape from host defenses which is achieved by antigenic variation. The variation is facilitated by differential expression of *Plasmodium falciparum* erythrocyte membrane protein 1 (PfEMP 1) by a diverse family of genes known as *var* genes (60 *var* genes are known in *Plasmodium*). Each individual parasite expresses one *var* gene at a time in a mutually exclusive manner and all other family members are maintained transcriptionally silent [78]. Antigenic variation is achieved by epigenetic regulation, by expression of monoallelic *var* transcripts and silencing of other *var* alleles by telomeric heterochromatin. In the schizont, multiple nuclear divisions and daughter merozoites formation occurs by schizogony. Several proteases are involved in the release of merozoites from schizonts. Possible proteins for the egress include cysteine proteases, like SERA family proteins and subtilisins like SUB1 and SUB2 [79]. After one round of asexual blood stage replication, released daughter merozoites infect fresh RBC and begins another round of asexual replication. Simultaneously a small population from newly invaded merozoites differentiates into male and female gametocytes, which are end stages of parasite development in the vertebrate host and ensure transmission [80]. The process of gametocytogenesis in *Plasmodium* biology is obscure. But certain hypothesis explains that stress and high parasitemia of host RBCs trigger gametocytogenesis. Endoplasmic reticulum stress prompts the conversion of heterochromatin *AP2-G* to euchromatin leading to *AP2-G* translation that acts as a transcription factor switching commitment from asexual cycle to sexual stages [81]. *AP2-G* gene deletion revealed its essential role in gametocytogenesis [82]. *Plasmodium falciparum* gametocyte development 1 (Pfgdv1) protein is essential for the sexual commitment and Pfgdv1 mutant parasites failed to produce gametocytes [83]. Exosome like microvesicles secreted by infected RBCs are ingested by other iRBCs which in turn act as signaling molecules for the sexual commitment [84], [85]. PfEMP1 trafficking protein 2 (PfPTP2) is one of the major protein involved in cell-cell communication [85]. The gametocytes from circulation will be taken up by the mosquito during blood meal and sexual reproduction takes place in the mosquito gut. Recent strategies to block transmission include, the usage of inhibitors that kill the gametocytes for complete malaria eradication [86].

1.2.2 Sexual development in the mosquito vector

Sexual development is a complex process regulated by many kinases and phosphatases, initiated by the activation of gametocytes. As soon as mosquito ingests infected blood, gametocytes experience a rise in pH and Ca^{2+} ion flux levels, drop in the temperature and exposure to xanthurenic acid induces parasite development in the midgut [87]. Male gametocyte undergoes three rounds of DNA replication within 15 min, which is known to be fastest DNA replication in eukaryotes and forms octoploid nucleus [88]. Activation of cGMP-dependent protein kinase (PKG) is critical for male gamete formation [89]. Kinases like calcium-dependent protein kinase 4 (CDPK4) and SR protein kinase (srpk) play a major role in assembly of the flagella on the surface these gametocytes (exflagellation), leading to the formation of mature micro male gametes [90], [91]. Metallo-dependent protein phosphatases [PPMs] have a significant role in mosquito stage development of the parasite. Depletion of PPM2 leads to 30% reduction in female gamete formation thereby resulting in subsequent reduction in ookinete formation [92]. PPM1 depleted parasites failed to produce ookinetes because of the blockade in male gamete exflagellation [91]. *Plasmodium berghei* mitogen activated protein kinase (PbMAP2) is required for cellular differentiation in male gametocytes in the mosquito midgut and its depletion resulted in lack of exflagellated microgametes formation [91]. In female gametocyte, activation takes place along with male gametocyte without DNA replication. Female gametocyte differentiates into a single female gamete and exits the erythrocyte. Female gametocytes synthesize transcripts which are essential for post fertilization development of the parasite and stored as P granules [93]. Few mRNA transcripts in female gametocytes undergo translational repression by DDX6-class RNA helicase binding to them (DOZI, Development Of Zygote Inhibited) [94]. Silenced mRNAs resume translation after zygote formation to develop into ookinetes. There are conserved 6-cysteine family member proteins like P230, P230p, P48/45 and P47 that are surface located and play a critical role in gamete formation. P230 and P48/45 are critical for male gamete fertility [95] whereas P47 is essential for female gamete fertility [96]. Haploid male and female gametes fertilize and forms non motile diploid zygote [97].

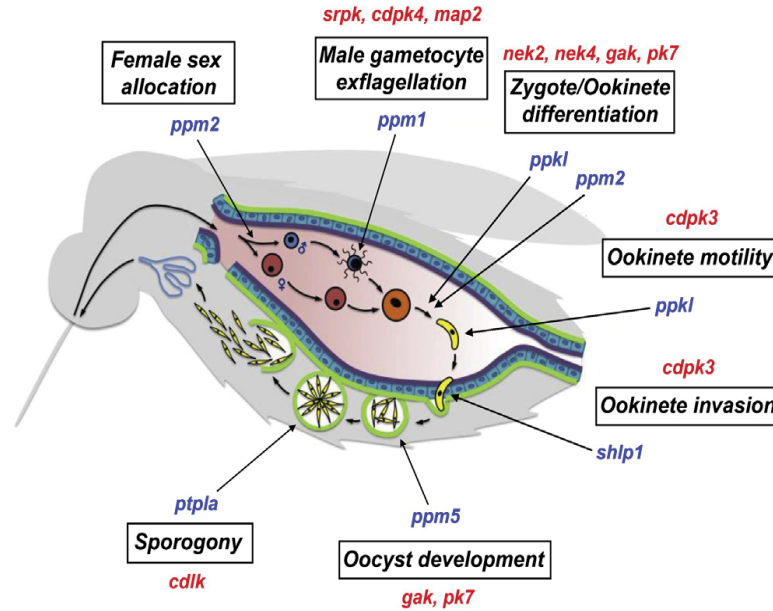


Fig 5: *Plasmodium* development in the mosquito vector. Male and female gametocytes ingested by the female *Anopheles* mosquito along with the blood develop into gametes. Male gametes emerge from male gametocyte after replication and exflagellation, fuse with differentiated female gamete to form zygote. Within 24 h post blood meal, zygote differentiates into motile ookinete which breaches midgut epithelium and develops into oocyst. Inside oocyst, sporogony takes place and approximately after 12 – 14 days, the oocyst ruptures to release sporozoites into the hemocoel. Through hemolymph, sporozoites glide and come in contact with salivary glands. They invade into salivary glands and reside here prior to their inoculation into vertebrate host. Most of these developmental processes are controlled by kinases (red) and phosphatases (blue) as represented in the diagram. (Image is adopted and modified from [92]).

Zygote differentiates into motile ookinete where DNA replication and meiosis occur [98]. Cyclin G-associated kinase (GAK) is essential for clathrin-mediated vesicle trafficking [99] and GAK mutant failed to develop into ookinetes, demonstrating the function of vesicular trafficking to protein export through secretory organelles in *Plasmodium* life cycle [91]. Nima-related protein kinase 2 and 4 (Nek2 and Nek4) are required for DNA replication in ookinete meiosis [100], [101]. After 10 h post fertilization, gene expression is initiated in the zygote.

AP2-O transcription factor, produced at this stage is essential for ookinete and oocyst development. Depletion of AP2-O leads to deformed ookinete formation resulting in absence of midgut oocyst and salivary gland sporozoites, suggesting it's essentiality for ookinete development [102]. Ookinete breaches through midgut epithelium with the help of chitinases, reaches the basal lamina facing the hemocoel and differentiates into oocyst [103]. The requirement of CDPK3 is critical for motility of ookinete and midgut invasion [104].

Shewanella-like protein phosphatase 1 (Shlp1) is required for secretory organelle (micronemes) development and *Shlp1* deletion leads to the absence of oocysts in the midgut [105]. In oocyst, sporogony occurs by multiple nuclear divisions without cytokinesis, concomitantly, cytoplasm is subdivided forming sporoblasts [106], [107]. Pfk7, a protein kinase and PPM5, a phosphatase both are required for oocyst development [108], [92]. Individual sporozoites bud from the sporoblast and enter into the hemolymph. CDPK like kinase plays a critical role in late oocyst development and depletion of this kinase leads to reduced sporozoite burden in salivary glands [91]. The development of sporozoites in the oocyst is CSP dependent. CSP depleted parasites failed to form oocyst sporozoites and mutations in the region II-plus of CSP lead to blockade in egress from oocyst [109], [110]. Proteases play a critical role in egress of the sporozoites from oocyst. An aspartic protease Plasmepsin-VIII deletion leads to defect in sporozoite egress from oocysts with impaired gliding motility of the sporozoites [111]. Thousands of the sporozoites released into the hemolymph migrate to the salivary gland by gliding motility and remain in the salivary glands until they are inoculated into the mammalian host [112], [113], [114].

1.2.3 Sporozoite

Formation and maturation of sporozoites take place in the oocyst and major surface protein CSP plays a critical role in the process [109]. Another transcription factor AP2-Sp that is upregulated in oocysts and salivary gland sporozoites regulates the transcription of many sporozoite genes and its disruption leads to impaired sporozoite formation [115]. Sporozoite is sickle cell shaped, with a large elongated nucleus, mitochondria, endoplasmic reticulum and Golgi apparatus. At the apical end, secretory organelles such as rhoptries and micronemes are located [116]. CSP is secreted by the secretory organelles and forms a dense coat on the surface. CSP contains a signal peptide, NANP region at the N terminus that binds to HSPGs and a thrombospondin-like type I repeat (TSR) domain at the C-terminus. Sporozoites are the only parasitic forms in the life cycle that invade two different cell types viz., the midgut sporozoites invade salivary gland and salivary gland sporozoites invade hepatocyte [117]. TRAP is another secretory protein which is continuously shed on to the sporozoite surface and plays a critical role in parasite locomotion [53]. TRAP structure comprises of a cytoplasmic C-terminal tail, a transmembrane domain, a proline-rich region and two adhesive domains including thrombospondin type-I repeat (TSR) domain and von Willebrand factor A (vWA)-like N-terminal A domain [118], [119]. The cytoplasmic tail of TRAP helps in locomotion and adhesive domains help in host cell attachment [120], [121]. The mammalian host infection starts with the

deposition of sporozoites by the infected mosquito while taking a blood meal and the exo-erythrocytic cycle will be initiated in short time span. But in *P. vivax* and *P. ovale*, few sporozoites may not follow asexual reproduction step in the humans, instead, they remain dormant in the liver and these stages are called as hypnozoites. They may be activated after weeks, months or even years and after maturation they are released into the blood to infect RBCs, leading to relapse of the disease [122], [123].

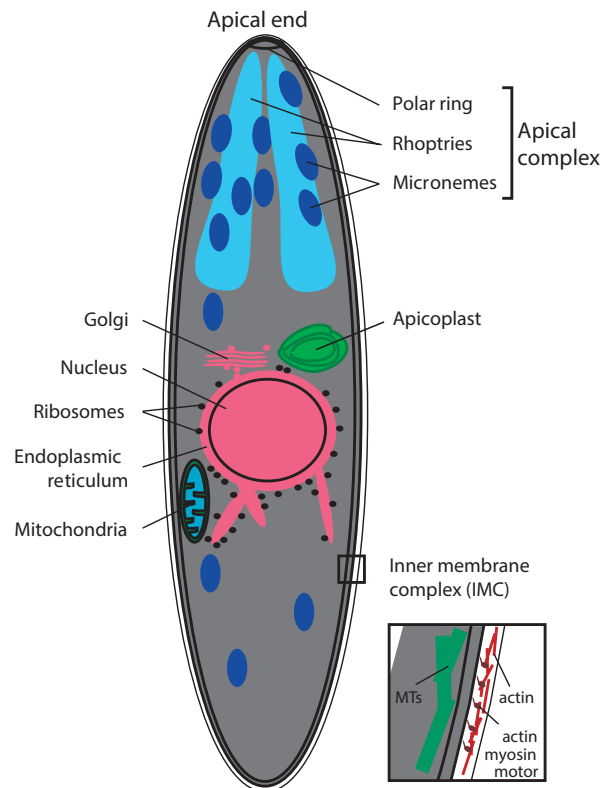


Fig 6: Typical spindle shaped sporozoite structure that measures about 10 – 15 μm in length and 1 μm in diameter. Major organelles are represented in the image. Actin myosin motor is presented beneath the membrane helps in gliding motility of the sporozoite. Image is adopted from [124].

Several high throughput transcriptomic and proteomic studies revealed that ~2000 genes are active in salivary gland sporozoites [125]. Among them, only a few were characterized such as CSP and TRAP. The involvement of CSP and TRAP in sporozoite functions like gliding motility, host cell attachment and invasion are well known [126], [42], [53]. The transcripts of sporozoite proteins required to establish infection in the mammalian host are known to be synthesized at sporozoite stage and these transcripts are translationally repressed by Pumilio (puf) proteins which bind to 3' untranslated regions of the target mRNA. Deletion of Puf2 gene leads to sporozoite maturation into early intrahepatic like forms (round) in salivary glands [127],

[128] demonstrating that Puf proteins are essential for stage transitions in *Plasmodium* life cycle from mosquito vector to the human host. AMA1 antigen present on sporozoite surface, is a target for anti- AMA neutralizing antibodies and inhibit the host cell entry of the sporozoites [129].

1.3 Clinical manifestations of malaria

Malaria is a febrile illness that can be categorized into mild, uncomplicated, severe or complicated malaria with flu like symptoms causing death. The outcome of the disease depends on many factors like individual immunity, age, host genetic composition and parasite virulence. Liver stage infection does not exhibit any clinical symptoms [130], [131]. Disease symptoms appear in asexual blood stage cycle when RBC lyse releasing daughter merozoites and toxins into the blood which activates host defense responses. The immune response induces cytokine release such as the pro-inflammatory TNF- α and promotes the production of reactive nitrogen species to clear asexual and sexual forms except for rings which are heat resistant [132], [133]. Each asexual erythrocytic cycle takes approximately 48 h and after every cycle, host shows symptoms including fever, chills, headache, dizziness, general malaise, body aches and sweating.

The infected individual becomes anemic and develops spleen enlargement due to hemolysis. If uncomplicated malaria is left untreated, it converts into severe or complicated malaria. RBC membrane loses its fluidity and becomes rigid as malaria parasite grows in it. This deformed infected RBC (iRBC) causes blockade in microvasculature by cytoadherence to endothelium that leads to severe malaria. *Plasmodium falciparum* erythrocyte membrane protein 1 (PfEMP 1) secreted by the parasite is exported onto the surface of RBC and forms knob like structures that acts as a ligand for receptor mediated adhesion. This molecule makes iRBC to adhere to the endothelium of microvasculature. The iRBC forms rosettes with other non-infected RBCs resulting in sequestration in the capillaries. Cytoadherence and rosetting in vital organs like brain, lung, liver and placenta cause obstruction to the blood flow, which is believed to be the reason for the development of complications [134], [135]. Sequestration in the brain causes cerebral malaria which may lead to death in many cases. Sequestration in the placenta of pregnant woman causes placental malaria leading to spontaneous abortions and maternal deaths. Because of the compromised immunity in the malaria infection, there is a likely possibility for the occurrence of other opportunistic infections which will make the situation more critical. In endemic areas, where malaria transmission is very high and some individuals are constantly getting exposed to parasite develop partial immunity. These individuals do not show any disease

symptoms but can act as carriers [136]. Overall malaria attacks bring a social, physical, psychological and economic burden [6].

1.4 Diagnosis and treatment

Individual with high fever, chills and other flu like symptoms will be tested for malaria by most commonly used rapid diagnostic tests (RDTs) and microscopic examination of peripheral blood smears [137]. In RDTs, malaria antigens such as HRP-II, pLDH or aldolase are tested for their presence in the human blood and in microscopic observation, blood smears stained with Giemsa are checked for malaria parasites in RBCs [138]. Other diagnostic tests include polymerase chain reaction (PCR), serological procedures and fluorochrome microscopic techniques [139], [140]. Malaria in pregnancy is tested by both peripheral blood microscopy and PCR [139]. There are different antimalarial therapeutic options available today. The therapeutic and treatment choice depends on several factors such as *Plasmodium* strain, the efficacy of the drug, availability, cost effectiveness and geographical location, which might be having a drug resistant species [141]. Many drugs are available such as chloroquine, mefloquine, sulfadoxine, pyrimethamine, artemisinin, etc. Most of the drugs like chloroquine and mefloquine inhibit hemozoin crystallization, thereby killing the parasite by accumulating toxic heme released by hemoglobin degradation [77]. Primaquine is an effective drug in eliminating hypnozoites and gametocytes [142], [141]. Artemisinin and its derivatives appear to be activated by cleavage of endoperoxide bridge after reacting with heme and ferrous oxide resulting in the production of free radicals that kills the parasite [143]. The emergence of drug resistance is a major problem in eradicating malaria. In this scenario, artemisinin based combination therapies (ACT) are commonly used. ACTs slower or clear the parasites because of the combinatorial drugs having a different mode of actions against the parasite development. Currently available ACTs are artesunate–amodiaquine, artemether–lumefantrine, artesunate–mefloquine, artesunate–sulfadoxine–pyrimethamine and dihydroartemisinin–piperaquine [144].

1.5 Control measures and prophylaxis

Control measures are aimed to break human-vector contact cycle of transmission and includes both vector control and inhibition of sexual stages of parasites in human, use of mosquito repellent liquids and coils to prevent mosquito bites. Other methods include use of window screen and insecticide treated nets that are helpful to reduce malaria transmission [145]. Destruction of larvae by using Paris green insecticide will facilitate killing of both larvae and pupae on stagnant waters where mosquitoes lay the eggs. Gambusia is a larvivorous fish, cultivated to kill larvae of mosquitoes. Indoor residual spraying (IRS) with

dichlorodiphenyltrichloroethane (**DDT**) kills adult mosquitoes by opening sodium ion channels in neurons [146]. Environmental conditions play a crucial role in malaria transmission. In endemic areas, awareness about environmental management practices, vector control and knowledge about parasite help to fight against malaria transmission.

Despite the availability of many drugs to cure malaria, prophylactic vaccines are more effective because of the constant emergence of drug resistant parasites. Several approaches are available to develop vaccines against malaria infection. In vaccine development strategies, injection of live radiation attenuated sporozoite was shown to be most effective [147]. However, over or under irradiation of sporozoites leads to suboptimal immunity. Also it is unrealistic for the production of irradiated sporozoites as vaccines for large endemic populations. To overcome these limitations and for mass production of vaccines, generation of subunit vaccines has gained more importance. For subunit vaccine designing, different parasite epitopes which can trigger high immunogenicity have been identified and are being tested for their efficacy. Some challenging aspects with subunit vaccines pertains to the poor immunogenicity in human and the use of advanced adjuvants formulation. The usage of various adjuvants with subunit vaccines to boost the immunity is under trails [148], [149]. At present, there are no effective vaccines for malaria recommended by WHO. Till now, SPf66 and RTS,S subunit vaccines have been tested in phase III clinical trials. Owing to their limited efficacy there is an urgent need to develop better vaccines to combat malaria. For malaria vaccine development, pre-erythrocytic stages, erythrocytic stages and sexual stages are suitable targets for disease prevention, elimination and transmission blocking respectively.

To achieve potential vaccine development, pre-erythrocytic stages are excellent targets for several reasons, such as they are metabolically active but clinically silent, sporozoites infect very less number of hepatocytes and attenuated sporozoites are capable of antigen presentation and activation of T cells [150]. Genetically attenuated parasites (GAPs) can be obtained by targeted deletion of genes which are essential for liver stage development. Arresting the parasite development in the liver to elicit immunity qualifies these mutants to be used as whole organism vaccines. For example, deletion of *UIS3* and *UIS4* genes led to the early arrest of the parasites in the liver and elicits CD8+ T cell immunity [151], [35], [36]. Targeting the parasite's fatty acid synthesis pathway (FAS-II) resulted in the arrest of the parasites at late liver stage development that have potential also to confer cross stage immunity [152]. Blockage of the very late liver stage development of the parasites is achieved by deleting genes like cGMP-dependent protein kinase (PKG) [153], *Plasmodium*-specific Apicoplast protein for Liver Merozoite formation (PALM)

[154] and Liver Specific Protein-1 (LISP-1) [50]. Amongst the subunit vaccines, RTS,s was formulated using hepatitis B surface antigen as a carrier for epitopes derived from CSP of *P. falciparum* [149]. Apart from this, several liver stage antigens such as TRAP [155], LSA1 [156], LSA3, SPf66 [148], SALSA [157] and STARP [158] are studied for their efficacy as vaccine candidates. Among all only SPf66 is under phase III clinical trials.

Blood stage vaccines are mainly designed to decrease disease symptoms by reducing parasite growth and elimination of the parasite by antibody production. Major parasite proteins for blood stage vaccines development that are available so far are MSP1 and AMA1 which are essential for merozoite attachment and entry [159], [160]. PfEMP1 that is essential for parasite cytoadherence to microvasculature resulting in severe form of the disease, is also another potential vaccine candidate [161]. But, limitations with the development of blood stage vaccines include antigenic variation and polymorphism. In endemic areas, transmission blocking strategies are essential to prevent disease dissemination. This can be achieved by targeting metabolic enzymes or signaling molecules like phosphatases and kinases that play a role in the sexual development of the parasites. These signaling molecules can be excellent targets for developing inhibitors for transmission blocking. PfS25 and PfS28 are parasite antigens expressed on zygote and ookinete surface [162], [163]. Immunization with PfS25 protein in mice produced transmission blocking antibodies and has undergone phase I clinical trials [164]. Multistage vaccines are under development which are made up of many antigens from different parasitic forms and may elicit immunity across different stages. For example, CSP, TRAP, LSA1, MSP-1, SERP, AMA-1 and Pfs25 were used in NYVAC-Pf7 vaccine design and though has undergone I phase I/II trial, it was not successful [165].

1.6 Current challenges to control malaria

Malaria is the most serious threat to the mankind and major challenge to combat malaria parasite is its complex multi-stage life cycle. Parasite expresses many antigens throughout the life cycle for interaction with the host. A poor knowledge about these host-parasite interactions and immune responses against the parasite proteins are major challenges in the disease control. Different *Plasmodium* species exhibit antigenic variation and polymorphism which makes drug and vaccine design strategies highly complicated. Production of malaria vaccines like irradiated sporozoites is challenging for large scale use. Further, many subunit vaccines are poorly immunogenic and are not able to confer sterile immunity even in 30% of the cases. Only RTS,S vaccine confers protection up to 36.3% as tested in African infants [166]. To achieve this, pre-erythrocytic stages are more suitable for several reasons. More recently, depletion of proteins

essential for liver stage development by genetic approaches have shown to arrest the parasite in the liver and the concept is being used to create whole organism vaccine to elicit immunity against the malaria parasite.

Designing blood stage vaccines is highly difficult because of the antigenic variation of the parasite. In many endemic countries, mosquitoes are becoming resistant to insecticides. The emergence of drug resistance parasites against artemisinin has been found in five countries including Thailand, Vietnam, Cambodia, Myanmar and Laos [167]. Even though combination therapies are available, the emergence of resistance to anti-malarial drugs is a constant risk. Travelers moving from drug resistant areas to other areas are also instrumental in spreading malaria to areas where the disease has been eliminated. For transmission blocking strategies, development of drugs which kills mature gametocytes is necessary as these stages are recalcitrant to anti-malarial drugs because of their less metabolic activity. For transmission blocking vaccines, only Pfs25 and Pfs28 are used which are surface antigens present on zygote and ookinete [162], [163]. Conjugation of recombinant Pfs25 with EPA (Pseudomonas aeruginosa exoprotein A) adjuvant made it highly immunogenic resulting in transmission blocking immunity [168]. Immunization with Pfs25 protein in mice produced transmission blocking antibodies and this is the only transmission blocking vaccine that has undergone phase I clinical trials [164]. Many of the uncharacterized parasite proteins might be playing an essential role in disease dissemination and parasite development which could be potential drug targets or form basis for efficient vaccine development. Further research into the biology of the parasite is of paramount important to enable development of new therapeutics and vaccine formulation required to curtail and cure malaria.

1.7 *Plasmodium berghei* as model

Plasmodium berghei parasite species infects specifically the rodent mammals. It was first discovered by Vincke and Lips in 1948 from rodents in Central Africa [169]. It is being widely used as a model in *Plasmodium* genetics for delineating the mechanisms of disease physiology and immunology because it can be genetically manipulated more easily than other species. The life cycle and symptoms of the disease in mouse species are almost similar to that of *P. falciparum* including sequestration and cytoadherence [170]. It allows to study the mosquito stages and *in vivo* development in the mammalian host because of the limitation to study these stages in human owing to ethical consideration. High throughput sequencing and phylogenetic analysis identified most of the genes of *P. berghei* to be conserved in *P. falciparum* that may also implicate conserved function across both species [171], [172]. For vaccine and drug development, *P. berghei* parasites

are more suitable because they are amenable to genetic manipulation using standard genetic engineering tools like single crossover [173], [174], double homologous recombination [175], [96], promoter swap method [176] and conditional silencing at sporozoite stages [177]. These tools allow the functional characterization of a gene by disrupting or deleting it and study the dependency of specific gene or its product protein in parasite development across all the life cycle stages. Availability of reporter parasite lines like GFP [178], mCherry [179], red star [180], luciferase [181] and gametocyte defective lines [96], [182] make this organism more tractable.

1.8 Objectives

In the current study, reverse genetics approach was used to functionally characterize two *Plasmodium* genes. Reverse genetics is an approach to discover the function of the gene by analyzing the phenotypic effects of specific gene sequence engineered. In the reverse genetics approach used in this study, the target gene was replaced through double homologous recombination with construct carrying GFP reporter and pyrimethamine drug resistance cassette. The successful integration of the cassette at the desired locus allows both selection of the transfected population, as well as live monitoring of different stages as genetically altered parasite passes from mammalian host to mosquito and back to the mammalian host. This approach investigates the stage specific importance of the target gene as a block at a particular stage may reveal the critical importance of the gene product at that stage. In the event of target gene product being essential either at the selection stage (blood stages), sexual stage or development at oocyst stage, thus precluding the analysis of salivary gland sporozoite stages and subsequent liver stage development, a conditional gene silencing approach can be employed. A conditional mutagenesis system developed for *P. berghei* that is widely in use is based on the yeast Flp/FRT system. This system achieves the excision of a FRTed DNA sequence (FRT sites engineered in target gene locus) through the expression of an FLP recombinase driven by a *Plasmodium* mosquito stage specific promoter.

Using both the gene replacement strategy by double homologous recombination and conditional mutagenesis approach, we have characterized in the current study two genes: (i) *Plasmodium berghei* nicotinamidase (*Pbnic*) gene that encodes a metabolic enzyme required for conversion of nicotinamide into nicotinic acid and appears in the NAD⁺ biosynthetic pathway and demonstrate its role in sexual development and (ii) *PbS10* - gene encoding a sporozoite secretory antigen, upregulated in sporozoite stage and demonstrate its role in liver stage development.

In addition, we have also investigated host long noncoding RNA profiles during *Plasmodium berghei* and *Toxoplasma gondii* infections *in vitro* and showed their modulation during host-pathogen interactions. The rationale for the study and results are explained in following sections.

*Functional characterization of
Plasmodium berghei nicotinamidase
by reverse genetics approach*

2.1 Introduction

Malaria in humans is caused by an Apicomplexan parasite that belongs to genus *Plasmodium* and is responsible for nearly 500 million clinical cases annually imposing a huge burden on healthcare and economic development [183], [184]. *Plasmodium* exhibits complex life cycle with asymptomatic liver stages and clinically symptomatic blood stages in the vertebrate host and sexual stages in the mosquito vector. Despite immense research for decades to eradicate malaria, it still remains as a global problem affecting millions of people. Most of the anti-malarial drugs available till to date are schizonticidal that target either inhibition of hemozoin crystallization or generation of free radicals. Other probable potential mechanisms include inhibition of nucleic acid synthesis. These anti-malarial drugs are not effective against gametocytes because gametocytes are metabolically inactive and developmentally arrested. The emergence of drug resistant parasites has drawn the focus of researchers towards the identification of novel drug targets that can be exploited for designing effective anti-malarial therapeutics. Asexual replication of the malaria parasite in erythrocytes results in metabolic stress placed on the host when the parasite develops within the red blood cell (RBC). The parasites are greatly dependent on glycolysis for energy production and to meet this requirement, the parasite infected erythrocytes (iRBC) consume glucose at approximately one hundred times the rate of uninfected erythrocytes [185], [186]. The dependence of parasites on anaerobic respiration lead to most characteristic clinical manifestations of malaria like hypoglycemia and lactic acidosis. Therefore, a thorough understanding of the *Plasmodium* metabolism is essential to unravel the host-parasite interactions and these approaches hold key to target unique enzymes therapeutically. It is also important to identify the key metabolic regulators that are essential for transmission of malaria from vertebrate host to the mosquito vector as this information may hold potential for designing novel drugs that prevent malaria transmission.

As an obligate intracellular parasite, *Plasmodium* is auxotrophic for several essential metabolites including heme, vitamins, purines, amino acids and NAD^+ that are acquired from the host. During erythrocytic development of the parasite, 80% of the RBC hemoglobin is consumed by the parasite. Hemoglobin is a major food source, degraded into proteins and free heme. Free heme is detrimental to the parasite, so the parasite crystalizes heme into hemozoin (target for anti-malarial drugs) [187]. However, heme is an essential cofactor in many metabolic enzymes and parasite has its own heme biosynthetic pathway [188]. Enzymes involved in heme biosynthesis were believed to be excellent targets to inhibit blood stage development of the parasite. Deletion of heme biosynthetic pathway enzymes led to no apparent defect in the growth of blood stages, however it affected the transmission of parasites to mosquito because

of reduction in the formation of male gametes. So, enzymes of heme biosynthesis could be targeted for designing of transmission blocking drugs [188].

In both hepatic and erythrocytic stages, glucose uptake from the host is an obligatory step for its energy source and host GLUT1 transporter plays a critical role in glucose uptake by the infected cell. Chemical inhibition of GLUT1 impairs parasite development in the cell [189]. Glucose taken up by the parasite is converted to pyruvate by glycolysis pathway and it is well reported that *Plasmodium* has all the necessary enzymes required for glycolysis pathway [190]. Even in the mosquito, *Plasmodium* induces glucose uptake by the mosquito to support enormous oocyst development and to inhibit mosquito immune system as high glucose levels inhibit nitric oxide production [191]. Enzymes required for pentose phosphate pathway have been identified, which is essential for the production of NADPH and ribose 5-phosphate (R5P). NADPH is a cofactor in anabolic reactions like lipid, nucleic acid synthesis and R5P acts as a precursor for nucleic acid synthesis. In pentose phosphate pathway, the Glucose-6-phosphate dehydrogenase (G6PD) enzyme converts D-glucose 6-phosphate to 6-phospho-D-glucono-1,5-lactone by reducing NADP to NADPH. This enzyme plays a critical role in maintaining NADPH level that is required for the antioxidant role against oxidative stress given by iRBC. G6PD deficiency in humans confers resistance against malaria [192], has drawn the attention towards drug designing against glycolytic and pentose phosphate pathway enzymes. *P. falciparum* hexose transporter (PfHT) transports glucose and fructose into the parasite through the plasma membrane [193]. Glucose derived inhibitors showed the effect on *in vitro* *P. falciparum* asexual growth and *in vivo* *P. berghei* development, suggesting that it could be a good drug target [194]. Hexokinase is the subsequent enzyme in the glycolysis pathway, phosphorylates glucose to glucose 6 phosphate (G6P). G6P can either enter into subsequent steps in glycolysis or may act as starting substrate for pentose phosphate pathway that is required for ATP synthesis and antioxidant systems. Glucose analogs 2-deoxy-D-glucose and 2-fluoro-2-deoxy- D-glucose is a competitive inhibitor of hexokinase and showed anti-*Plasmodial* activity suggesting its potential for drug designing [195]. Glucose uptake is 100 fold more in iRBC, when compared to uninfected RBC [196], suggesting that glucose is an energy source for parasite and its metabolic enzymes are essential for *Plasmodium* survival and need to be validated for anti-malarial therapies.

Plasmodium genomic sequence analysis revealed that there are no enzymes for protein metabolism, which are required for amino acid synthesis. All the amino acids required for parasites are acquired by either scavenging from the host or by degrading hemoglobin [197]. But enzymes required for conversion of cysteine to alanine, glycine to serine and aspartate to

asparagine etc., are known to be expressed [190]. There is a high demand for lipids to support rapidly growing parasite population, lipids are produced in the parasites from the raw sources taken up from the host cells and serum. Comparatively a large amount of lipid synthesis takes place in *Plasmodium*, making it a target for anti-malarial drug design [198]. Phosphatidylcholine constitutes major portion in the parasite membrane and extensive research is going on the identification of chemotherapeutic targets in choline biosynthetic pathway [199]. G25 or Tritium-labeled compound VB5-T (N,N,N',N'-tetramethyl-N, N'-di{2-N[2-(p-3H-benzoyl)benzoyl]-aminoethyl}-1,12-dodecanediaminium dibromide) an G25 analog, are competitive inhibitors for choline and inhibits choline uptake by parasite shows anti-Plasmodial activity [200]. Type II fatty acid synthase (FASII) is localized to the apicoplast and involved in the *de novo* synthesis of fatty acids. FASII pathway is an attractive target because of its essentiality in making fatty acids. There are several bacterial inhibitors for FASII pathway such as cerulenin, triclosan and thiolactomycin have shown antimalarial activity *in vitro* [201].

Nucleic acid metabolism in rapidly dividing parasites is another well-known target for drug discovery. Parasite synthesize purines by salvage pathway from hypoxanthine scavenged from host plasma, which is finally converted into ATP or GTP through a series of enzymatic events, while pyrimidines are synthesized by *de novo* pathway from its precursors obtained from the host [202]. However, humans can synthesize nucleic acids, both by *de novo* and salvage pathways. Because of the limited ways of nucleotide synthesis in *Plasmodium*, the scope for targeting these reactions may have important therapeutic implications. Folate derivatives act as cofactors involved in pyrimidine biosynthesis. Dihydrofolate to tetrahydrofolate conversion is catalyzed by dihydrofolate reductase (DHFR) and these folate derivatives act as carbon donors in the synthesis of pyrimidine nucleotides. Antimalarial drugs such as pyrimethamine and cycloguanil preferentially inhibit *Plasmodium* DHFR activity [203]. Parasites synthesize dihydrofolate from glutamate, para-aminobenzoic acid and GTP. Sulfadoxine and other sulfa drugs inhibit parasite growth by targeting the dihydrofolate *de novo* synthesis [204]. Vitamins and cofactors play a key role in parasite metabolism, most of them are all scavenged from the host.

Nicotinamide adenine dinucleotide (NAD^+) is a cofactor found in all living cells. The intracellular NAD^+ levels are regulated/maintained by the *de novo* and/or salvage pathway, and through its catabolic activity as co-enzyme or co-substrate. It exists in two forms: NAD^+ and its phosphorylated (NADP^+) and reduced forms (NADH and NADPH) (Fig 7 A) that play a role as important redox cofactors [205]. In recent years, however, NAD^+ has gained recognition for its diverse role as an enzyme substrate in several essential

cellular processes including epigenetic regulation, calcium signaling and DNA repair [206], [207].

In human erythrocytes, the synthesis of NAD^+ is by either *de novo* (Fig 7 B) or by salvage pathway (Fig 7 C). In salvage pathway, parasite utilizes either nicotinic acid (Na) or nicotinamide (Nam) referred to as niacin or vitamin B3 that is acquired extracellularly [208] (Fig 7 C). The conversion of Na to NAD^+ occurs through the Preiss-Handler pathway in three steps: 1) Na is first converted into nicotinate mononucleotide (NaMN), a reaction catalysed by nicotinic acid phosphoribosyl transferase (NAPRT), then to nicotinate adenine dinucleotide (NaAD) via the nicotinamide mononucleotide adenylyl transferase (NMNAT) and finally the glutamine-dependent NAD^+ synthetase (NADSYN) generates NAD^+ [209], [210]. Alternatively, Nam can be converted to NAD^+ in a two-step pathway involving nicotinamide riboside kinase (NRK) and NMNAT [211]. In the *de novo* synthesis pathway, prokaryotes can utilize aspartate as a precursor to feed into the synthesis of NAD^+ , whereas eukaryotes rely on intermediates of tryptophan breakdown [212]. Both pathways produce NaMN, which integrates with the final two steps of the salvage pathway. The reconstruction of *P. falciparum* genome revealed that the parasite encodes only enzymes necessary for a functional NAD^+ salvage pathway (NAPRT: PFF1410c, NMNAT: PF13_0159 and NADSYN: PFI1310w) (Fig 7 C) and does not appear to possess the enzymes for *de novo* synthesis [190], [213]. While both the host and parasite possess the NAD^+ salvage pathway, there is a significant divergence between the two pathways due to the presence of nicotinamidase (nic) enzyme (PFC0910w) in the *P. falciparum* genome that is able to convert Nam to Na.

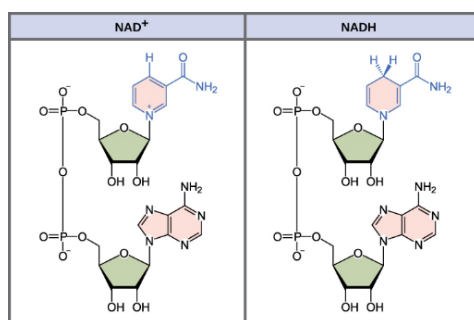
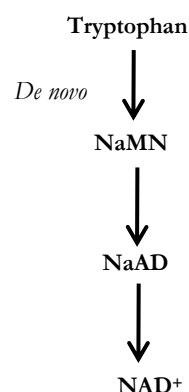
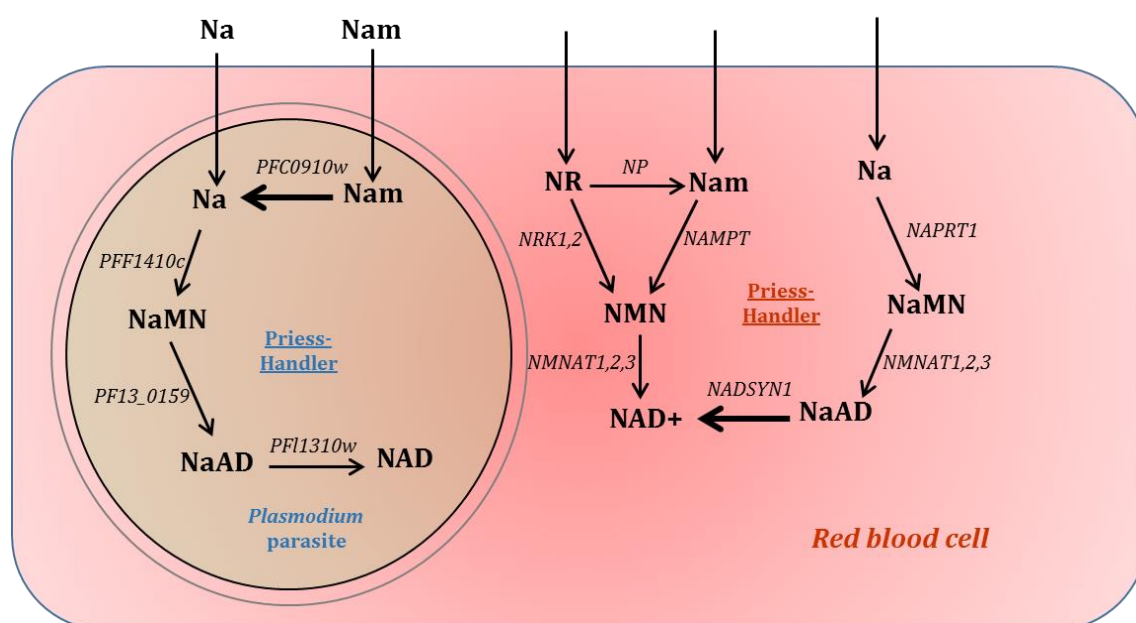
A**B****C**

Fig 7: *Plasmodium falciparum* NAD⁺ biosynthesis. **A)** Oxidized and reduced forms of NAD. **B)** NAD⁺ *de novo* synthesis from tryptophan amino acid. **C)** Outline of NAD⁺ biosynthesis by salvage pathway (Priess-Handler pathway) in human red blood cells and in *Plasmodium* parasites. Precursors of NAD: Nam: nicotinamide, Na: nicotinic acid, NR: nicotinamide riboside, NaMN: Nicotinic acid mononucleotide, NaAD: Nicotinic acid adenine dinucleotide, NMN: Nicotinamide mononucleotide. Enzymes of the pathway: 1 or Nicotinamidase, 2 or Nicotinate, 3 or Nicotinate nucleotide adenylyl transferase, 4 or NAD synthetase (Numbers represent *Plasmodium* and abbreviations represent human enzymes). NP: Nucleotide phosphorylase, NRK: Nicotinamidase riboside kinase, NAMPT: Nicotinamide Phosphoribosyl transferase, NMNAT: NMN/NaMN adenylyl transferase. (Image adapted from [214])

Owing to the unique expression of *nic* only to *Plasmodium*, it is expected that targeting this enzyme may lead to overall imbalance in the cellular NAD^+ levels thus affecting several NAD^+ dependent biological processes like electron transport (catalysed by oxidoreductases), ADP-ribosylation reactions, secondary messenger activity and NAD^+ dependent Sir2 activity required for deacetylation of histones. The *P. falciparum* genome appears to encode significantly fewer NAD^+ utilizing enzymes than other organisms, containing only two putative sirtuin proteins (Sir2) and no homologs of poly(ADP-ribose) polymerase [190]. Owing to the catabolic dependency of NAD^+ by the Sir2s [215], and its role as a cofactor in many other NAD^+ dependent enzymes, it is likely that NAD^+ dependent metabolic pathway provides a link between metabolism and a variety of important biological processes in the *Plasmodium*.

Extensive work on NAD^+ salvage pathway enzymes has been done by various groups using biochemical and genetic approaches. Their studies confirmed the constituents of a canonical salvage pathway, while the enzymes of *de novo* synthesis were shown to be completely lacking suggesting that *P. falciparum* is a NAD^+ auxotroph [213]. To characterize the parasite's NAD^+ synthetic pathway, stable isotope labeling was done by using labeled ^{13}C -U-glucose and the labeled carbon was traced in newly synthesized NAD^+ throughout development. This study revealed a continuous synthesis of NAD^+ throughout the 48-hour parasite life and also high levels of NAD^+ was shown to be synthesized and utilized by the parasite and not the host cell during infection [216]. Further, the ability of the parasite to take up exogenous niacin and synthesize NAD^+ was functionally demonstrated nonetheless, the removal of niacin from culture media only reduced but did not impact the intracellular parasite growth suggesting that niacin derived from the host cell is sufficient to provide the required amount of NAD^+ [216]. Expression analysis of NAD^+ metabolic enzymes revealed that they exhibit an uncoordinated transcriptional profile. Interestingly, the NAD^+ synthesis did not peak with NAD^+ synthase expression, but rather showed a steady NAD^+ production throughout the erythrocytic stages, likely to maintain NAD^+ pools that are lost to turnover and ensure sufficient increase in total NAD^+ required for the development of new merozoites [217], [218].

NANAT is a rate limiting enzyme in the NAD^+ biosynthetic pathway, present in all the organisms. However the solved crystal structures of both *E. coli* and humans have revealed significant structural divergence between their respective active sites, suggesting the feasibility

to selectively target the bacterial enzymes [216]. Due to similarities in PfNMNAT and bacterial homologs and a significant divergence from the host enzyme, it constitutes an excellent target for chemical inhibition. Co-crystallisation of bacterial NMNAT and one of the effective inhibitors, compound 1a-a, revealed that it binds to the enzyme in its *apo* form and interact with both the NaMN binding pocket and the ATP binding site [219]. Owing to the conservation of this region in PfNMNAT, the chemically modified 1a-a, was tested on *in vitro* cultures of *P. falciparum* that showed significant inhibition. These studies likely raise the possibility of using NMNAT inhibitors to cure human malaria as they are selective only to *P. falciparum* and do not impact host metabolism. The solved X-ray structures of PfNaMNAT in the product-bound state with NADH together with an a,p-non-hydrolyzable ATP analog, to a resolution of 2.2 Å and 2.5 Å respectively revealed that PfNaMNAT possesses two cysteine residues within the active site that is unique only to PfNaMNAT and have not been described for any other NaMNATase described so far. These two cysteine residues are likely involved in redox regulation. Further, a comparison with the active site of *E. coli* NaMNAT showed very similar architecture despite different substrate preferences [220].

Investigation of the genetic and biochemical aspects of *Leishmania infantum* nicotinamidase (*Lipnc1*), involved in the NAD⁺ biosynthetic pathway revealed its role stage specific transition and in insect stages of *Leishmania*. The *Leishmania nic* mutants manifested a decrease in NAD⁺ content, resulting in the metabolic shut down and extensive lag phase of growth *in vitro*. However, complementing the mutants with a copy of *nic* or supplementing niacin exogenously to cultures restored the phenotype. In addition, *Leishmania nic* mutants were not successful in a sustained infection in a rodent model. Further, the crystal structure of *Leishmania nic* was also solved to facilitate the design of rational inhibitors [221]. Further studies demonstrated the role of *nic* during *L. infantum* development in its natural sand fly vector, *Phlebotomus perniciosus* (Diptera, Phlebotominae) using *Leishmania nic* mutants [222]. These mutants manifested no developmental defect as compared to wild type *L. infantum* at early time points post ingestion of blood meal. However, following completion of blood meal digestion, the mutants failed to develop further and establish late-stage infections. These studies reiterate the importance of endogenous nicotinamidase for *Leishmania* development in the sand fly. Loss of infectivity in *Leishmania nic* mutants is reminiscent with earlier findings in other species like yeast and bacteria. For example, mutations in bacterial *nic* or pyrazinamidase leads to reduction in virulence [223]. Yeast *nic* helps to adapt to various stress conditions and nutrient depletion [224].

Alignment of amino acid sequence of Pb_{nic} with rodent and human *Plasmodial* species revealed that Pb_{nic} is highly conserved, possibly suggesting a conserved role across all these species. In the current study, we deleted *Pb_{nic}* by double homologous recombination and performed phenotypic characterization of *Pb_{nic}* knockout (KO) parasites throughout all the *Plasmodium* life cycle stages. While *Pb_{nic}* KO parasites did not manifest any defect in asexual blood stages, they however failed to form ookinetes and oocysts. For studying the role of Pb_{nic} beyond sexual stages, FLP/*FRT* conditional gene silencing approach was employed. Conditional silencing of *Pb_{nic}* using transgenic TRAP/FLPL parental line revealed dispensable role of Pb_{nic} in the development of salivary gland sporozoites, sporozoites infectivity and completion of liver stage development. These findings demonstrated the unique role of Pb_{nic} during *Plasmodium* transmission stages to mosquito and this informs the feasibility of developing nic inhibitors to block malaria transmission.

2.2 Materials and Methods

2.2.1 Experimental animals

Female Swiss albino (SA) mice were used for mosquito feeding and parasite production. C57BL/6J mice were used to investigate the prepatent period in the knockout parasites as compared to WT parasites. All the mice used in the study were 6-8 weeks old with approximately 25 grams weight. Male New Zealand White rabbit, aged 3-4 months was used as a source of blood meal for adult female mosquitoes to facilitate egg laying. All the animals were purchased from National Institute of Nutrition (NIN), fed with pelleted food and maintained at 24 °C with relative humidity 50-60% and 12:12 light:dark cycle. All animal experimentation was in accordance with Institutional Animal Ethical Committee (IAEC) protocols (approval no: UH/SLS/IAEC/2014-1/9b and UH/SLS/IAEC/2014-1/9c).

2.2.2 Parasite lines

Wild type *P. berghei* ANKA strain was as a parental line for all genetic manipulations. Wild type *P. berghei* ANKA GFP line [225] was used as a control in all experiments pertaining to phenotypic characterization of knockout parasites. All phenotypic characterization were done in SA mice, C57BL/6J mice and *A. stephensi* mosquitoes.

2.2.3 Bacteria

Cloning and expansion of gene targeting constructs were carried out using *E. coli* XL-1 Blue MRF cells ($\Delta(mcrA)183 \Delta(mcrCB-hsdSMR-mrr)173 \text{ endA1 supE44 thi-1 recA1 gyrA96 relA1 lac [F' proAB lacIqZ}\Delta\text{M15 Tn10 (Tetr)]}$).

2.2.4 Retrieval of *Pbnic* gene sequence, amino acid sequences, alignment and similarity analysis of *Pbnic*

Plasmodium database, Plasmodb (www.plasmodb.org) and Sanger's Gene database (<http://www.genedb.org/Homepage/Pberghei>) were used for retrieval of *Pbnic* gene, untranslated region sequences and amino acid sequence using PBANKA_121800 as a query. The gene ID of other *Plasmodium* nic orthologues were also retrieved from the same data base. Following are the gene IDs of different the orthologues: Pynic: *Plasmodium yoelii* (rodent) PY05269, Pfnic: *Plasmodium falciparum* (human) PF3D7_0320500 and Pvnic: *Plasmodium vivax* (human) PVX_095210. All these orthologue sequences were aligned by Clustal Omega tool (<http://www.ebi.ac.uk/Tools/msa/clustalo/>). Nic amino acid sequences from *Plasmodium* species were aligned with those of yeast, *E.coli*, *mycobacterium tuberculosis* and *Leishmania* to analyze conserved domains and catalytic site. Nic amino acid similarity among *Plasmodium* species was done by NCBI BLASTP tool (<https://blast.ncbi.nlm.nih.gov/Blast.cgi?PAGE=Proteins>).

Primers used for amplification of *P. berghei nic* sequences for quantitative real-time PCR (qRT-PCR), generation of knock out plasmids, conditional silencing plasmids and for integration confirmations are listed below.

S. No	Name of the primer	Primer sequence (5'-3')
1	<i>Pbnic</i> TA FP	TGACCTCGTTAAATAGCCATT
2	<i>Pbnic</i> TA RP	TCACACTATTTCGGGATATTTC
3	<i>Pb18S rRNA</i> TA FP	AAGCATTAATAAAAGCGAATACATCCTTC
4	<i>Pb18S rRNA</i> TA RP	GGAGATTGGTTTTGACGTTTATGT
5	<i>Pbnic</i> 5' FP (FP1)	AGA <u>CTCGAG</u> AGAATATCCTTCTCCTTTAT
6	<i>Pbnic</i> 5' RP (RP1)	CGT <u>ATCGAT</u> TTTCAAAATTCAGTAAATCGATA
7	<i>Pbnic</i> 3' FP (FP2)	ACA <u>GCGGCCGC</u> AGCGATGTTTCATATATACTT
8	<i>Pbnic</i> 3' RP (RP2)	ACT <u>GCGGCCGC</u> ATAATATCTCGCATAGTCCT
9	<i>Pbnic</i> 5' confirmation FP (FP3)	AATTGTGATTATTTTGGAAA
10	HSP705' UTR RP (RP3)	TTCCGCAATTTGTTGTACATA
11	DHFR FP (FP4)	GTTGTCTCTTCAATGATTCATAAATAG
12	<i>Pbnic</i> 3' confirmation RP (RP4)	AAACCTATTCAAGCATT
13	<i>Pbnic</i> ORF FP (FP5)	AACTCTAAAGATGAATTTATG
14	<i>Pbnic</i> ORF RP (RP5)	TTATGATTATTGCTAAAATGG
15	<i>Pbnic</i> cKO CDS FP (FP1)	TGA <u>AGATCT</u> AATTAATACTTTAACAGATGT
16	<i>Pbnic</i> cKO CDS RP (RP1)	ATA <u>GCGGCCGC</u> ATATGTTTATTAAAATTATGT GAGAAACATTGTTT
17	<i>Pbnic</i> cKO 3' FP (FP2)	ATA <u>GCATGCA</u> AAAATATATTGAGCGATGT
18	<i>Pbnic</i> cKO 3' RP (RP2)	TGA <u>AGATCT</u> ATGGTATAAAAACATGTATTTT
19	<i>Pbnic</i> cKO 5' confirmation FP (FP3)	GAACGAATGTATAAATGACAA
20	TRAP RP (RP3)	TATATAATTGAATAAATAACATAAAAAAGATGG CA
21	HSP70 3' UTR FP (FP4)	ATACAACAAAAAGGAGGTACA
22	<i>Pbnic</i> 3' cKO confirmation RP (RP4)	TTAATAATACCCAGAATTATA
23	Excision confirmation FP (FP5)	ACTAAGCTTTTTTAGACAG
24	Excision confirmation RP (RP5)	TTCCGCAATTTGTTGTACATA
25	<i>Pbnic</i> CDS ORF FP (FP6)	ATGAACTGCTTGGTTATAGTCGAT

Table 2: List of primers used for *Pbnic* qRT-PCR (Fig 12), generation and integration confirmation of *Pbnic* KO line (Fig 13) and *Pbnic* conditional KO line (Fig 17). (Restriction sites are in bold and underlined).

2.2.5 Total RNA isolation and cDNA synthesis

Total RNA was isolated from synchronized *P. berghei* parasites at various time points during the development. Erythrocytic stages were synchronized by injecting purified schizonts into SA mice by tail vein intravenous injection. Synchronized erythrocytic stages were confirmed by Giemsa staining and the ring stage and mixed blood stage parasites were collected into the heparinized RPMI complete medium. The infected RBCs were lysed in a 0.5% saponin solution, centrifuged at 10,000 rpm for 5 min. The saponin lysis was repeated for 2 times. The pellet was washed with 1X PBS and centrifuged at 10,000 rpm for 5 min. RNA was isolated from pelleted parasites. For RNA isolation from mosquito stages, the midguts and salivary glands were dissected from 100 *P. berghei* ANKA infected *A. stephensi* mosquitoes on day 14 and 21 respectively. Midguts and salivary glands were separately collected in an eppendorf tube maintained on ice and both the tissues were mechanically disrupted using a plastic pestle. The samples were centrifuged at 800 RPM for 3 min at 4 °C and supernatant containing partially purified sporozoites was taken for RNA isolation. For RNA isolation from liver stages, HepG2 cultures were infected with sporozoites and cells were pelleted at different time points (16 h, 25 h, 42 h, 50 h and 65 h post infection). From all these samples, RNA was extracted by Ambion pure link RNA mini kit (Cat No# 12183020). All the parasite samples were lysed by adding lysis buffer, vortexed and passed through insulin syringe 10-15 times for homogenization. To the homogenate, one volume of 70% ethanol was added and vortexed for thorough mixing. This homogenate was loaded onto the spin cartridge having silica membrane and centrifuged at 12,000g for 15 seconds. After this, 700 µL wash buffer was added and the column was centrifuged at 12,000g for 15 seconds. Flow-through was discarded, 500 µL wash buffer II was added, centrifuged at 12,000g for 15 seconds and flow-through was discarded. The wash with wash buffer II was repeated one more time. After this, the column was centrifuged at 12,000g for 2 min to dry the membrane. Then, 25-30 µL RNase free water was added to the membrane, incubated for 1 min and RNA was eluted by centrifuging at 12,000g for 2 min. RNA concentration was quantified using Nanodrop 2000 (Eppendorf) at wavelength of 260 nm using RNase free water as a blank. In order to remove DNA contamination, DNase I treatment was set up in a reaction mixture that contained 1x DNase I reaction buffer, 2µg of RNA and 1 U of DNase I in a final volume of 10 µL made up with DEPC treated nuclease free water. The reaction mixture was incubated at room temperature for 20 min. Following DNase I treatment, 1µL of 25mM EDTA was added to the mixture and DNase I was heat inactivated at 65 °C for 10 min. The DNase I treated RNA was reverse transcribed into cDNA. For cDNA synthesis, PCR was set up with 1X PCR buffer, 1 µL of dNTPs (2.5mM each), 1 µL of random hexamers,

1 μ L of RNase inhibitor, 1 μ L of MuLV reverse transcriptase (Applied biosystems) and 1-2 μ g of RNA used as template. Thermal cycling was performed in Eppendorf mastercycler PCR machine, and the cycling conditions were as follows: 25 °C for 10 min, 42 °C for 20 min, 98 °C for 30 and 5 °C for 5 min.

2.2.6 Quantitative real time PCR analysis of *Pbnic* expression across all the life cycle stages of *P. berghei*

The expression of the *Pbnic* was measured by absolute quantification method. cDNA was generated from equal concentrations of RNA derived from rings, mixed blood stages, midgut sporozoites, salivary gland sporozoites and liver stages at 16 h, 25 h, 42 h, 50 h and 65 h post infection with *Plasmodium* sporozoites. Gene specific standards were generated for *Pbnic* by amplifying 141 bp product from *P. berghei* genomic DNA and ligated into pTZ57R/T vector. Similarly, 180 bp of *Pb18S rRNA* was cloned into pTZ57R/T vector and used as an internal control. The sequences of forward primer and reverse primers used for real time gene expression analysis were listed in table 2.

The clone was confirmed for presence of insert by double digestion. Gene specific standards were generated over a range of plasmid concentrations from 10^8 to 10^2 per μ L by log dilution at each step. The cDNA samples were run alongside with gene specific standards generated within a log range from 10^2 to 10^7 per μ L. The target gene was expressed as equivalents of gene specific standards. Similarly, gene specific standards for *Pb18S rRNA* were also generated in a log range. qRT-PCR was carried out in a 10 μ L reaction containing SYBR Green PCR master Mix (Bio rad, Cat No # 1708882) and 0.25 μ M gene specific primers. qRT-PCR was performed using the EPPENDORF REALPLEX 2 qPCR machine. A ratio of transcript numbers of *Pbnic* and *Pb18S rRNA* was obtained to normalize the gene expression data.

2.2.7 Agarose gel electrophoresis

Agarose gel electrophoresis was used to resolve DNA or RNA molecules based on their size and confirmation. For standard analysis, 1% agarose gel was prepared by dissolving agarose (Lonza, Cat No# 50004) in TAE buffer (Tris base, Acetic acid and EDTA). Agarose was melted by boiling in the microwave for 2 min. Melted agarose was cooled, 2-4 μ L of ethidium bromide (0.4 μ g/ml) was added to it and solution was poured into gel tray. Immediately comb was placed in the tray to make wells in the gel and was allowed to solidify. The DNA samples was mixed 6X DNA loading dye and samples were loaded in wells. A DNA ladder used as marker in the range of 100 bp – 1kb was loaded in one of the wells (Thermo Scientific, Cat No# SM0333). The agarose gel electrophoresis was performed at 100 – 150 V for 45 – 1 h in 1X TAE running buffer. Then, agarose gel was visualized and documented using gel doc with UV illuminator.

2.2.8 Generation of *Pbnic* (PBANKA_121800) knockout construct

2.2.8.1 PCR

Double homologous recombination strategy was used to delete *Pbnic*. To achieve this, *Pbnic* targeting construct was generated using pBC-GFP-hDHFR vector. *P. berghei* genomic DNA was used as template to amplify 521bp of 5' upstream flanking region of *Pbnic* with *Pbnic* 5' forward primer (FP1) and *Pbnic* 5' reverse primer (RP1). A 578bp of 3' downstream flanking region of *Pbnic* was also amplified using *Pbnic* 3' forward primer (FP2) and *Pbnic* 3' reverse primer (RP2). PCR was set up with 1X PCR buffer, 0.25 μ M FP, 0.25 μ M RP, 1mM dNTPs each (Thermo Scientific, Cat No# R72501), 2.5 mM MgCl₂, 30-50 ng genomic DNA and 2.5 units of Taq DNA polymerase (Thermo Scientific, Cat No# 11615010). Thermal cycling was performed in Eppendorf mastercycler PCR machine, and the cycling conditions were as follows: initial denaturation at 94 °C for 2 min and 94 °C for 30 sec, annealing at 54 °C for 30 sec followed by synthesis at 72 °C for 1 min. The cycles were repeated for 35 times except initial denaturation and final extension was done at 72 °C for 10 min. Amplified products were visualized by UV illuminator after resolving on 1% agarose gel by loading 5 μ L sample and the gel image was documented. PCR amplified products were purified by DNA clean up and gel extraction kit (Fermentas, Cat No#K0831). DNA concentration was measured by Nanodrop 2000.

2.2.8.2 XL-1 Blue MRF competent cell preparation by calcium chloride treatment and transformation

XL-1 Blue MRF colony was inoculated in 5ml LB broth having tetracycline antibiotic (Sigma, Cat No# 87128) and incubated at 37 °C with 200 rpm shaking for overnight. Following day, 1% inoculum added to 20ml broth having tetracycline and incubated for 2 to 3 hour till the OD (600 nm) reached to 0.5. After this, the culture was kept on ice for 30 min, followed by centrifugation at 6000 rpm for 10 min. The supernatant was discarded and the pellet was re-suspended in 0.1 mM CaCl₂. Re-suspended cells were incubated for 1 h on ice and were pelleted by centrifuging at 6000 rpm for 10 min. Pellet was resuspended in 0.1 mM CaCl₂ for immediate transformations. For long term purposes, the pellet was resuspended in 13% glycerol in 0.1 mM CaCl₂. Approximately 50 – 100 μ L was aliquoted into 1.5 ml tubes and stored in -80 °C (pre-treated with liquid nitrogen). These competent cells were used for transformation of the ligation mixtures.

Competent cells were taken out from -80 °C and kept on ice for thawing. Approximately 5-10 μ L of ligation mixture was added to the cells and incubated for 20-25 min on ice. Then,

heat shock was given at 42 °C for 60 – 90 seconds and kept on ice for 5 min. One ml of LB broth was added to the cells and incubated for 1 h at 37 °C with shaking at 200 RPM. Following incubation, the culture was centrifuged at 4000 rpm for 5 min. The supernatant was discarded, and the pellet was re-suspended in 100 µL LB broth. Re-suspended pellet was plated on LB agar plate having appropriate antibiotics that allowed the growth of only recombinant colonies. The LB agar plates were incubated at 37 °C for overnight in an upright position.

2.2.8.3 Cloning of 5' flanking region of *Pbnic*

PCR amplified 5' flanking part was purified and concentration was measured by Nanodrop 2000. Amplified PCR product was cloned into pBC-GFP-hDHFR vector. This vector was a generous gift by Dr. Robert Menard from Pasteur Institute, France. PBC-GFP-hDHFR has two multiple cloning sites (MCS). MCS1 is located upstream to the GFP cassette (GFP ORF flanked with HSP70 promoter and 3' UTR) and MCS2 is located downstream to hDHFR cassette (hDHFR ORF flanked with EF1 α promoter and PBDHFR/TS 3' UTR). Approximately 1-2 µg of PCR product was kept for double digestion with 1 U of XhoI and 1 U of ClaI restriction enzymes (MCS1) using 3 µL fast digest buffer (Thermo scientific) and the reaction mixture was made up to 30 µL with nuclease free water. Approximately 2 µg of pBC-GFP-hDHFR plasmid was also subjected to restriction digestion for 1 h at 37 °C using same enzymes. After double digestion, both vector and inserts were purified by DNA clean up and gel extraction kit (Fermentas, Cat No#K0831) and concentration was measured by Nanodrop 2000. Ligation was set up with 1:3 vector insert ratio in 1X ligation buffer and 1 U of T4 DNA ligase (Thermo scientific) in a final volume of 20 µL made up with nuclease free water. The ligation mixture was kept at 22 °C for 3-5 hours. Nearly 10 µL ligation mixture was subsequently transformed into XL-1 Blue MRF competent cells and plated them on LB agar plate containing chloramphenicol (HIMEDIA, Cat No# CMS218) and tetracycline (Sigma, Cat No# 87128) antibiotic and incubated overnight at 37 °C. Next day, 10 colonies were inoculated in LB broth and colony PCR was performed to select the positive clones. After preliminary screening, plasmid was isolated by GeneJET Plasmid Miniprep Kit (Thermo scientific, Cat No# K0502) and the clones were confirmed for the presence of insert by double digestion with XhoI and ClaI restriction enzymes. This intermediate vector was named as 5' *Pbnic*-pBC-GFP-hDHFR.

2.2.8.4 Cloning of 3' flanking region of *Pbnic*

PCR amplified and purified 3' flanking part and 5' *Pbnic*-pBC-GFP-hDHFR intermediate vector were kept for double digestion with AscI and NotI restriction enzymes (Thermo scientific) for 1 h. After digestion, insert and vector were purified and concentration was

measured. Ligation was performed at 22 °C for 3-5 hours. Nearly 10 µL of the ligation mixture was used for transforming XL-1 Blue MRF competent cells and positive clones were preliminarily confirmed by colony PCR and reconfirmed by double digestion with AscI and NotI restriction enzymes. Sequencing was done for both 5' and 3' inserts that were cloned into the pBC-GFP-hDHFR vector resulting in *Pbnic* knockout construct. This construct was purified in large scale by Sureprep plasmid MAXI kit (Genetix, Cat No# NP-15162).

2.2.9 Release of *Pbnic* targeting cassette from knockout vector by double restriction digestion

The plasmid was subjected to restriction digestion with XhoI and AscI enzymes to release targeting cassette containing GFP-hDHFR flanked on either ends with 5' and 3' flanking regions of *Pbnic*. The restriction digestion products were resolved in 1% agarose gel and the targeting cassette was extracted by DNA clean up and gel extraction kit (Fermentas, Cat No#K0831) and concentration was measured with Nanodrop 2000. The purified targeting cassette was for electroporation of WT *P. berghei* schizonts to target the *Pbnic* locus as using protocol described in following sections.

2.2.10 Propagation of *P. berghei* ANKA WT line in SA mice and Giemsa staining of blood stage parasites

The *P. berghei* ANKA WT parasites were freshly thawed and injected intraperitoneally into SA one mouse. The parasitemia was monitored by making blood smears from caudal vein puncture. The smear was air dried and fixed by immersing slide in methanol for 5-10 sec. After methanol was evaporated, Giemsa stain [(Sigma, Cat No# GS1L) diluted by 5 times with distilled water] was poured over the smear and stained for 10 min. The slide was gently washed under running tap water and air dried. One drop of immersion oil was put on stained smear and slide was observed under light microscope with 100X objective lens (Nikon). Different parasite stages were observed and were identified in infected RBC based on their morphology. For measuring parasitemia, uniform thin fields were selected which were having approximately 300 RBC. Nearly 25 fields were analysed and parasitemia was calculated as a percent of RBCs infected.

2.2.11 *In vitro* culture of *P. berghei* ANKA asexual stages

In vitro culture of *P. berghei* ANKA asexual stages, purification of schizonts, transfection of purified schizonts and drug selection of recombinant parasites were performed as described earlier [2]. SA mice were intraperitoneally injected with cryopreserved *P. berghei* ANKA parasites.

When parasitemia reached to 2-3 %, blood was collected and passaged into 5 donor mice (10^6 – 10^7 parasites/mouse). When parasitemia reached 3-5 % in donor mice, mice were anesthetized by 200 μ L of xylazine/ketamine mix (prepared by mixing 300 μ L of Xylazine, 800 μ L of ketamine and making up the final volume to 5 ml with PBS). Blood was collected by cardiac puncture with heparinized capillary tubes into 50 ml falcon tube containing 250 U of 1X heparin (anticoagulant). Collected blood was used for culturing of schizonts in schizont media. Schizont media was prepared by mixing RPMI (Lonza BioWhittaker, Cat No# 12-115F), 10% Fetal Bovine Serum (Hyclone, Cat No# SH30071.03) and gentamycin (3.5 ml for 500 ml of media) (Sigma, Cat No# G1397) and sterilized by filtration. To the blood, 10 ml of schizont media was added and centrifuged at 200 g in swinging bucket rotor for 8 min with 9 acceleration, 0 deceleration (Eppendorf 5810R). After the spin, the supernatant was discarded, the pellet was resuspended in 2 ml of schizont media and gently distributed into 3 T75 flasks containing 20 ml of schizont media. These T75 cultures were gassed with a mixture gas composed of 5% O₂, 5% CO₂ and 90% N₂ for nearly 3 min. The culture flasks were subsequently (T75 closed caps flasks, Nunc, Cat No# 156472) incubated at 36.5 °C for 16 – 18 hours with gentle shaking of approximately 40 rpm. Following day morning, 100 μ L blood was taken, centrifuged at maximum speed for 5 sec, the supernatant was discarded and the pellet was used to make smears. The smears were stained with Giemsa to observe the maturation status and frequency of schizonts. The schematic outline of the transfection protocol is shown in Fig 8B.

2.2.12 Purification of schizonts

After confirming the presence of schizonts in culture, they were purified by Nycodenz density gradient. Nycodenz was prepared by mixing 27.6 g Histodenz (Sigma, Cat No# D2158), 3 mM KCl, 5 mM Tris-HCl, 0.3 mM EDTA and final volume made up to 100 ml with sterile water. This solution was autoclaved and stored in 4 °C. Before using for purification, 60% Nycodenz was prepared in 1X PBS and warmed at 37 °C for 15 min. In a 50 ml tube, 25 ml of schizont culture was taken and 10 ml of 60% Nycodenz was added to the culture slowly at the bottom. The culture layered over the Nycodenz with clear differentiation between both the solutions. Culture with Nycodenz was centrifuged at 380 g for 20 min with acceleration 9 and no deceleration using swinging bucket rotor. Clear separation of schizonts was observed at the interface between media and pellet. Schizonts were collected with a capillary tube (Fig 8 C). Purified schizonts were washed with 10 ml of schizont culture media for 2 times by centrifuging at 1500 rpm for 8 min with acceleration 9 and no deceleration using swinging bucket rotor. These purified schizonts were used for electroporation.

2.2.13 Electroporation of *Pbnic* knockout construct into schizonts

Electroporation of *Pbnic* knockout construct was done using the Amaxa nucleofector kit (Lonza). For electroporation, 90 μ L of mouse T cell nucleofector solution was mixed with 20 μ L of supplement to prepare nucleofector solution. The nucleofector solution was mixed with 10 μ g of purified *Pbnic* knockout construct. This mixture was then added to the pelleted $\sim 5 \times 10^7$ schizonts and gently transferred into nucleofector cuvette and placed in Amaxa nucleofector device. Electroporation was done using U033 program (Fig 8 F). Following electroporation, 100 μ L of schizont culture media was added immediately into the cuvette and the contents were immediately injected intravenously into mice (Fig 8 G).

2.2.14 Drug selection of transfected parasites

Twenty four hours post transfection, caudal blood smears were made from mice and were Giemsa stained. Following confirmation of parasites, the mice were given an orally administration of pyrimethamine, that was prepared by dissolving 7 mg drug in 1ml of DMSO and made up to 100 ml in sterile water following adjustment to pH 4.0. After 5-7 days, the non-transfected parasites were cleared and drug resistant population emerged gradually.

2.2.15 Observation of GFP parasites in the infected blood

When parasitemia reached around 3-5%, approximately 5-10 μ L of blood was collected from mouse tail by caudal vein puncture and placed in a 1.5 ml eppendorf tube containing 2 U of heparin. Blood was pelleted, washed twice with 1X PBS. Pellet was resuspended in 200 μ L of 1X PBS containing 0.2 μ L of 1000X DAPI (4', 6' diamidino-2 phenyl indole, Sigma, Cat No# 9542, prepared by dissolving 1 mg of DAPI in 1ml of sterile water) and incubated for 1h at 37° C. Following incubation, cells were pelleted by centrifugation at 5000 rpm, washed with 1X PBS and resuspended in 10 μ L of 1X PBS. From this solution, 3 μ L was placed on a clean glass slide, and covered with cover slip. Cover slip was sealed with nail polish and slide was observed for GFP fluorescence under an upright fluorescent microscope (Nikon Eclipse).

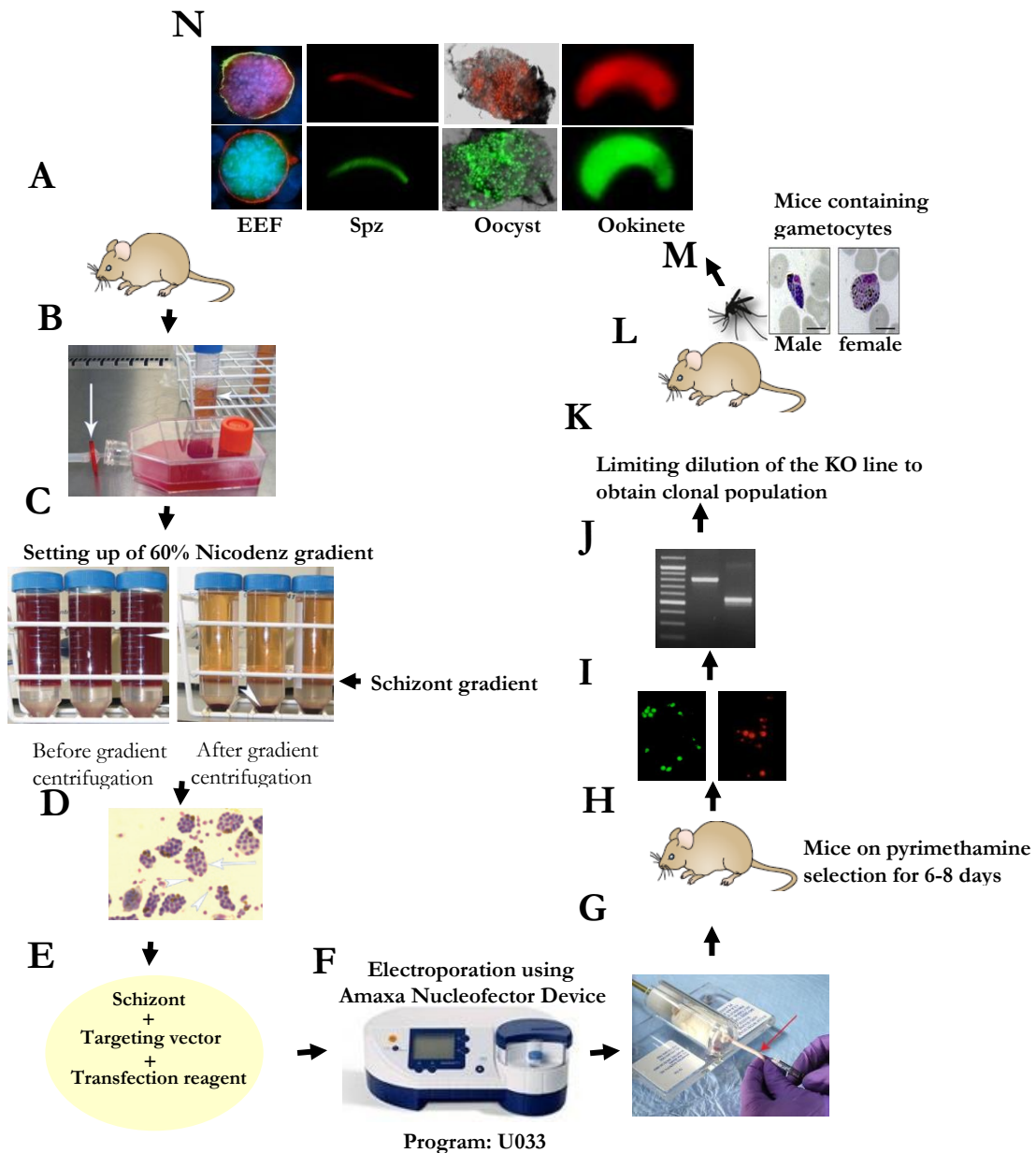


Fig 8: Schematic representation of *P. berghei* transfection, drug selection, confirmation of target construct site specific integration and phenotypic characterization of transgenic parasites. **A)** *P. berghei* parasites were injected into mice. When parasitemia reached to 3-5%, blood was collected and **B)** schizont culture was kept overnight. **C)** Following day, schizonts were enriched by 60% Nycodenz density gradient centrifugation. **D)** Purified schizonts confirmed by Giemsa staining. **E)** To the purified schizonts, targeting construct and transfection reagent were mixed, **F)** electroporated using Amaxa electroporator and **G)** medium was added to it and immediately injected by intravenous route to Swiss albino mouse. **H)** The mice were subjected to pyrimethamine drug administered orally in drinking water. **I)** Following 7 days of stringent drug selection, the parasites were analysed for GFP/mCherry fluorescence. **J)** Genomic DNA was isolated from drug resistant parasites and correct integration was confirmed by integration PCR. **K)** Limiting dilution was done to isolate single clonal population and to eliminate drug resistant wild type and non transfectants. **L)** These clones were used for phenotypic characterization; **M)** asexual blood stage propagation in the mouse, **N)** ookinete, oocyst and salivary gland sporozoite stages in the mosquito and liver stages the vertebrate host. (Images adapted and modified from [2])

2.2.16 Cryopreservation of the *P. berghei* blood stage parasites

After confirming the presence of GFP parasites in the blood, infected blood was collected in freezing medium containing 250 U of heparin. The freezing medium was composed of 9 parts Alsever's solution (Sigma, Cat no# A3551) and 1 part glycerol (Invitrogen, Cat No# 15514011). One part blood and 2 parts freezing media were mixed gently and nearly 250-300 μ L was aliquoted into cryo vials (Corning, Cat No# CLS430658) and stored at -80°C in a freezing container (Nalgene, Cat# 5100) which cools gradually at 1°C per 1 min and the samples were shifted to liquid nitrogen after 24 h for long term preservation.

2.2.17 Confirming the stable integration of *Pbnic* knockout construct in endogenous locus

The infected RBCs were lysed in 0.5% saponin solution, centrifuged at 10,000 rpm for 5 min. The saponin lysis was repeated for 2 times. The pellet was washed with 1X PBS and centrifuged at 10,000 rpm for 5 min. Genomic DNA was isolated from pelleted parasites by using the DNASure tissue mini kit (Genetix, Cat No# NP-61305). The integration of *Pbnic* knockout construct into endogenous locus was confirmed by integration specific PCRs. For 5' integration confirmation, FP3 primer was designed beyond the site of integration and RP3 primer was designed within GFP cassette. For 3' integration confirmation, FP4 primer was designed in hDHFR cassette and RP4 primer was designed from genomic sequence after the site of integration.

2.2.18 Clonal dilution of *Pbnic* knockout parasites

Following confirmation of correct integration by PCR as described in above section, limiting dilution was done to isolate single clones of the *Pbnic* knockout parasites. To obtain the single clone, blood was collected from mice and its precise parasitemia was determined. A small volume of blood was collected and was diluted at 1:10,000 and the number of RBCs were counted using hemocytometer. Twenty mice were intravenously injected with approximately with 1 or less than one parasites/mouse. After 7-9 days, nearly 2-3 mice became positive for infection out of 20 mice used for intravenous injections. To confirm if the clonal population of parasites were derived from a single parasite, genomic DNA was isolated from two clones selected from two independent transfections. A diagnostic PCR was set up with genomic DNA using FP5 and RP5 that amplified 510 bp PCR product from wild type genomic DNA whereas no amplification was observed in *Pbnic* knockout clone out lines. This PCR confirmed that *Pbnic* ORF was replaced with the GFP-hDHFR cassette in both KO lines.

2.2.19 Phenotypic analysis of *Pbnic* knockout (KO) parasites in blood stages

Since *Pbnic* KO parasites were generated as GFP line, as an appropriate control, we obtained a WT *P. berghei* ANKA GFP line by targeting the non-essential *p230P* locus by by disrupting the gene by integration of GFP-hDHFR cassette [225]. This line was designated as WT GFP. Nearly 1×10^3 mixed blood stage parasites of both WT GFP or *Pbnic* KO parasites were injected into 4-6 week old SA mice by intravenous route. Parasitemia was monitored daily to assess the asexual growth kinetics of the *Pbnic* KO parasites by making Giemsa stained blood smears. Parasitemia was determined by checking 25 random fields under light microscope.

2.2.20 Breeding of *A. stephensii* mosquitoes

To study the transmission and development of the parasite in the mosquito, the *A. stephensii* mosquitoes were reared and a colony was maintained. In brief, freshly emerged 1 week old male and female *Anopheles* mosquitoes were kept in a mosquito cage to facilitate mating (Fig 9 A). Mosquitoes were starved for 4 h and subsequently were allowed to obtain a blood meal from anesthetized rabbit. The rabbit was sedated by intramuscularly injection of 0.5 ml of ketamine (50 mg/ml) and 0.25 ml of xylazine (20 mg/ml). The blood feeding was done for two successive days (Fig 9 B). On day 3-4 post blood feeding, a water bowl was placed inside the cage for egg laying. The eggs were collected daily for 4 days and shifted to mosquito breeding chamber that was maintained at 27 °C with relative humidity of 70-80%. In this chamber, the eggs hatched into larvae. The larvae were transferred to plastic trays having 2 L water. Larvae were fed on powdered food prepared with Kellogg's special K low fat cereal and wheat germ (Avees) in the composition of 60:40 ratio. After 5-7 days, the larvae transformed into pupae (Fig 9 D). Pupae were manually picked and kept in a mosquito cage for emergence of adult mosquitoes. The adult mosquitoes emerged within 24-48 h. These were fed on 10% sucrose solution (provided as soaked in cotton balls) and dry raisins (soaked for 3-4 hours in water).

2.2.21 Transmission of *Pbnic* KO parasites to *A. stephensii* to study mosquito stages of the parasite

A cage of 250-300 female *A. stephensii* mosquitoes were prepared for transmission of malaria. Approximately 10^6 iRBCs of either WT GFP or *Pbnic* KO parasites were injected into SA mice that were nearly 6 weeks old. Following confirmation of gametocytes in these mice, the *A. stephensii* mosquitoes were allowed to obtain blood meal for 15 min (Fig 9 E). During this process, the position of the mice was moved for every 4-5 minutes to ensure that a maximum number of mosquitoes obtained blood meal from more than one mice. The same procedure was

repeated on the second day. Following 2 feedings, the mosquitoes were maintained at 20 °C temperature and 80% humidity for 21 days (Fig 9 F). After 24 h of post blood feeding, midguts were dissected, crushed and smear was done. Giemsa stained smears were observed for ookinetes under light microscope with 100X objective lens (Nikon).

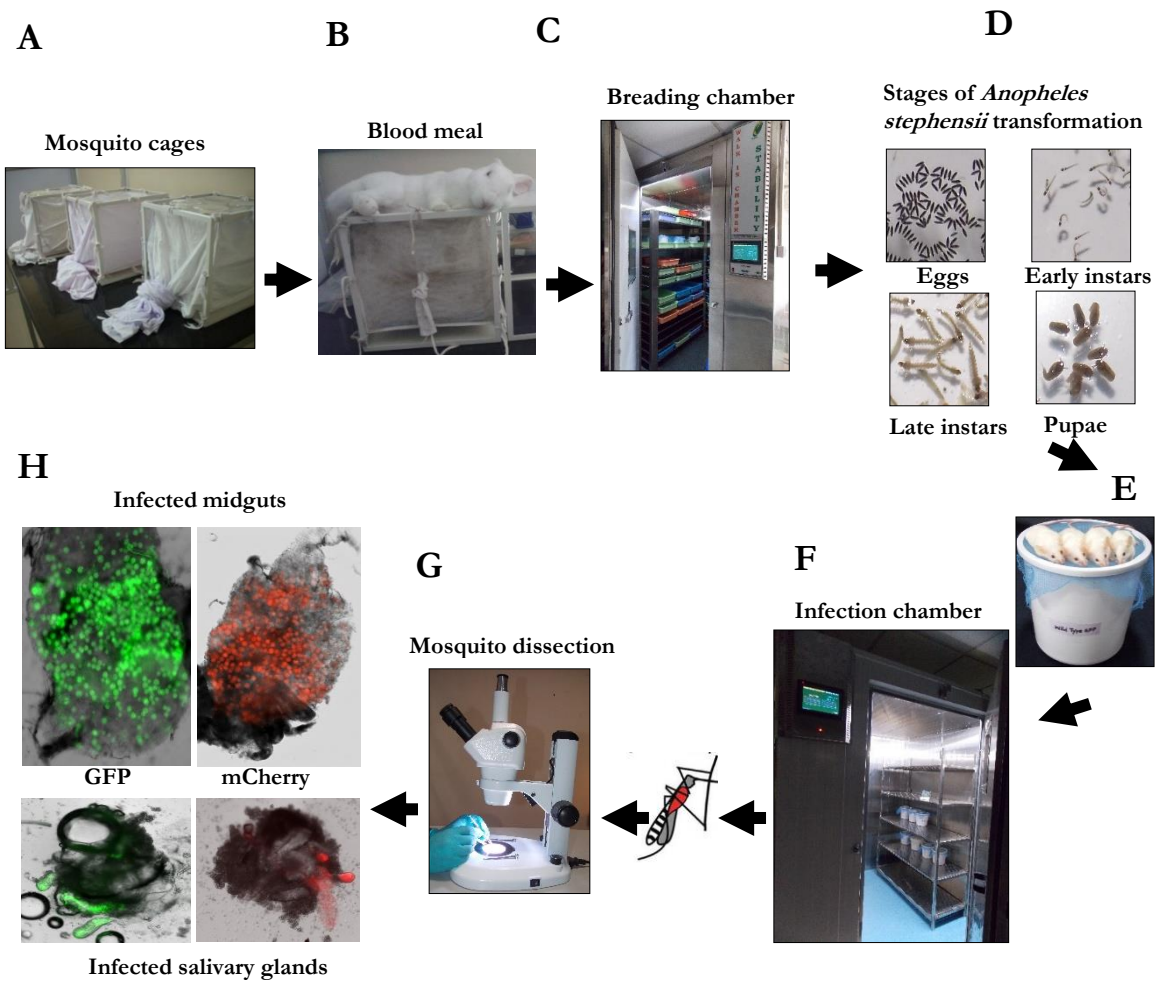


Fig 9: Breeding of *Anopheles stephensi* mosquitoes and transmission of *P. berghei* parasites to the mosquitoes to study the ookinete, oocyst and salivary gland sporozoite stages. **A)** Emerged male and female mosquitoes were kept in breeding cage. **B)** Anesthetized rabbit blood meal was given to mosquitoes for 20 min with 24 h interval for 2 successive days. **C)** Following day, water bowl was kept in the cage in which mosquitoes laid eggs. Next day, eggs were shifted to mosquito transformation chamber maintained at 28 °C with 80% relative humidity. **D)** Eggs hatch into larvae, then larvae further develop into pupae. **E)** Pupae were manually collected, kept in a mosquito cage and within 24 h, pupae emerged into mosquitoes. Female mosquitoes were collected with the help of vacuum pump and allowed to feed on mice harboring gametocytes in the blood circulation. **F)** These blood fed mosquitoes were shifted to infected mosquito chamber maintained at 20 °C with 80% relative humidity for 20 days. **G)** Mosquitoes were dissected at day 14 for midgut oocysts and at day 18 post blood meal for salivary gland sporozoites under dissection microscope. **H)** Dissected midgut oocysts and salivary glands were visualized under fluorescence microscope for oocyst numbers, sporulation pattern and salivary gland sporozoite load respectively. (Images adapted and modified from the thesis of Dr. Surendra Kumar Kolli).

On D14 post blood feeding, midguts were dissected and the oocyst infectivity was observed under a fluorescence microscope. On D18 post infection, the salivary glands of mosquitoes were dissected and were observed for sporozoite loads (Fig 9 H). Both midguts and salivary glands were mechanically disrupted in an eppendorf tube with a plastic pestle and centrifuged at 800 RPM for 3 min at 4 °C and supernatant containing partially purified sporozoites were collected. Sporozoite numbers were counted using hemocytometer. The oocyst and salivary gland sporozoites were observed under an upright fluorescent microscope (Nikon Eclipse). The images were captured, processed and deconvoluted by NIS software.

2.2.22 Genetic crosses to investigate the effect of *Pbnc* depletion on gamete formation

Sexual development in *Plasmodium* is an elaborate process that involves many events like male and female gamete formation from respective male and female gametocytes in the mosquito gut. Followed by this, there is a fusion of gametes to form zygote, which differentiates into motile ookinete that breaches midgut epithelium and develops into oocyst. In order to investigate the precise defect associated with the sexual reproduction, genetic cross experiments were performed that allowed investigation of the *Pbnc* KO parasites to generate functional gametes. Towards this end, the asexual blood stages of *Pbnc* KO line and *P. berghei* ANKA mCherry line (WT *Pb* mCh) were mixed in equal proportions and these mixed lines were propagated in SA mice. Following the confirmation of gametocytes from all the mice harboring mixed lines, the malaria was transmitted to mosquitoes. Midguts were dissected at D14 post blood meal and analysed for oocyst development. The principle behind the genetic cross experiments is as follows: if either male or female gamete is functional in *Pbnc* KO, it will fertilise respectively with the female and the male gamete of WT *PbmCh* resulting in oocysts that will express both mCherry and GFP. As an appropriate control, WT *Pb* GFP and WT *Pb* mCh lines were crossed.

2.2.23 Generation of *Pbnc* conditional KO parasites

If the target gene is essential for parasite development during sexual stage development, it may limit the possibility to study the function of the gene at oocyst stage salivary gland sporozoite stage and during the development of sporozoite in the liver. To address this issue, a conditional knockout strategy was used to study the role of *Pbnc* beyond sexual stages. Towards construction of a conditional targeting construct, a 509 bp *Pbnc* CDS part preceding the stop codon was PCR amplified with *Pbnc* CDS FP1 and *Pbnc* CDS RP1 and cloned in the TRAP-GFP-hDHFR vector using SphI and NotI restriction enzymes. The vector was further modified by cloning a 532 bp 3' region after stop codon that was amplified using primers- *Pbnc* 3' UTR

FP2 and RP2 and cloned with KpnI and EcoRI restriction enzymes. The targeting vector was digested with SphI and EcoRI and the integration cassette consisting of the following genetic elements: *PbniC* CDS part, 1st FRT site, 3' UTR of TRAP, hDHFR, 2nd FRT site, GFP and *PbniC* 3' UTR was released and gel purified. The concentration of the purified *PbniC* conditional KO was determined by Nanodrop 2000. Gel purified targeting cassette was electroporated into purified schizonts using Amaxa nucleofector device with U033 program. The conditional construct was electroporated on a TRAP/FLPL parental line where FLPL (a thermolabile variant of FLP) expression is driven by TRAP promoter that is active in the oocyst stages. Drug selection was done as described earlier. Genomic DNA was isolated from drug resistant parasites and successful integration of cassette was confirmed by site specific integration PCRs. For CDS part integration, PCR was done with a set of primers- *PbniC* cKO FP3 designed beyond the site of integration and RP3 within the 3' UTR of TRAP that amplified 964 bp product from transfected parasites. For 3' part integration, PCR was done with a set of primers- *PbniC* cKO FP4 and *PbniC* cKO RP4 that were designed respectively within the GFP cassette and after the site of integration that amplified 732 bp product. Limiting dilution was done to isolate single clones of the *PbniC* conditional knockout parasites. Two clones were selected from two independent transfections. In these clones, replacement of 3' UTR of *PbniC* with 3' UTR of TRAP was confirmed by diagnostic PCR with primers *PbniC* cKO FP5 within the *PbniC* CDS and *PbniC* cKO RP3 in 3' UTR of TRAP.

2.2.24 Transmission of *PbniC* conditional KO (cKO) parasites to *A. stephensi* to achieve inactivation of *PbniC* in mosquito stages

Approximately 10⁶ iRBCs of either WT GFP or *PbniC* cKO parasites were injected into 6-8 weeks old SA mice. Following confirmation of gametocytes in these mice, the *A. stephensi* mosquitoes were allowed to obtain blood meal for 15 min as described earlier in 2.2.19. Following 2 feedings, the mosquitoes were maintained at 20 °C temperature and 80% humidity for 16 days then shifted to 25 °C with 80% humidity where FLPL activity is optimum. Mosquitoes were maintained for 7 days at 25° C. TRAP promoter is active from oocyst stages and expresses FLPL that excises the DNA flanked by FRT sites (Fig 10). On D14 post blood feeding, midguts were dissected and the oocyst infectivity was observed under a fluorescence microscope. On D18 post infection, the salivary glands of mosquitoes were dissected and were observed for sporozoite loads (Fig 9 H). Both midguts and salivary glands were mechanically disrupted with a plastic pestle, centrifuged at 800 RPM for 3 min at 4 °C and supernatant containing partially purified sporozoites was collected. Sporozoite numbers were counted using

hemocytometer. Oocysts, salivary glands and sporozoites were observed under an upright fluorescent microscope (Nikon Eclipse). The images were captured, processed and deconvoluted by NIS software.

Excision was confirmed in midgut sporozoites at day 14 and in salivary gland sporozoites at day 21 post blood meal with the help of excision specific PCRs. For excision confirmation, two different sets of primers were used, one set was *Pbnic* cKO FP5 present in *Pbnic* CDS and RP5 present in GFP cassette and the PCR amplicon length encompassed the DNA sequence from CDS till GFP cassette. Another set of primers- *Pbnic* cKO FP5 and RP3 that informs about presence or absence of TRAP 3' UTR in tandem to *Pbnic* CDS.

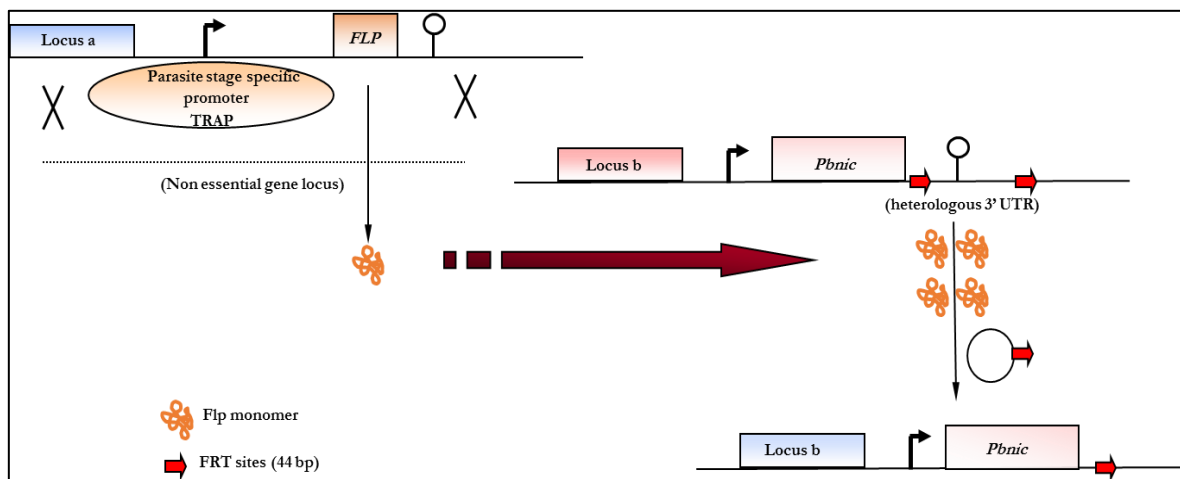


Fig 10: Schematic showing conditional silencing of *Pbnic* using yeast FLP/*FRT* system.

TRAP/FLPL transgenic line was generated by integrating the ORF of FLP recombinase under oocyst stage specific promoter TRAP by stable integration into non-essential gene locus. For conditional silencing of *Pbnic*, PCR amplified 509 bp *Pbnic* CDS part preceding the stop codon and another 532 bp 3' region after stop codon of the *Pbnic* and cloned respectively at SphI/NotI and KpnI/EcoRI in the TRAP-GFP-hDHFR vector. The targeting vector was linearized with SphI and EcoRI. Targeting cassette was gel purified and electroporated into purified schizonts of TRAP/FLPL parental line where FLPL (a thermolabile variant of FLP) expression is driven by TRAP promoter that is active in the oocyst stages. After successful double homologous recombination, integration of 3' TRAP UTR–GFP-hDHFR by replacing 3'UTR of *Pbnic* ensured the stabilization of *Pbnic* transcript at blood stages. When these parasites were transmitted to mosquito, TRAP promoter drives the expression of FLP that excised a FRTed DNA sequence i.e 3' UTR of *Pbnic* in the oocyst stages was confirmed by diagnostic PCR from gDNA of D17 oocyst. From this oocyst stage, even though transcript is made from *Pbnic* gene, that transcript won't be stabilized due to lack of functional 3'UTR, thus resulting in the failure of translation (protein synthesis).

2.2.25 *In vitro* infectivity of *Pbnic* cKO salivary gland sporozoites

A 24 well plate (Nunc, Cat No# 142475) was coated with 1X collagen (Sigma, Cat No# C3867-1VL) over night and on following day, 2×10^5 cells were seeded and maintained in complete DMEM (cDMEM) at 37 °C in a CO₂ incubator. After confirming the establishment of a monolayer of HepG2 cells under phase contrast microscope, approximately 2×10^4 sporozoites of WT GFP or *Pbnic* cKO sporozoites were added to cultures and the plate was centrifuged at 1500 rpm for 4 min. The culture medium was changed after 3 h and to avoid contamination, the medium was subsequently replenished every 8 h till 65 h time point with complete DMEM containing 2X antibiotic and antimycotic medium (Gibco, Cat No# 15240062). At 12 h, 36 h and 62 h cover slips were removed, fixed in 4% formalin solution (Sigma, Cat No# HT5011) and stored in 4 °C till it was taken for immunofluorescence assay.

2.2.26 Immunostaining for assessing EEF development of *Pbnic* cKO.

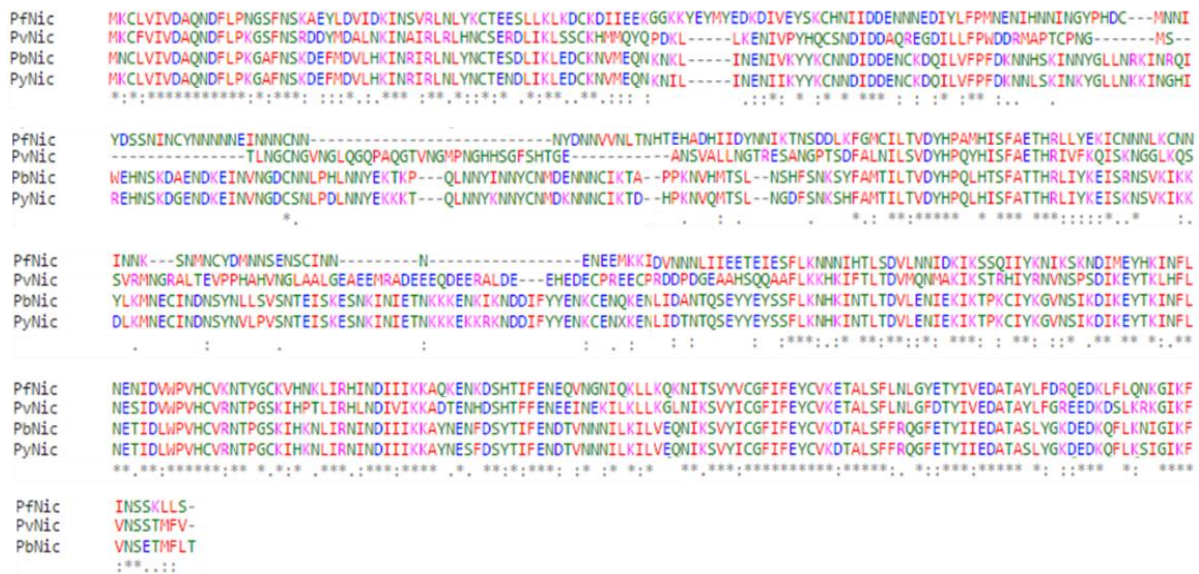
Formalin solution was removed from the wells, followed by permeabilisation with pre chilled (1:3) Acetone Methanol for 20 min. The fixative was removed and wells were gently washed with 1X TBS. Nonspecific blocking was done with 3% BSA in 1X TBS for 1 h at 37 °C. Following blocking, cells were gently washed with 1X TBS and cells were incubated with primary antibody, rabbit anti UIS4 (stains PVM, 1:500 dilution) diluted in 1% BSA. After primary antibody treatment, cells were washed with TBS, TBST (0.1% of tween 20 in 1X TBS) and TBS, with each wash for 30 min. Cells were incubated for 1h at 37 °C with secondary antibody, anti rabbit Alexa flour 594 (Thermo scientific, Cat No# A-11037) diluted in 1% BSA along with DAPI (used in 1:1000 dilution). After this incubation, the cells were washed with TBS, TBST and TBS. Coverslips were taken out from 24 well plate, allowed for air drying and mounted with ProLong gold antifade mountant (Thermo scientific, Cat No# P36930). The borders of cover slip were sealed with nail polish (inhibits the desiccation and contraction of mounting media because of impermeability to water and air), air dried and stored in dark. Mounted slides were observed for EEF growth under an upright fluorescent microscope (Nikon Eclipse). The images were captured, processed and deconvoluted by NIS elements software.

2.3 Results

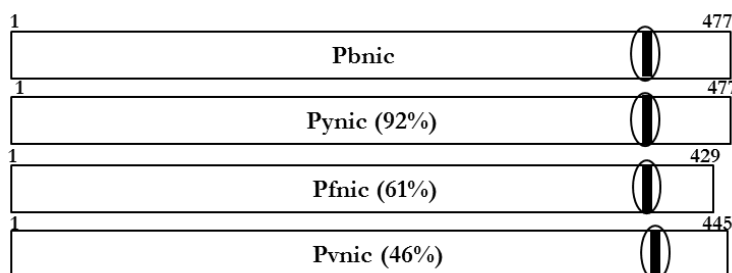
2.3.1 Pbnic is conserved among all the *Plasmodium* species

Protein sequence alignment of Pbnic (PBANKA_121800) with its orthologues from another rodent species- *P. yoelii* (PY05269) showed 92% similarity where as it showed respectively 61% and 46% similarity with human parasites *P. falciparum* (PF3D7_0320500) and *P. vivax* (PVX_095210) (Fig 11 A and B). Nicotinamidase belongs cysteine – hydrolases superfamily and all the *Plasmodium* orthologues have a conserved Cys – peptide bond at C-terminus (Fig 11 B). Multiple sequence alignment of Nic from different species like yeast, *E.coli*, *Mycobacterium tuberculosis* and *Leishmania* revealed that the catalytic triad (D, K, C) is highly conserved (Fig 11 C).

A



B



Conserved cys – peptide bond (cysteine – hydrolases super family)

C

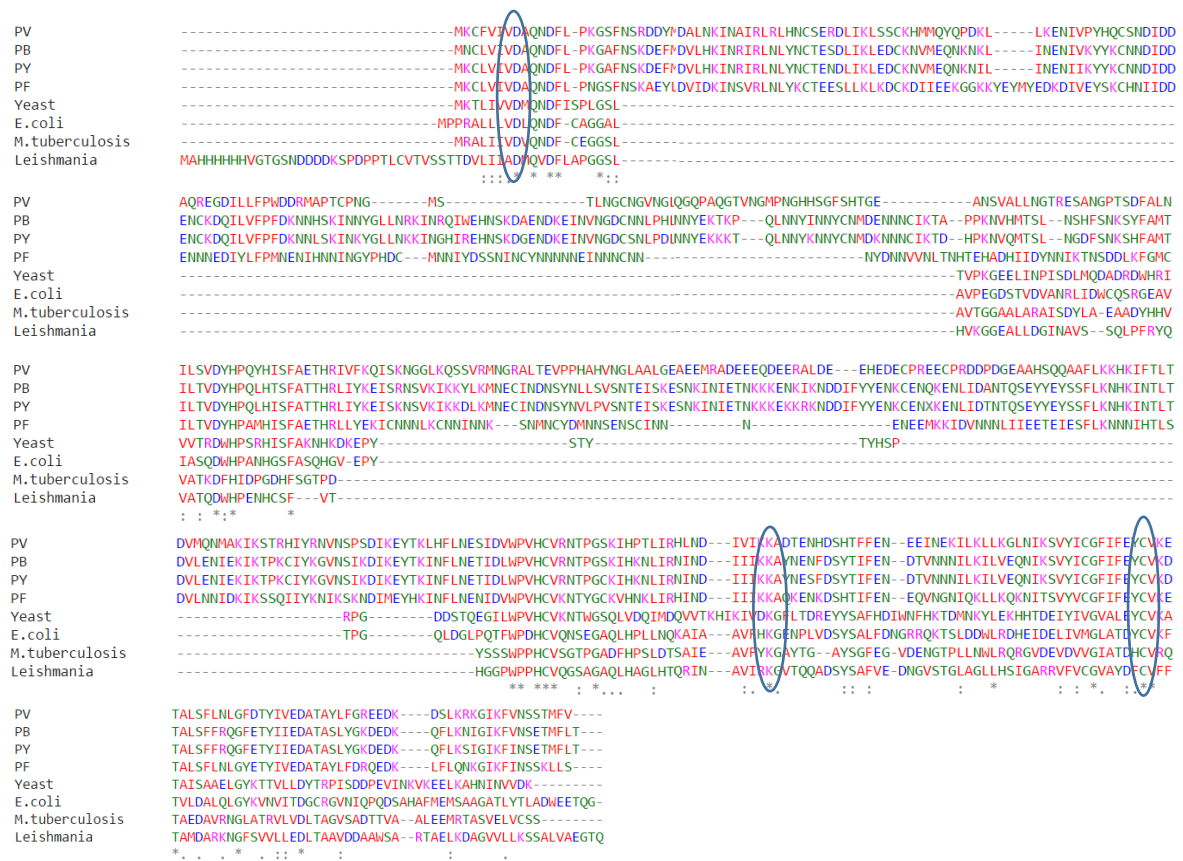


Fig 11: A) Multiple sequence alignment of nic amino acid sequence from different *Plasmodium* species. **B)** Conservation of Pbnic protein among *Plasmodium* species. The predicted conserved cys-peptide bond (shown in black color), conserved amino acid identities were shown in *Plasmodium* orthologues as percentage in comparison with Pbnic: *Plasmodium berghei* (rodent) (PBANKA_121800) to Pynic: *Plasmodium yoelii* (rodent) (PY05269), Pfnic: *Plasmodium falciparum* (human) (PF3D7_0320500) and Pvnic: *Plasmodium vivax* (human) (PVX_095210). **C)** Multiple sequence alignment of nic from *Plasmodium*, yeast, *E. coli*, *Mycobacterium tuberculosis* and *Leishmania* showing conserved catalytic triad (D, K, C).

2.3.2 *Pbnic* is expressed in in all the life cycle stages of *Plasmodium*

Gene expression analysis of *Pbnic* across all the parasite stages as measured following normalization with *Pb18S rRNA* revealed that *Pbnic* is expressed at all the life cycle stages with maximal expression in ring and midgut sporozoite stages (Fig 12).

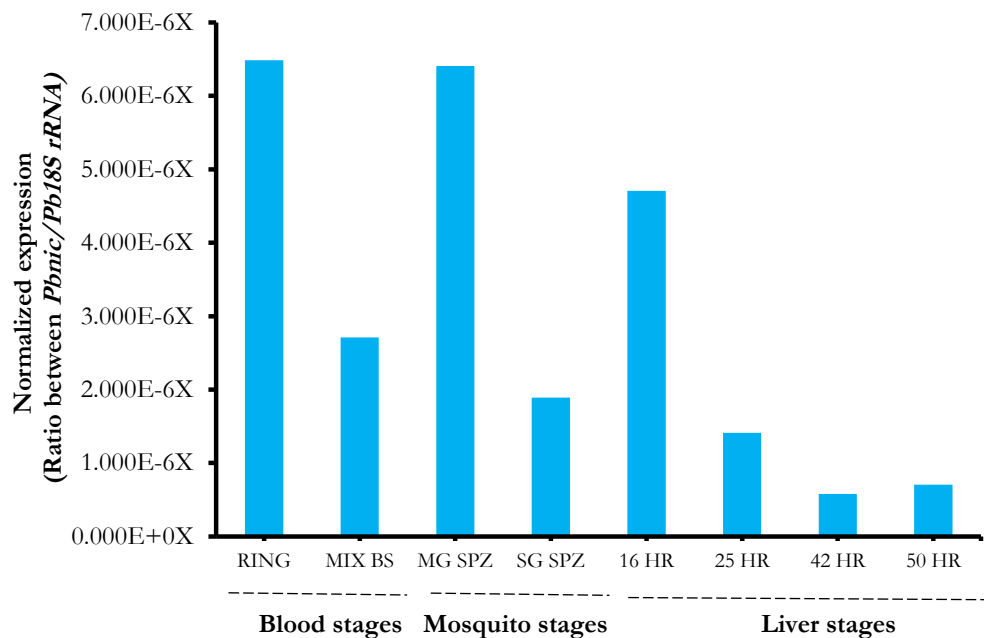


Fig 12: Quantitative real time PCR analysis of *Pbnic* across all *Plasmodium* life cycle stages. Analysis of *Pbnic* gene expression by qRT-PCR revealed maximum expression in the ring stages followed by midgut sporozoites. *Pbnic* absolute transcript numbers were normalized to *Pb18S rRNA* (internal control gene) absolute copy numbers and expressed as a ratio for each of the stage. **Blood stages:** RS; rings, AS; asexual mixed blood stages. **Mosquito stages:** MG SPZ; midgut sporozoites (14 days post infection to mosquitoes), SG SPZ; salivary gland sporozoites (18 days post infection). **Liver stages:** 16 h, 25 h, 42 h and 50 h of liver stages.

2.3.3 Successful deletion of *Pbnic* locus with GFP-hDHFR cassette by double homologous recombination

The genomic organization of *Pbnic* gene locus is shown in Fig 13 A. The targeting construct carrying the 5' and 3' parts of the *Pbnic* cloned on either ends of GFP-hDHFR cassette is shown in Fig 13 B. Following successful recombination, the endogenous *Pbnic* was deleted resulting in the recombined locus as shown in Fig 13 C. Fig 13 D shows the PCR amplified products of 5' and 3' flanking regions of *Pbnic*. Fig 13 E shows the release of the targeting cassette from vector back bone using restriction enzymes Xho1 and Asc1. The adjacent lanes show the release of the respective of 5' and 3' fragments following restriction digestion with Xho1/Cla1 and Not1/Asc1. A diagnostic PCR was set up to confirm correct site specific integration using genomic DNA obtained from drug resistant parasites from two independent transfections. In Fig 13 F, an expected product size of 695 bp with primer set FP3 and RP3 in clones C1 and C2 indicated correct integration of the GFP-hDHFR cassette at the 5' end of *Pbnic*. Also, an expected product size of 732 bp with primer set FP4 and RP4 in clones C1 and C2 indicated correct integration of the GFP-hDHFR cassette at the 3' end of *Pbnic*. Genomic DNA of both clones C1 and C2 did not amplify a PCR product with primer set FP5 and RP5 while WT genomic DNA amplified a PCR product of 510 bp confirming the complete absence of WT parasites in clonal populations, C1 and C2 as shown in Fig 13 G. Consistent with the correct integration of the GFP-hDHFR cassette, both clones expressed GFP constitutively, as shown Fig 13 H.

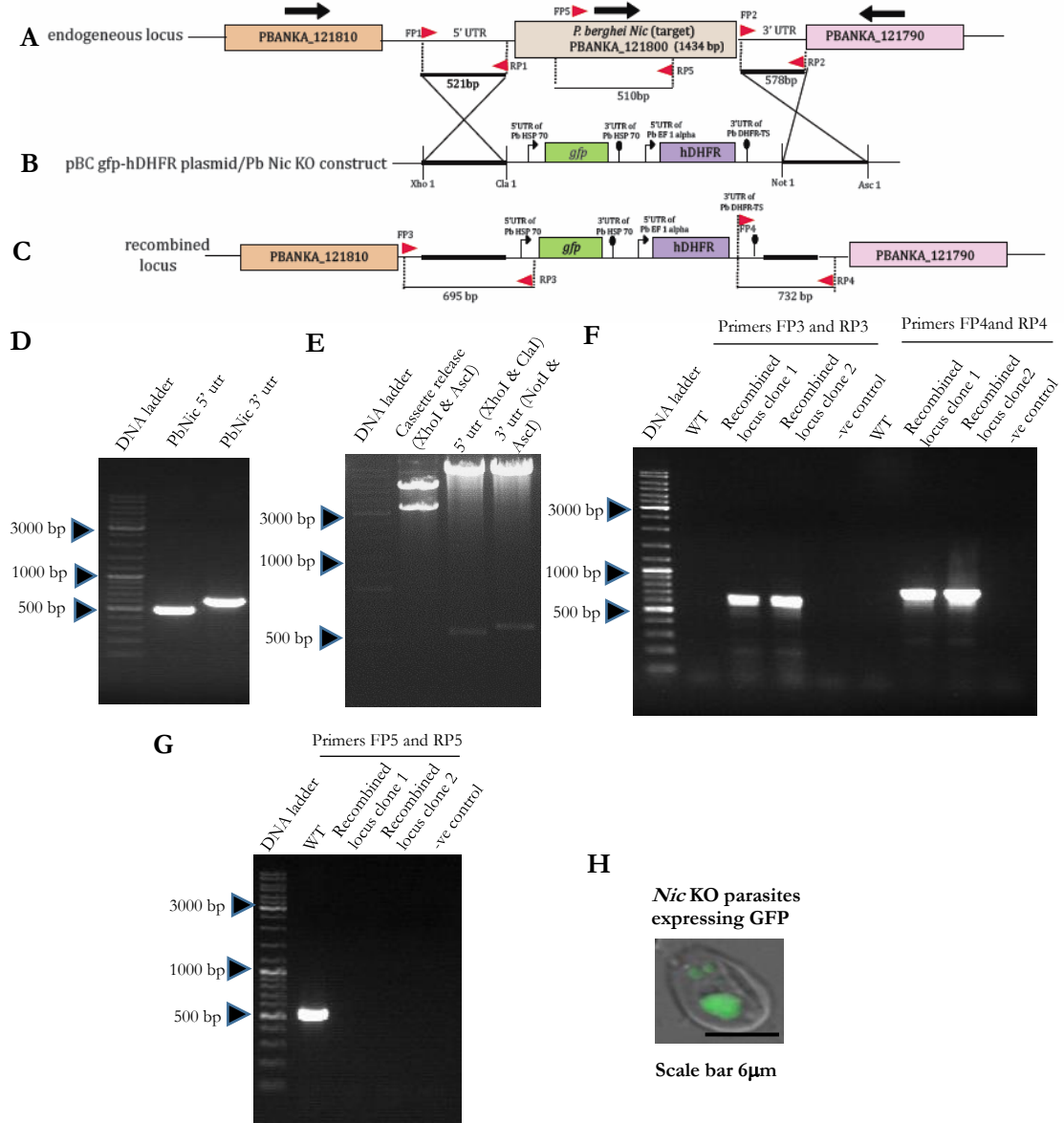


Fig 13: Generation of *Pbnic* knockout parasites. **A)** Representation of *Pbnic* endogenous locus showing *Pbnic* ORF, 5' and 3'UTR regions. **B)** Elements of targeting construct showing, 521 bp of 5' UTR and a 578 bp 3' of UTR of *Pbnic* cloned on either ends of pBC-GFP- DHFR vector using XhoI/ClaI and NotI/AscI respectively, GFP reporter and hDHFR drug resistance marker. *Pbnic* targeting vector was linearized with XhoI and AscI, transfected into schizonts to replace the gene. **C)** Representation of endogenous locus after integration of targeting vector into *Pbnic* gene by double cross over. **D)** A 1% agarose gel showing PCR amplified 521 bp of 5' UTR and 578 bp 3' of UTR of *Pbnic* with FP1/RP1 and FP2/RP2 primers respectively, **E)** digestion products of 521 bp of 5' UTR and 578 bp 3' of UTR of *Pbnic* following release with XhoI/ClaI and NotI/AscI respectively and construct linearized with XhoI and AscI. **F)** Diagnostic PCR with one primer beyond the site of integration in endogenous locus and the other within the targeting construct. FP3/RP3 primers for 5' integration confirmation and FP4/RP4 primers were used for 3' integration. **G)** Drug resistant parasites were clonal diluted for single clone without wild type contamination and was confirmed by FP5/RP5 primers. **H)** Merged DIC image of infected RBC showing GFP expressing parasite.

2.3.4 *Pb*nic has no role in blood stage propagation

Investigation of asexual blood stage propagation of *Pb*nic KO parasites as compared to WT GFP following infection with 1×10^3 iRBC into SA mice did not show any difference in their rates of propagation. (Fig 14 A). All asexual forms like rings, trophozoites and schizonts as well as sexual gametocyte stages were readily observed in *Pb*nic KO parasites. We conclude that *Pb*nic depletion does not affect the asexual development of parasite in the blood.

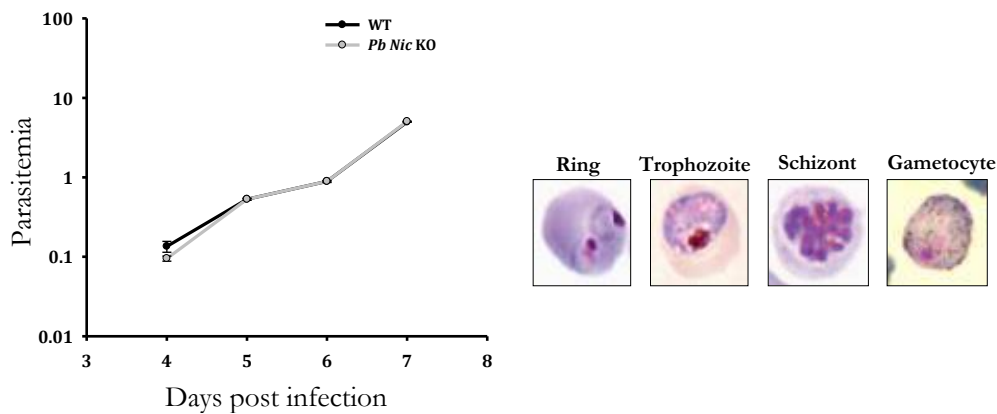
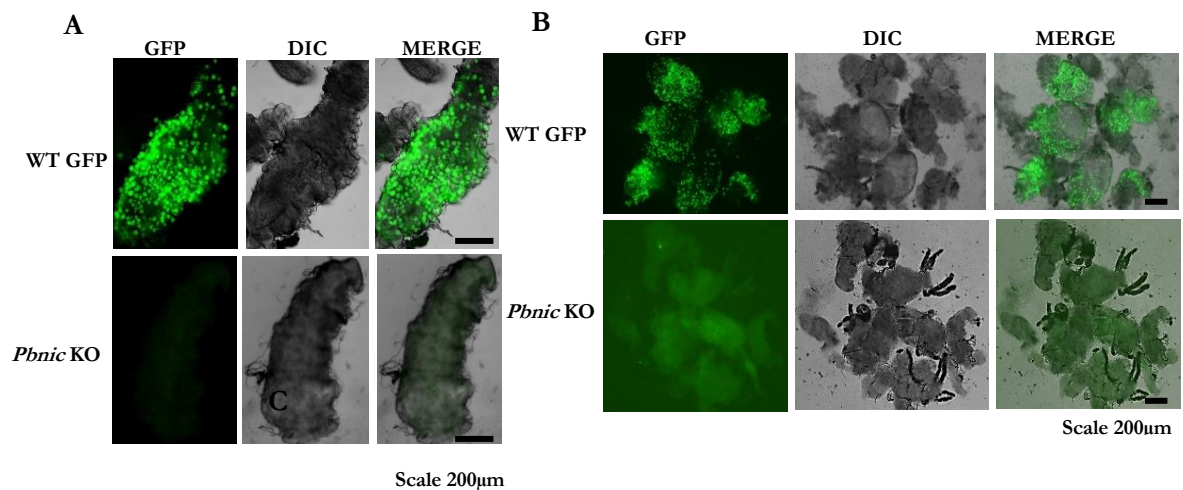


Fig 14: Asexual blood stage propagation of *Pb*nic KO parasites: A) Thousand mixed blood stage parasites of both WT GFP and *Pb*nic KO parasites were injected into 4-6 week Swiss albino mice through intravenous route. Parasitemia was monitored by daily blood smears stained with Giemsa and found no difference with wild type propagation. **B)** Shown are representative images of rings, trophozoite, schizont and gametocyte obtained from [226].

2.3.5 *Pb*nic KO parasites failed to produce ookinetes and oocysts

Following transmission of *Pb*nic KO parasites to female *A. stephensi*, the development of the parasite was analysed in mosquito at 20-24 h post blood meal. No ookinetes were detected in 30 fields of the Giemsa stained smears made from blood meal obtained from dissected midguts. During the same time point, an appreciable number of ookinetes were observed in WT GFP parasites. On D14 post blood meal, oocyst development was observed by dissecting midguts. In accordance with the absence of ookinetes, oocysts were absent in the midgut of the mosquitoes infected with *Pb*nic KO parasites. As expected, the control group showed considerable number of oocysts (Fig 15 A). These experiment was repeated for 3 times.



* Percentage of infected mosquitoes in each group were scored only on the presence of oocyst but not actual numbers (burden)



















Fig 15: *Pbnic* KO parasites do not produce oocyst in mosquito. Mosquitoes were fed on infected mice either with WT GFP or *Pbnic* KO parasites harboring gametocytes in the blood circulation and analysed for oocyst development at day 14 post blood meal. Dissected midguts of mosquitoes infected with WT GFP and *Pbnic* knockout parasites at day 14 of post blood meal shows oocysts in WT GFP infected, whereas absence of oocysts in *Pbnic* KO infected mosquito. **A)** Individual dissected midgut of WT GFP infected mosquito showing oocysts, *Pbnic* KO infected mosquito showing absence of oocysts. **B)** Pool of dissected midguts from WT GFP infected mosquitoes, most of them were positive for oocysts and none were positive in *Pbnic* KO infected mosquitoes. **C)** Table indicating the mosquito midgut infectivity in 3 independent experiments. WT GFP infected mosquitoes showed 88%, 76% and 92% infectivity respectively in 3 independent experiments, whereas *Pbnic* KO infected mosquitoes showed 0% infectivity.

Each time nearly 88%, 76% and 92% mosquitoes were positive for oocysts in WT GFP, but in *Pbnic* KO infected groups, none of the mosquitoes were having oocyst (Fig 15 B, C) (Percentage was calculated based the number of oocyst positive midguts from total number of blood meal positive mosquitoes). We conclude that *Pbnic* is essential for completion of *P. berghei* sexual reproduction.

2.3.6 *Pbnic* KO parasites failed to produce functional gametes

Following genetic crosses and transmission to mosquitoes, formation of functional gametes was revealed by analyzing the kind of oocysts formed at D14 post blood feeding. In the cross of *Pbnic* KO line and *P. berghei* *ANKA* mCherry line (WT *PbmCh*), oocysts were found that were positive only for mCherry. Whereas, in the genetic cross between WT *PbGFP* and WT *PbmCh*, three kinds of oocyst were observed on mosquito midguts (Fig 16 B). This included oocyst that were positive only for GFP (product of cross between male and female gamete expressing GFP), oocyst that were positive only for mCherry (product of cross between male and female gamete expressing mCherry) and oocyst that were positive for both mCherry and GFP expression [a product of male gamete (GFP expressing) with female gamete (mcherry expressing) or vice versa]. This indicated a defect in both male and female gametes in *Pbnic* KO line. While these results clearly demonstrated an essential role of *Pbnic* in sexual reproduction, the inability of *Pbnic* mutants to complete development in mosquito precluded us from investigating its role in oocyst stages, sporozoites stages and liver stages.

A

S. No.	Nature of sample	Cross between	Possible combinations of gametes formed	Phenotype of oocyst in midguts	Inference
1.	+ve control	WT GFP X WT mCherry	       	   	Both male and female gametes are functional Both male and female gametes are functional Both male and female gametes are functional Both male and female gametes are functional
2.	Test	<i>Pbnic</i> X WT mCherry	  (?)   (?)	 	<i>Pbnic</i> KO has no male & female gametes <i>Pbnic</i> KO has either male or female gamete

B

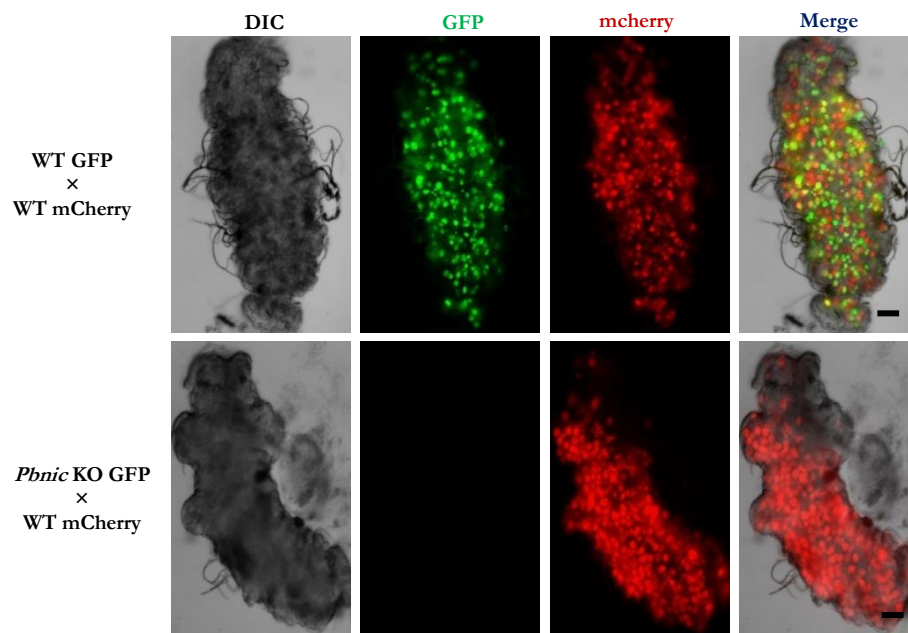


Fig 16: Genetic cross experiments. A) Schematic showing the genetic cross of WT GFP with WT mCherry and cross of *Pbnic* KO (GFP) with WT mCherry. The possible gametes derived from each line and oocysts formed are indicated. Genetic cross reveals that *Pbnic* KO do not form functional male and female gametes. B) Top panel shows a cross of WT GFP and WT mCherry, having 3 kinds of oocysts include oocyst that were positive only for GFP, oocyst that were positive only for mCherry and oocyst that were positive for both mCherry and GFP expression, and lower panel shows a cross of *Pbnic* KO with WT mCherry having oocysts expressing only mCherry.

2.3.7 Successful integration of *Pbnic* conditional silencing construct at *Pbnic* locus by double homologous recombination

The genomic organization of *Pbnic* gene locus is shown in Fig 17 A. The targeting construct carrying *Pbnic* CDS part preceding the stop codon that is cloned upstream to 1st FRT site at MCS1 and *Pbnic* 3' region cloned after GFP cassette at MCS2 is shown in Fig 17 B. Following successful recombination, the endogenous *Pbnic* 3' UTR was replaced with TRAP 3' UTR resulting in the recombined locus as shown in Fig 17 C. Fig 17 D shows the recombined locus following excision of *FRT*ed sequence. Fig 13 E shows the PCR amplified products of 509 bp CDS part preceding the stop codon and another 532 bp 3' region after stop codon of *Pbnic*. Fig 13 F shows the release of the targeting cassette from vector back bone using restriction enzymes Sph1 and EcoR1. The adjacent lanes show the release of the respective of CDS part and 3' fragments following restriction digestion with Sph1/Not1 and Kpn1/EcoR1. A diagnostic PCR was set up to confirm correct site specific integration using genomic DNA obtained from drug resistant parasites from two independent transfections. In Fig 13 G, an expected product size of 964 bp with primer set FP3 and RP3 in clones C1 and C2 indicated correct integration of the conditional targeting cassette after the CDS of *Pbnic*. Also, an expected product size of 732 bp with primer set FP4 and RP4 in clones C1 and C2 indicated correct integration of the targeting cassette at the 3' end of *Pbnic*. Genomic DNA of both clones C1 and C2 did not amplify a PCR product with primer set FP5 and RP2 while WT genomic DNA gave a product of 682 bp confirming the complete absence of WT parasites in clonal populations, C1 and C2 as shown in Fig 13 H. Consistent with the correct integration of the targeting construct which has GFP cassette, both clones expressed GFP constitutively, as shown Fig 13 I. A diagnostic PCR was set up to confirm the excision of TRAP 3' UTR using genomic DNA obtained from midgut and salivary gland sporozoites. In Fig 13 J, an expected product size of 1584 bp with primer set FP5 and RP5 in midgut and salivary gland sporozoites indicated excision of TRAP 3' UTR. Also, an expected product size of 366 bp with primer set FP5 and RP3 in mixed blood stage genomic DNA and absence of amplicon in sporozoite genomic DNA further confirms complete excision.

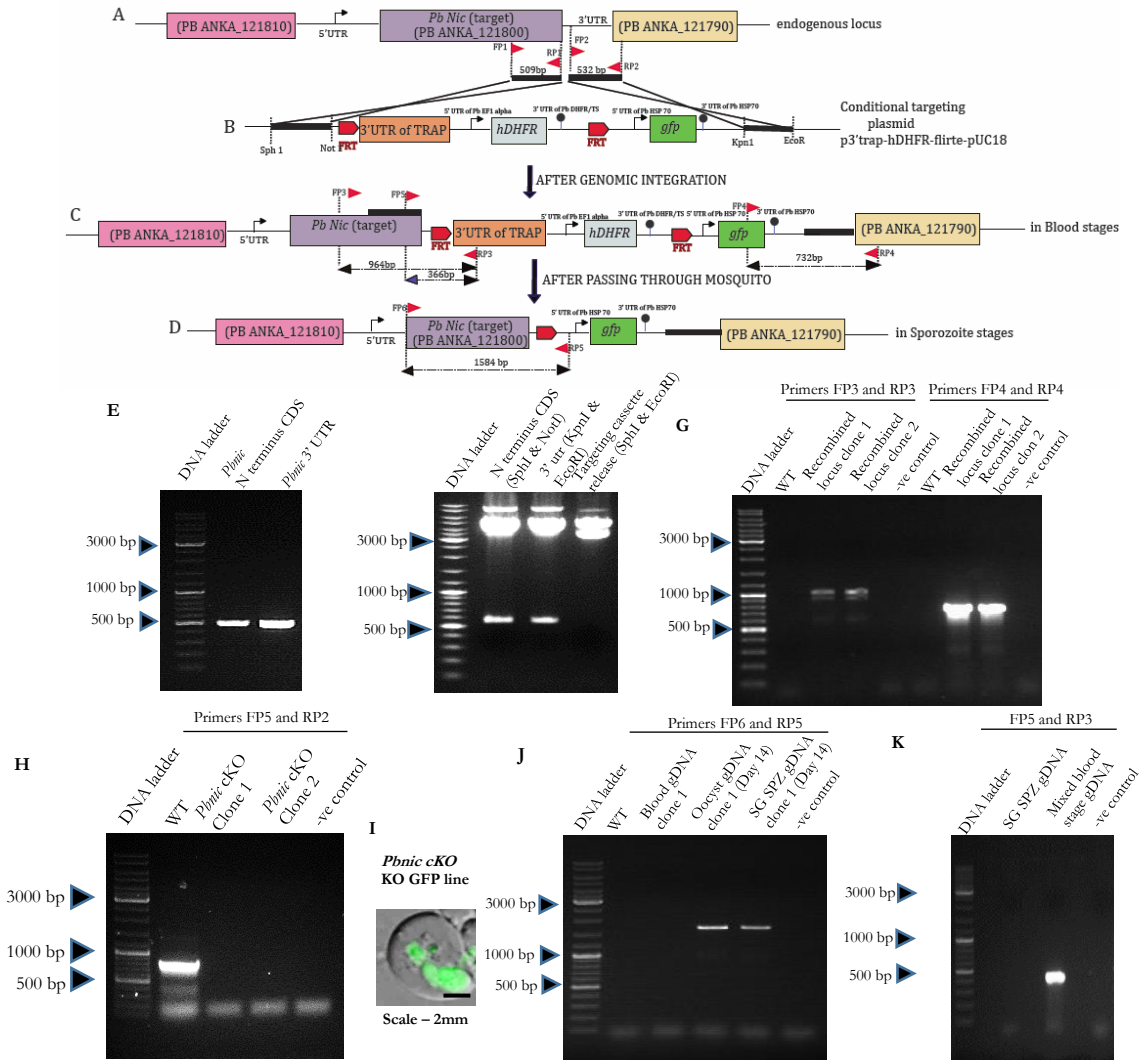


Fig 17: Generation of *Pbnic* conditional knockout parasites. **A)** Representation of *Pbnic* endogenous locus showing *Pbnic* ORF, 5' and 3'UTR regions. **B)** Elements of targeting construct showing, 509 bp *Pbnic* CDS part preceding the stop codon and another 532 bp 3' region after stop codon of the *Pbnic* cloned on either ends of TRAP-GFP-hDHFR vector using SphI/NotI and KpnI/EcoRI respectively, TRAP 3' UTR and hDHFR drug resistance marker flanked by *FRT* sites, and GFP reporter. *Pbnic* cKO targeting vector was linearized with SphI and EcoRI, transfected into schizonts. **C)** Representation of endogenous locus after integration of targeting vector by replacing *Pbnic* 3' UTR by double cross over. **D)** Representation of endogenous locus after excision at oocyst stages where TRAP promoter drives the expression of FLP recombinase that excises *FRT*ed DNA resulting in conditional silencing. **E)** A 1% agarose gel showing PCR amplified 509 bp *Pbnic* CDS part and 532 bp 3' region of the *Pbnic* with FP1/RP1 and FP2/RP2 primers respectively, **F)** digestion products of 509 bp *Pbnic* CDS part and 532 bp 3' region of *Pbnic* following release with SphI/NotI and KpnI/EcoRI respectively and construct linearized with SphI and EcoRI. **G)** Diagnostic PCR with one primer beyond the site of integration in endogenous locus and the other within the targeting construct. FP3/RP3 primers for CDS part integration confirmation and FP4/RP4 primers for 3' integration. **H)** Drug resistant parasites were clonal diluted for single clone without wild type was confirmed by FP5/RP2 primers. **I)** Merged DIC image of infected RBC showing GFP expressing parasite. **J)** Excision specific PCR was done with blood stage genomic DNA with FP5/RP3 showed TRAP 3' UTR in the *Pbnic* endogenous locus and at day 14 post blood meal oocyst genomic DNA with FP5/RP5 showed complete excision of TRAP 3' UTR and was confirmed by FP5/RP5 primers. **K)** Excision confirmation PCR with salivary gland sporozoite genomic DNA confirmed the complete excision of TRAP 3' UTR.

2.3.8 Excision of TRAP 3' UTR and conditional silencing of *Pbnic* in mosquito stages of the parasite

Pbnic cKO parasites revealed their blood stage propagation on par with wild type parasites. Following transmission of *Pbnic* cKO parasites to female *A. stephensi*, the development of the parasite was analysed at D14 by observing the oocyst and the sporulation pattern within it. We noted that the mutants showed similar number of oocysts as WT GFP (Fig 18A and B). Further, there was no difference in the sporulation pattern (Fig 18C) and enumeration of the midgut oocyst sporozoites also showed similar frequency (Fig 18D).

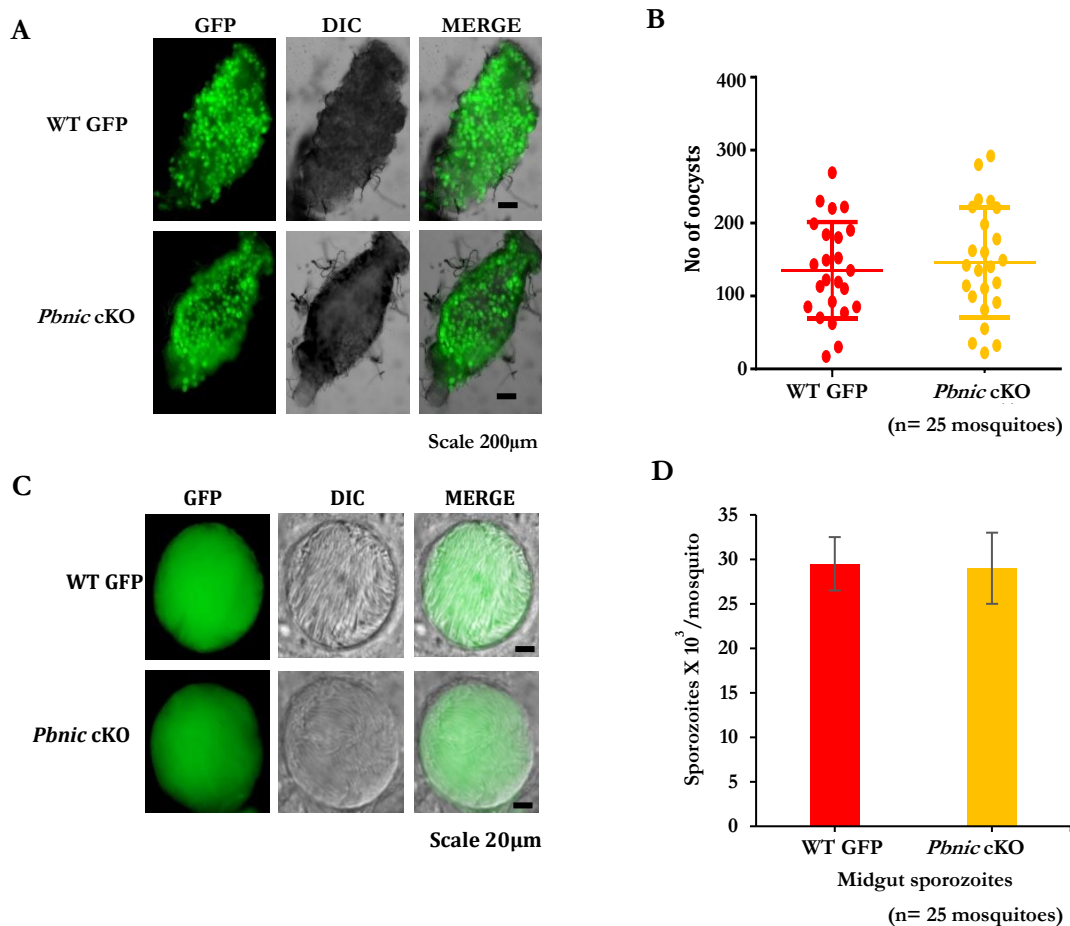


Fig 18: *Pbnic* has no role in oocyst infectivity. Mosquitoes were fed on infected mice either with WT GFP or *Pbnic* cKO parasites harboring gametocytes in the circulation and analysed for oocyst development at day 14 post blood meal. **A)** Dissected midguts of mosquitoes infected with WT GFP and *Pbnic* cKO parasites at day 14 of post blood meal shows oocysts in similar rates. Individual dissected midgut of WT GFP infected mosquito, *Pbnic* cKO infected mosquito showing oocysts. **B)** Dot plot showing quantified oocyst numbers in each of 25 mosquitoes for WT GFP and *Pbnic* cKO infected mosquito. **C)** Individual oocyst from both WT GFP and *Pbnic* cKO showing sporulation. **D)** Bar graph drawn from average number of midgut sporozoites from 25 infected mosquitoes from WT GFP and *Pbnic* cKO showing comparable number.

On D18-21 post infection, dissected salivary glands showed *Pbnic* cKO sporozoites whose numbers were similar to WT GFP sporozoites (Fig 19A and B). In *Pbnic* cKO parasites, FLPL excises TRAP 3' UTR and hDHFR elements flanked by two *FRT* sites. As TRAP is active from oocyst stages, excision is expected to begin at this stage. Maximal excision of 3' UTR at oocyst and salivary gland sporozoites was confirmed by excision specific PCRs (shown in Fig 17 J&K). The non-essential role of *Pbnic* in sporozoite formation and its infectivity to salivary gland was revealed. These conditionally silenced sporozoites were used to analyze the role of *Pbnic* in liver stage development.

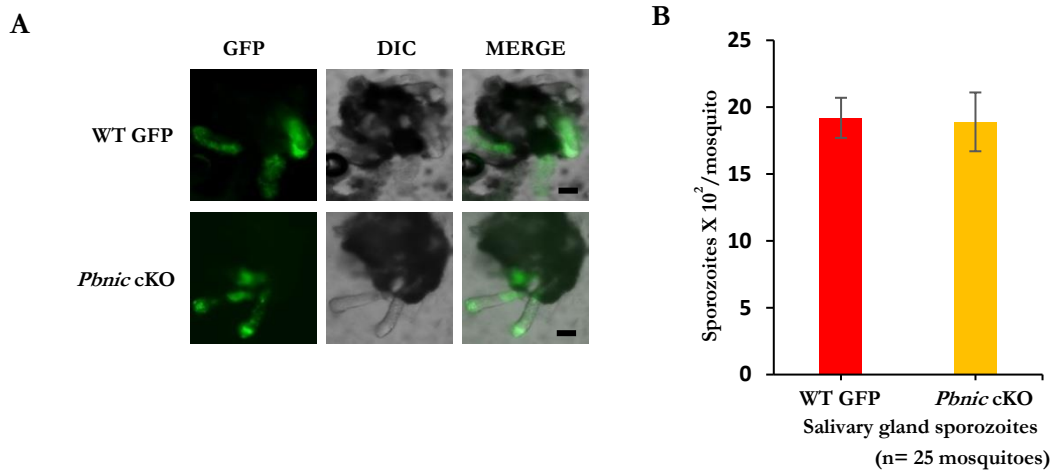


Fig 19: Conditional deletion of *Pbnic* depletion does not affect salivary gland sporozoite load. Dissected salivary glands of mosquitoes infected with WT GFP and *Pbnic* cKO parasites at day 23 of post blood meal shows sporozoites in similar rates. **A)** Individual dissected salivary gland of WT GFP parasites infected mosquito and *Pbnic* cKO infected mosquito. **B)** Bar graph drawn from average number of Salivary gland sporozoites from 25 infected mosquitoes from WT GFP and *Pbnic* cKO showing comparable numbers.

2.3.9 *Pbnic* cKO showed normal EEF development as WT parasites

Analysis of EEF development in HepG2 cultures at 12h, 36h and 62h time points revealed that *Pbnic* cKO EEFs were indistinguishable from WT GFP EEFs, both in morphology and development, thus suggesting the dispensable role of *Pbnic* in EEF development (Fig 20).

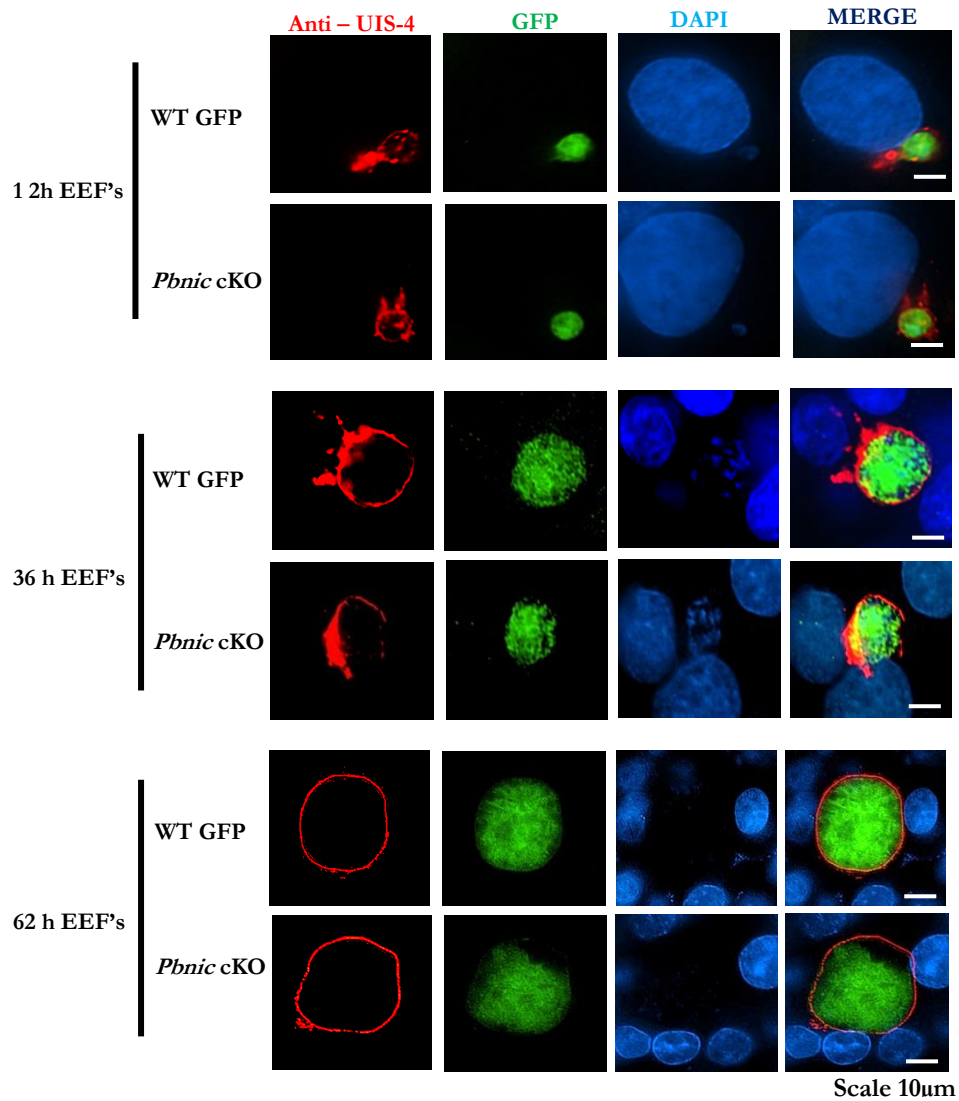


Fig 20: *Pbnic* is not essential for liver stage development: Salivary gland sporozoites were extracted from the dissected mosquito and 2X10⁴ sporozoites of either WT GFP or *Pbnic* cKO sporozoites were added to HepG2 cultures that support *P. berghei* sporozoite growth. The growth of EEF at 12 h, 36 h and 62 h was revealed by staining with UIS4 (PVM marker) and DAPI was used to stain nuclei of HepG2 and parasite. It was observed that *Pbnic* cKO parasites have grown as normal as wild type EEFs in HepG2 cells.

2.4 Discussion

Ongoing research on NAD⁺ bio-synthetic pathway is opening multiple intervention strategies for many parasitic and bacterial infections. NAD⁺ is a co-factor for many oxidoreductases that catalyze redox reactions required for energy metabolism [227], [228]. NAD⁺ plays an important role in regulating the activity of sirtuins that are NAD⁺-dependent histone deacetylases that influence diverse activities pertaining to gene silencing, cell cycle regulation, apoptosis and energy homeostasis [229]. NAD⁺ is an ADP-ribose donor in ADP-ribosylation to proteins, a post-translational modification essential for many cellular processes, including gene regulation, DNA repair, apoptosis and cell signaling [230]. Because of the essential functions of NAD⁺ in many cellular processes, enzymes of the pathway became excellent drug targets for anti-microbial and anti-protozoan infections. Bacterial and *Plasmodium* nicotinate mononucleotide adenylyl transferase is structurally diverge from the human form, catalyzes the conversion of nicotinate mononucleotide to nicotinate adenine dinucleotide in NAD⁺ metabolism. Small molecule inhibitors against this enzyme showed anti-bacterial and anti-malarial properties [216], [213]. These findings demonstrate that NAD⁺ synthesis is critical for microbial viability and the feasibility of targeting other enzymes of the salvage pathway as a means of developing anti-malarial therapies.

Nic is the enzyme involved in NAD⁺ metabolism, catalyzes the conversion of nicotinamide to nicotinic acid in bacteria, yeast and protozoan parasites. The absence of this enzyme in higher eukaryotes makes it an excellent target for drug designing. In *Plasmodium*, enzymes required for *de novo* synthesis of NAD⁺ were not identified in bioinformatics analysis, suggesting that the parasite is dependent on salvage pathway to meet its requirement [213]. Previous studies using isotope labeling revealed elevated NAD⁺ levels in infected RBC that are synthesized and utilized by *Plasmodium* [214]. NMR spectroscopy studies on uninfected RBCs and purified parasites showed increased NAD⁺ concentrations in trophozoites [231]. These findings suggest the ability of *Plasmodium* to scavenge precursors like nicotinamide and nicotinic acid from the host milieu in order to meet the required levels of NAD⁺. Niacin deprivation did not affect the *P. falciparum* *in vitro* growth but led to reduction in NAD⁺ levels [216]. However, in *Leishmania* and other yeast species, niacin dependency for the growth was reported [221], [222]. These findings suggest the importance of salvage pathway to maintain NAD⁺ levels. Following niacin starvation, Na (TNA1) and NR (TNR1, TNR2) high-affinity transporters are

being upregulated in *Candida glabrata* and in other yeast species as characterized by transcript profiling [232]. However, no homologs for these corresponding transporters are found in *Plasmodium* database.

Quantitative gene expression studies revealed *Pbnic* expressions throughout the all life cycle stages, likely pointing to the indispensable metabolic requirement of this enzyme. Such an obligatory dependence may mean that its locus may be recalcitrant to genetic manipulation. While such a phenotype may reveal the essential nature of nic and qualify it as a blood stage target, surprisingly our attempts to knock out *nic* in *P. berghei* readily yielded a KO mutant that was unaffected with regard to its ability to propagate asexually or to form gametocytes. However, they failed to transmit malaria to the mosquito as judged by the complete absence of ookinete and oocyst stages. Further, a defect in both male and female gametes was noted in *Pbnic* KO line as revealed by genetic crosses. Conditional approaches to deplete *Pbnic* in mosquito stages yielded mutants that were able to form oocyst sporozoites and salivary gland sporozoites, which upon introduction into hepatocytes in vitro, showed complete EEF development till 62 h. These observation demonstrated the essentiality of *Pbnic* exclusive to sexual stages. Similar findings were reported in *Leishmania* where *Lipnc1* was shown to be essential for the parasite growth *in vitro* and establishment of infection in mice [221]. *Lipnc1* null mutants developed as wild type parasites at early time points in the sand fly, post blood feeding whereas they failed to develop further when the blood meal was digested completely and the remnants were defecated [222].

What explains the fitness of the *Pbnic* KO mutants during blood stages while manifesting a striking transmission blocking phenotype? A likely explanation for this phenotype may be that the *Pbnic* deleted parasites use alternative pathways for NAD^+ synthesis by recruiting nicotinic salvaged from host RBC. However once the *Pbnic* deleted parasites are taken up by the mosquito, they fail to complete sexual development. This may imply that the parasite is dependent on nicotinamidase at this stage, and the possibility of acquiring the nicotinic acid from the mosquito gut milieu is limited. While nicotinic acid may not be a limiting factor in the blood meal, one speculation for its lack of effective deployment to parasite may be due to absence of specific transpoters that mediate nicotinic acid uptake. Further, the inability of *Pbnic* mutants to complete sexual reproduction may also be due to failure to survive within the hostile environment of mosquito midgut. *Plasmodium* sexual development starts in the mosquito within 15 min post blood meal when gametocytes egress from RBC to differentiate into gametes. Human pro-inflammatory cytokines, reactive nitrogen species (RNS) such as nitric oxide (NO) and reactive oxygen species (ROS) produced against *Plasmodium* infection inactivates gametocyte by DNA

damage [233]. After mosquito ingests blood, the remenants components such as white blood cells, complement proteins, and cytokines are active for several hours post blood meal [234], [235], [236]. WBC, byproducts of RBC digestion, including oxyhemoglobin, heme and mosquito midgut epithelium release RNS that causes DNA damage to the parasite. Blood, as a nutrient source promotes bacteria growth in mosquito midgut which in turn triggers the mosquito innate immune response limiting *Plasmodium* growth [237], [238]. Since NAD^+ acts as co-factor in antioxidant systems and essential for sirtuins, whose activity is required for DNA repair, it is likely that one mutant may fail to maintain an efficient antioxidant system thus succumbing to DNA damage in the absence of NAD^+ . Sirtuins are a class of histone deacetylases involved in chromatin condensation and heterochromatin formation thereby affecting gene silencing, specifically act at telomeres [229]. *Plasmodium falciparum* has two sirtuins viz., PfSir2a and PfSir2b. While PfSir2b is not well characterized, the PfSir2a was shown to play a role in *var* gene silencing [239]. Nicotinamide is a noncompetitive inhibitor of the Sir2 enzyme, so nicotinamide must be catabolised by *nic* for the function of Sir2. In *Pbnic* deleted parasites, it is speculated that accumulated nicotinamide might be inhibiting NAD^+ dependent Sir2 enzymes thereby inhibiting DNA repair. Or deletion of *Pbnic* leads to reduced NAD^+ levels thus inhibiting Sir2 mediated DNA repair which is detrimental to the parasite.

Several *Plasmodium* metabolic enzymes like asparagine synthetase [240], dipeptidyl aminopeptidases [241], S-adenosyl methionine decarboxylase/ornithine decarboxylasekinases [242] and chitinases [243] are critical for malarial transmission which makes them potential targets of transmission blocking interventions. Our current study adds one additional metabolic enzyme called nicotinamidase to the previously existing list, essential for *Plasmodium* sexual stage development. Owing to the absence of *nic* homologues in humans (higher eukaryotes), the design of *nic* specific inhibitors could exclusively inhibit the *Plasmodium* development without the risk of compromising with the host metabolism. Furthermore, *Pbnic* is conserved across all the *Plasmodium* species, bacteria, yeast and other parasites such as *Toxoplasma* and *Eimeria tenella*, implicating *nic* as a potential drug target beyond *Plasmodium*.

In conclusion, our studies highlight a metabolic aspect of *Plasmodium* parasite development in the mosquito midgut by revealing the essential role of the *Pbnic* enzyme, which catalyses the initial step of NAM to NA conversion. The identification and validation of *Plasmodium* *nic* specific inhibitors will be an exciting avenue that opens up from these studies. If effective it may offer a great advantage to tackle *Plasmodium* that manifests striking ability to acquire drug resistance. The NAD^+ biosynthetic pathway appears to be an interesting new field

of investigation for the identification of new therapeutic targets against *Plasmodium* and other related Apicomplexan parasites.

*Functional characterization of
Plasmodium berghei S10 by reverse
genetics approach*

3.1 Introduction

Plasmodium sporozoites are the infective forms of the malaria parasite to humans and undergo development in the oocyst and upon release into the mosquito hemocoel, colonise the salivary glands [244]. Several lines of evidence demonstrate the distinct transcriptional changes associated with sporozoites while developing within oocyst [51] and during their maturation within the salivary glands [225]. Concomitant to such transcriptional changes are coordinated expression of distinct proteins that are required for infectivity and development of parasite [245]. Analysis of the proteomes from oocyst sporozoite stages and salivary gland sporozoites stages reveals marked differences in their composition, a pre-requisite that likely potentiates the sporozoites to establish liver stage infections [245]. A deeper understanding of the sporozoite biology may offer better interventional strategies to prevent completely the sporozoite infection to hepatocytes or subsequent development into liver stages.

Sporozoites and merozoites are two distinct invasive stages of *Plasmodium* that invade respectively the hepatocytes and erythrocytes. Since these stages are adapted to invade a particular cell type and undergo further development only in these cellular niches, it is very likely that stage specific gene expression may play a key role in determining the host cell tropism. In order to identify the stage specific transcripts uniquely upregulated in sporozoite stages, a suppression subtractive hybridisation was carried between salivary gland sporozoite stage and merozoite stage [52]. Sequencing the SSH library and aligning the cDNA sequences to *P. yoelii* genome yielded 25 tags (Fig 21), of which the only 2 were previously characterised, namely the circumsporozoite protein (CSP) and thrombospondin related anonymous protein (TRAP). Several interesting features emerged following a preliminary inspection of the genes discovered in SSH screen. Twelve genes encoded for proteins with signal peptide, likely implicating their role in the process of secretion. In addition, a product bearing a thrombospondin like repeats was shown to reside in the rhoptries, an organelle associated with storage of sporozoite secretory proteins. Interestingly, there were also 2 proteins that exhibited expression pattern similar to TRAP, likely suggesting their localisation to micronemes. Thus the uniquely upregulated transcripts in sporozoite stages can be envisaged to express products important only for sporozoites and not merozoites thus aiding commitment to hepatocyte infection.

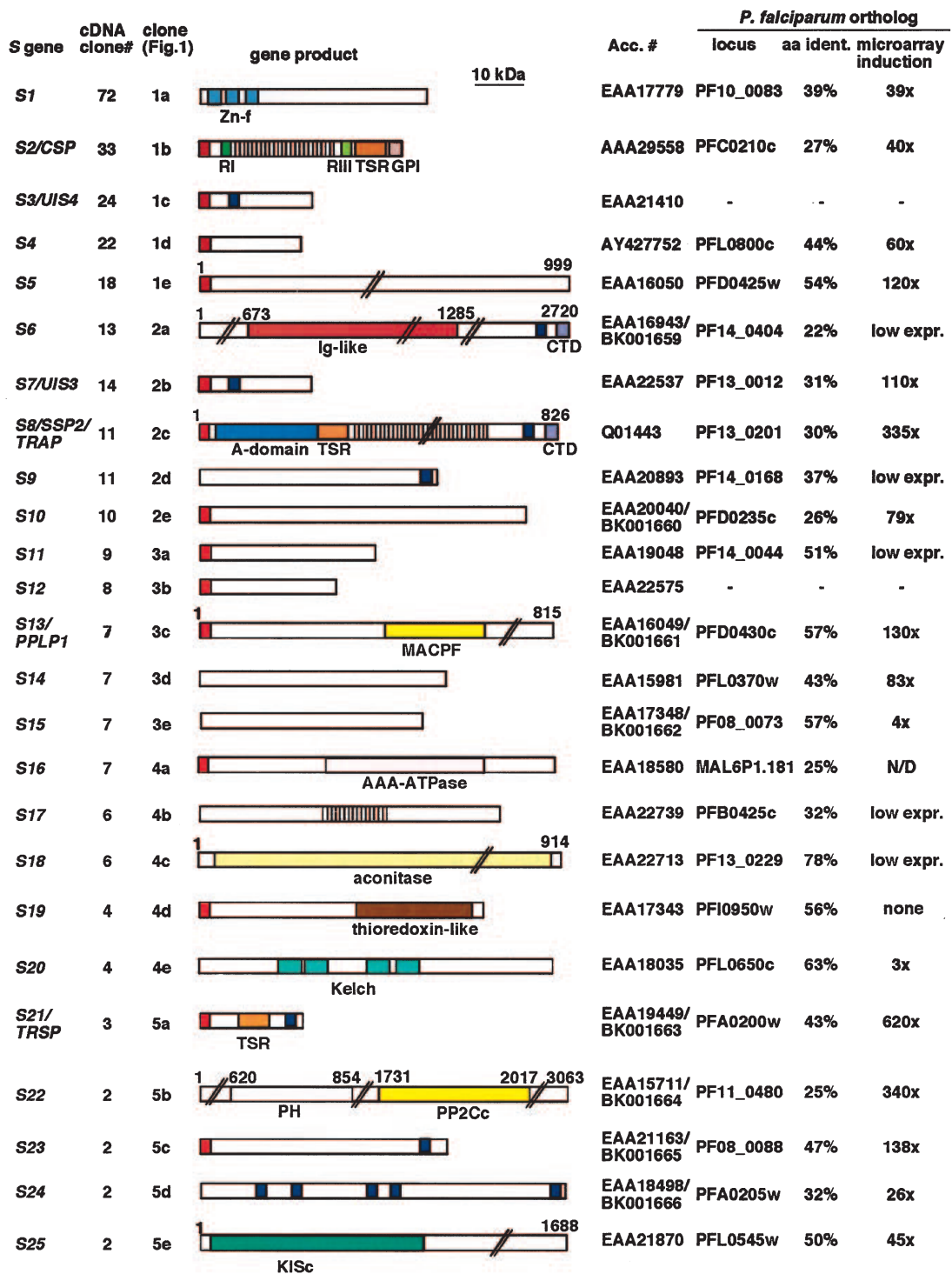


Fig 21: Schematic diagram showing predicted primary structure of 25 sporozoite specific (S) gene products of *P. yoelii* in SSH of salivary gland sporozoite stages versus merozoite stages. For each S orthologue in *P. falciparum*, the ratio of expression levels between sporozoite versus merozoite is displayed as microarray induction. Out of 25 S genes, 12 genes encoded proteins with signal peptides (represented with red box). S10 is one among them with signal peptide and showed 79 fold micro array induction. (Figure obtained from [52]).

These 25 genes were designated as “S” genes, as they were uniquely over expressed in sporozoite stage. The designated tags S2 and S8 recovered in SSH screen corresponded respectively to CSP and TRAP, was not surprising given their central role in sporozoite biology. Both S2/CSP and S8/TRAP showed an induction in microarray by 40X and 335X fold thus validating the SSH results. While no dearth of information exists for S2/CSP and S8 /TRAP mediated functions in sporozoite stages, more recently a majority of these “S” genes have been functionally investigated using approaches of reverse genetics. Consistent with sporozoite specific functions, the “S” genes have been implicated in development of sporozoites [109], gliding motility and malaria transmission [246], [54], [55], [53], [247], post transcriptional regulation of genes associated with sporozoite maturation or maintenance of sporozoite infectivity [57], [58], host cell entry [248], completion of EEF development [35], [36], cell passage ability of parasite in mosquito as well as in mammalian host [56] and breaching of liver sinusoidal cell layer prior to hepatocyte infection [22]. Based on the literature, we provide below detailed information about the role of each “S” genes in regulation of pre-erythrocytic biology.

The *S1* orthologues across the rodent and human species are annotated with three C3H1 zinc finger domains that bind to the class II AU-rich elements of the tumor necrosis factor alpha mRNA. While S1 showed sporozoite specific gene expression, surprisingly however, a KO of *S1* yielded a dispensable phenotype and was able to complete the life cycle similar to WT parasites. Owing to its non- essential role, the feasibility of utilising *S1* locus for stable heterologous transgene expression was demonstrated by targeting the *S1* locus a DsRed cassette driven by *P. berghei* elongation factor 1 alpha and stabilised by the *P. berghei* dihydrofolate reductase 3'UTR [249]. The successful integrants showed constitutive DsRed expression across all life cycle stages, with development and frequency of parasites similar to WT. Thus S1 locus can be successfully exploited for heterologous gene expression, complementation and also to test the stage specificity of promoters.

S2/CSP is one of the most widely studied candidate till to date, owing to its importance as a potential pre-erythrocytic vaccine candidate. It is the predominant sporozoite surface antigen that continues to be expressed on the exo-erythrocytic forms [250]. Using CSP transgenic mice, it was shown to be an immunodominant antigen on irradiated sporozoites, as these mice failed to elicit immune response, owing to recognition of CSP as self antigen [41]. The CSP transgenic mice failed to generate CD8+ T cell immunity. By further obtaining CSP transgenic mice in antibody deficient background, a total abrogation of humoral immune responses was achieved, thus providing an ideal immunological setting to study the efficacy of

the non-CSP T- antigens expressed in irradiated sporozoite following immunisation. While the CSP transgenics deficient in humoral responses were severely compromised in imparting protection against challenge with infectious sporozoites, yet multiple immunisations led to complete sterile protection revealing the presence of powerful, yet to be identified sporozoite and liver stage antigens that are targets of a strong protective response. The ability of CSP to enter secretory pathway and being shed as trails during sporozoite gliding motility under *in vitro* condition and during traversal of mammalian cells prior to hepatocyte infections, additionally renders a strong humoral and CD4+ T cell mediated immunity [251]. Thus many other sporozoite antigens that are likely sorted to the secretory pathway are of prime importance for inclusion as pre-erythrocytic vaccine candidates [252], [253], [254]. In addition to its role in protective immune responses, CSP is also essential for development of sporozoites within oocyst and CSP KO parasites have impaired sporulation and are unable to generate infectious sporozoites [109]. Further, the normal levels of CSP expression is required for sporozoite morphogenesis as reduced expression following the truncation of its 3' UTR region affected the development of the inner membranes and associated microtubules underneath the oocyst outer membrane, that are points of budding [255]. Taken together these studies reiterate the importance of CSP in normal development of sporozoites.

Owing to the importance of CSP as a prime vaccine candidate, the structural motifs of CSP have been investigated in great detail. In all *Plasmodium* species, the CSP structure is highly conserved consisting of the N-terminal domain, two conserved motifs referred to as regions I and a stretch of positively charged residues called region II plus flanking a species specific tandem repeat region that is target for B- cell responses, a C- terminal domain and a GPI sequence. Recent studies reveal the existence of CSP on sporozoite surface in two conformational stages- an adhesive conformation where the C-terminal cell adhesive domain is exposed and is required for sporozoite development and for commitment to hepatocyte infection and a non-adhesive conformation where the N-terminal domain masks the adhesive C- terminal domain, thus maintaining the sporozoites in a migratory state after its exit from oocyst till the time of invasion to the salivary glands [256]. Further, the role of region I and II plus were though implicated initially in the interaction of sporozoite with mosquito salivary glands and hepatocytes respectively, swapping the *P. berghei* CSP with *P. falciparum* CSP lacking the region I and II plus showed an unaltered phenotype with regard to salivary gland and hepatocyte invasion for region I mutants, while region II plus mutants demonstrated abolished gliding motility affecting mutant's ability to invade salivary glands and infect hepatocytes [26]. Mutation of the positive residues with alanines within region II plus resulted in failure of

sporozoites to exit the oocyst [110]. Further, the role of N- terminal and tandem repeat region together was shown to be required for sporozoite to reach salivary glands and hepatocytes [257]. Another independent study on the same lines showed that in both the mutants lacking tandem repeats and N- terminal plus repeats, the oocyst formation was unaffected but sporozoite development was defective [258]. The GPI addition sequence was also shown to be required for sporogenesis as deletion of signal sequence led to CSP localisation to the cytoplasm, resulting in failure of sporozoites to bud and develop. In addition to sporozoite stages, CSP continues expression during early liver stages. Infact one of the ways how the early liver stages usurp the host cellular machinery is by preventing an inflammatory responses and CSP plays a crucial role in this process. CSP has two *Plasmodium* export motifs (PEXEL) or Vacuolar Transport Signals (VTS), that are a stretch of positively charged amino acids that occur around 11-50 amino acids downstream to signal peptide. By virtue of these motifs, CSP translocates from the parasite across the PVM into the hepatocyte cytoplasm. The exported CS out competes the NF- κ B nuclear translocation using the nuclear importin- α , thus precluding the expression of nearly 1000 host genes, required for inflammatory response [42].

S3, also known as UIS4 (upregulated in infective sporozoites gene 4) was additionally identified as gene upregulated in salivary gland sporozoite stages, following SSH of oocyst sporozoites versus salivary gland sporozoites. S3 protein is expressed both in sporozoite stages and also in liver stages. Owing to its localisation to PVM, UIS-4 has been used as a marker to distinguish the host and parasite boundary inside hepatocyte. A KO of *UIS4* in the rodent parasite *P. berghei*, led to progression of parasite life cycle normally in asexual stages and in mosquito stages. However, upon entry into hepatocytes, the KO's experienced a block in the growth and were unable to initiate a break though infection. Interestingly, the inability of these mutants to initiate blood stage infection was exploited to induce a pre-erythrocytic immunity following a prime boost immunisation with UIS4 mutants, that showed complete sterile protection upon challenge with infectious sporozoites [35].

S4, also referred to as CelTOS is an acronym for Cell Traversal protein for ookinetes and sporozoites, localises to micronemes and is essential for cell traversal activity. Disruption of CelTOS locus resulted in a 200 fold reduction in infectivity in mosquito and reduced the sporozoite infectivity to hepatocytes. The CelTOS mutants, though were able to invade the midgut epithelial cells by disruption of the plasma membrane, yet they were unable to cross this layer owing due defect in cell migration. These observations suggest conserved cell passage

mechanisms used by sporozoites and ookinetes to cross cellular barrier to establish successful invasion [56].

S5, also known as SIAP-1 (Sporozoite invasion associated Protein-1) is unique to Apicomplexan hemoprotezoa like *Babesia*, *Theileria*, including *Plasmodium*. mCherry transgenics of SIAP-1 localised the protein to oocyst and salivary gland sporozoite stages, with characteristic accumulation at the apical end of the sporozoite. Disruption of SIAP-1 locus, while had no effect on oocyst sporulation, however the mutants manifested a partial defect in sporozoite egress and a concomitant abolition in sporozoite's ability to reach salivary glands. Further, the SIAP-1 mutants are unable to perform gliding motility. These studies point to the importance of SIAP-1 in sporozoite functions like oocyst egress and migration to salivary glands [246]. S5 protein was identified in the proteomic profiling of the sporozoite stage and targeted disruption of S5 led to failure in egress of oocyst sporozoites. The development of S5 (PB000251.01.1) mutants were normal till the point of mature oocyst formation and interestingly, contained similar number of sporozoites as WT oocyst. However, only a small fraction of these oocyst sporozoites were seen in hemocoel and salivary glands, an observation that concurred with accumulation of mutant sporozoites in oocyst. The S5 mutants also failed to establish infection in the mice following delivery of sporozoites through mosquito bite. An inspection of oocyst derived sporozoites, for their ability to infect mice or invade hepatocytes *in vitro*, following release by mechanical disruption, showed no difference as compared to WT. Infact, mechanically disrupted oocyst sporozoites also initiated infection in mouse, reflecting the infection competence of mature oocyst sporozoites, however, the ability of these sporozoites to get released into hemocoel depended on the presence of S5, as revealed by studies on mutants [245].

S6, referred to as TREP, is another transmembrane domain containing protein having short cytoplasmic tail and a large extracellular domain that contains Type I TSR domain, similar to TRAP/S8 described below. Disruption of TREP resulted in sporozoite mutants whose ability to invade salivary glands were dramatically diminished due to severe defect in gliding motility [55], [54]. A different study showed that S6 transcription is down regulated during sporozoite maturation, that likely involves a translational control similar to the translational repression reported previously for gametocyte specific genes that are repressed by DEAD box RNA helicases, referred to as development of zygote inhibition (DOZI) [94]. The S6 transcript abundance peaked during the ookinete and oocyst stage with a progressive decline in hemocoel sporozoite stage and lowest in salivary gland sporozoite stage. However the protein profiles of

S6 showed an increase in levels from oocyst stage to salivary gland sporozoite stages. Suggesting that the S6 translation was delayed as compared to its transcription rate. More detailed investigation is needed to address how such translational repression actually helps in regulation of sporozoite infectivity [54].

S7/UIS-3 (upregulated in infective sporozoites gene 4) was also another candidate that was discovered in gene expression profiling studies using an SSH screen of oocyst sporozoites versus salivary gland sporozoites. The *UIS-3* KO yielded sporozoites that were competent to invade hepatocytes but unable to initiate blood stage infections [36]. This report was a seminal of its kind, demonstrating the possibility of developing a safe and effective, genetically attenuated whole organism pre-erythrocytic vaccine. The liver stage parasites are targets for protective immune responses as they are capable of generating sterilising immunity, thus preventing malaria. The genetically attenuated parasites like *UIS-3* KO and *UIS-4* KO are indeed a proof of principle for their potential to elicit sterilising immunity thus paving way for creation of human genetically attenuated parasites.

S8/TRAP is another well studied sporozoite protein, after CSP. TRAP is a type 1 transmembrane protein required for parasite gliding motility and invasion of salivary glands and mammalian hepatocytes [53]. In the sporozoite, TRAP localises to the unique secretory organelles- the micronemes present at the apical end of the parasite, as well as on the surface of the sporozoite. When sporozoites contact the host cell surface, the intracellular TRAP accumulates on the parasite surface and forms a cap at the anterior end [259], [260]. An interesting feature of TRAP is the presence of two adhesive modules in its ectodomain. One is an integrin like A domain, and the other, a thrombospondin type 1 repeat. Mutations in these domains affected the invasion ability of sporozoites towards salivary glands and hepatocytes, without affecting its gliding and host cell adhesion [121]. TRAP acts as a link bridging the parasite cortical microfilaments and matrix or surface of the host cell. Genetic evidence for the role of cytoplasmic tail of TRAP in regulating sporozoite gliding and host cell invasion was shown by elegant point mutations. Further, the TRAP cytoplasmic tail was interchangeable with the cytoplasmic tail of *Toxoplasma* MIC2 protein, revealing a conserved makeup of the gliding machinery across apicomplexan parasites. Like MIC2 that undergoes an anterior to posterior redistribution during parasite host cell invasion, the amino acid substitutions also revealed a similar function of TRAP, emphasising its role in providing the necessary force to perform gliding motility [120].

S13 codes for a protein that bears a membrane attack complex/perforin (MACPF) related domain. The expression of this transcript in sporozoite stages is in agreement with its role in breaching sinusoidal barriers, prior to hepatocyte infection. The S13 protein localises to micronemes, an organelle that also harbors other proteins essential for host cell invasion. The *S13* KO mutants lacked membrane wounding activity required to cross sinusoids to access the hepatocytes [22]. Thus, the pore forming activity of sporozoites is highly essential for establishing infection. Similar to S13, another member of the MACPF family was shown to be highly expressed in the ookinete stages. Referred to as MAOP (membrane attack ookinete protein), it also localises to micronemes, confers the ookinetes with the ability to traverse the midgut epithelial cells [261]. Following ingestion of infected blood containing *MAOP* KO's, the mosquito midgut epithelial lining was intact in comparison to the damage caused by the WT ookinetes. The MAOP mutants reached the midgut epithelium and remain attached without gaining entry into the cytoplasm owing to a defect in their ability to rupture the cell membrane. Thus break down of cellular membrane seems to be a common theme to access the host cell and establish infection across different invasive stages of *Plasmodium*.

S16 (PB107027.00.0/PB107193.00.0/PB001101.03.0), orthologous to PFF1195c, when depleted, did not manifest defect in oocyst stage nor its ability to reach the salivary gland. The salivary gland sporozoites were able to establish infection in mice, similar to WT suggesting a dispensable role of S16 in *Plasmodium* life cycle [245].

S21, also referred to as thrombospondin-related sporozoite protein (TRSP) also possesses at its N- terminal end a thrombospondin type 1 repeat and *TRSP* KO did not manifest any defect in asexual development, transmission of malaria to mosquitoes, development of oocyst, sporulation and invasion to salivary glands. However, the mutants are highly compromised in their ability to invade hepatocytes, both under *in vitro* and *in vivo* conditions. Thus TRSP plays a role in facilitating and establishment of infection through initial contact with hepatocytes prior to invasion [248].

S22, also designated as Sporozoite Asparagine-rich Protein-1 (SAP-1) was interestingly known to play a role in regulating the expression of *UIS-3* and *UIS-4* that maintain the sporozoite infectivity to hepatocytes. Deletion of SAP-1 in rodent species did not affect the sporozoites ability to traverse hepatocytes under *in vivo* or *in vitro* conditions, however the mutants were severely compromised to initiate liver stage development [58]. Its localisation to sporozoite cytoplasm may likely hint to its involvement in post-transcriptional regulation of gene expression control of infectivity associated genes [57].

S23, also referred to as SSP3, is a conserved sporozoite surface protein unique to *Plasmodium* with a putative type 1 transmembrane domain. The protein is expressed both in midgut sporozoites as well as in salivary gland sporozoite stages with cytoplasmic and surface localisation respectively. Deletion of SSP3 resulted in a defect *in vitro*, in gliding motility that however did not impact the ability of these mutants to perform cell traversal activity or host cell invasion both, *in vitro* and *in vivo* [247]. In contrast to these findings, a mutant of S23 generated in our laboratory (Togiri Jyothi, S Rameswara Reddy and Kumar KA, unpublished) did not affect sporozoite gliding. The mutants invaded HepG2 cells and completed the liver stage development, as efficiently as WT parasites. However, infection of C57Bl6 mice with S23 mutants failed to initiate a blood stage infection. In 3 independent experiments, involving 3-5 mice C57Bl6 mice per group, we observed that more than 80% of the mice were unable to give rise to a breakthrough infection whereas all mice infected with WT parasites had a pre patent period of day 3. In mice that became positive for infection, the prepatent period was extended to day 5, suggesting a likely attenuation of the late liver stages following depletion of S23.

S24, (PB000251.01.0), orthologous to PFA0205w was also recovered in the proteomic profiling of the sporozoites stages [245]. Attempts to generate S24 KO was not successful suggesting the loci is recalcitrant to genetic modification, and hence highly essential for the survival of the parasite.

Thus, the above cited literature clearly justifies that majority of the S genes have crucial roles in mosquito and liver stages of *Plasmodium*. Beginning from the oocyst stages, in the salivary gland sporozoite stage, in interaction with hepatocytes, invasion into host cell, liver stage development and in regulation of infection inducing factors, the S genes play a myriad role in governing the sporozoite infectivity. In the current study we have selected S10, a yet to be characterised sporozoite gene and through functional investigation by reverse genetics approach, prove its role in early liver stage development. As demonstrated for other S gene mutants like S3/UIS-4, S7/UIS-3 and S22/SAP-1, we demonstrate the requirement of S10 in liver stage development and propose that it can be a target for achieving attenuation of liver stages in other *Plasmodium* orthologues, including human malaria, *P. falciparum*.

3.2 Materials and methods

Most of the experiments described in this chapter are similar to those mentioned in Chapter 2. Hence the materials and methods below are only mentioned briefly to avoid redundancy.

3.2.1 Retrieval of *Plasmodium berghei* (Pb) target gene, protein sequences, alignment and similarity analysis of PbS10

Plasmodium genomic database, Plasmodb (www.plasmodb.org) and Sanger's Gene database (<http://www.genedb.org/Homepage/Pberghei>) were used for retrieval of all *Pb* gene, protein and untranslated region sequences. Amino acid sequences of PbS10 from *Plasmodium berghei* (rodent) (PBANKA_100250), PyS10: *Plasmodium yoelii* (rodent) PY01067, PfS10: *Plasmodium falciparum* (human) PF3D7_0404800, PvS10: *Plasmodium vivax* (human) PVX_001000 were aligned by Clustal Omega tool (<http://www.ebi.ac.uk/Tools/msa/clustalo/>). PbS10 amino acid sequence similarity among *Plasmodium* species was done by using NCBI BLASTP tool (<https://blast.ncbi.nlm.nih.gov/Blast.cgi?PAGE=Proteins>). Primers used for amplification of *P. berghei* S10 sequences for quantitative real-time PCR (qRT-PCR), generation of knock out plasmids and for integration confirmations are listed below.

S. No	Name of the primer	Primer sequence (5'-3')
1	<i>PbS10</i> TA FP	ACATGAATCCCAAGAAAATGAT
2	<i>PbS10</i> TA RP	AACTAATTTCCCTTCTGTCTTCT
3	<i>PbS10</i> GD 5' FP (FP1)	AGA <u>CTCGAG</u> ATGAATAAACTATATGCTTG
4	<i>PbS10</i> GD 5' RP (RP1)	TAA <u>ATCGAT</u> TTTTTCGGTTTTTTCTTTTCT
5	<i>PbS10</i> GD 3' FP (FP2)	ACA <u>GCGGCCGC</u> TCGTATAGGAAATAAAGAAAA
6	<i>PbS10</i> GD 3' RP (RP2)	GAA <u>GGCGCGCC</u> TTATTCCATAGCAAACCTTGT
7	<i>PbS10</i> 5' confirmation FP (FP3)	ATAGAAGGTCAAAATGAATGA
8	HSP705' UTR RP (RP3)	TTCCGCAATTTGTTGTACATA
9	DHFR FP (FP4)	GTTGTCTCTTCAATGATTCATAAATAG
10	<i>PbS10</i> 3' confirmation RP (RP4)	CATGCTATACATGAAAAATGA
11	<i>PbS10</i> ORF FP (FP5)	AACTGAATACTAACAAAATTT
12	<i>PbS10</i> ORF RP (RP5)	TAAATCGATATCTTTAAAAAAT

Table 3: List of primers used for *PbS10* qRT-PCR (Fig 22) and generation and integration confirmation of *PbS10* GD mutants (Fig 23). Restriction sites are in bold and underlined.

3.2.2 Quantitative real time PCR analysis of *PbS10* expression across all the life cycle stages

The expression of the *PbS10* was measured by absolute quantification method. cDNA was generated from equal concentrations of RNA derived from rings, mixed blood stages, midgut sporozoites, salivary gland sporozoites and liver stages at 16 h, 25 h, 42 h, 50 h and 65 h post infection with *Plasmodium* sporozoites. Gene specific standards were generated for *PbS10* by amplifying 145 bp product from *P. berghei* genomic DNA and ligated into pTZ57R/T vector. The sequences of forward primer and reverse primers were listed in table 3.

The clone was confirmed for presence of insert by double digestion. Gene specific standards were generated over a range of plasmid concentrations from 10^8 to 10^2 per μL by log dilution at each step. The cDNA samples were run alongside with gene specific standards generated within a log range from 10^2 to 10^7 per μL . The target gene was expressed as equivalents of gene specific standards. Similarly, gene specific standards for *Pb18S rRNA* (internal control gene) were also generated in a log range. qRTPCR was carried out in a $10\mu\text{L}$ reaction containing SYBR Green PCR master Mix (Bio rad, Cat No # 1708882) and $0.25\mu\text{M}$ gene specific primers. qRTPCR was performed using the EPPENDORF REALPLEX 2 qPCR machine. A ratio of transcript numbers of *PbS10* and *18S rRNA* was obtained to normalize the gene expression data.

3.2.3 Generation of *PbS10* (PBANKA_100250) gene disruption construct

3.2.3.1 PCR

Double homologous recombination strategy was used to disrupt *PbS10*. To achieve this, *PbS10* targeting construct was generated using pBC-GFP-hDHFR vector. *P. berghei* genomic DNA was used as template to amplify 507 bp 5' CDS part of the *PbS10* with *PbS10* 5' forward primer (FP1), *PbS10* 5' reverse primer (RP1) and 530 bp 3' CDS part with *PbS10* 3' forward primer (FP2), *PbS10* 3' reverse primer (RP2). PCR was set up with 1X PCR buffer, $0.25\mu\text{M}$ FP, $0.25\mu\text{M}$ RP, 1mM dNTPs each (Thermo Scientific, Cat No# R72501), 2.5 mM MgCl_2 , 30-50 ng genomic DNA and 2.5 units of Taq DNA polymerase (Thermo Scientific, Cat No# 11615010). Thermal cycling was performed in Eppendorf mastercycler PCR machine, and the cycling conditions were as follows: initial denaturation at 94°C for 2 min and 94°C for 30 sec, annealing at 52°C for 30 sec followed by synthesis at 72°C for 1 min. The cycles were repeated for 35 times except initial denaturation and final extension was done at 72°C for 10 min. Amplified products were visualized by UV illuminator after resolving on 1% agarose gel by loading $5\mu\text{L}$ sample and the gel image was documented. PCR amplified products were purified

by DNA clean up and gel extraction kit (Fermentas, Cat No# K0831). DNA concentration was measured by Nanodrop 2000.

3.2.3.2 Cloning of 5' CDS region of *PbS10*

PCR amplified 5' CDS part was purified and concentration was measured by Nanodrop 2000. Approximately 1-2 µg of PCR product was kept for double digestion with 1U of XhoI and 1U of ClaI using 3 µL fast digest buffer (Thermo scientific) and the reaction mixture was made up to 30 µL with nuclease free water. Approximately 2 µg of pBC-GFP-hDHFR plasmid was also subjected to restriction digestion for 1 h at 37 °C using same enzymes. After double digestion, both vector and inserts were purified by DNA clean up and gel extraction kit (Fermentas, Cat No#K0831) and concentration was measured by Nanodrop 2000. Ligation was set up in a reaction mixture that contained 1x ligation buffer, 100 ng insert, 100 ng vector, 1 U of T4 DNA ligase (Thermo scientific) in a final volume of 20 µL made up with nuclease free water. The ligation mixture was kept at 22 °C for 3-5 hours and 10 µL ligation mixture was subsequently transformed into XL-1 Blue MRF competent cells and plated them on LB agar plate containing chloramphenicol and tetracycline antibiotic and incubated overnight at 37 °C. Next day, 10 colonies were inoculated in LB broth and colony PCR was performed to select the positive clones. After preliminary screening, plasmid was isolated by GeneJET Plasmid Miniprep Kit (Thermo scientific, Cat No# K0502) and the clones were confirmed for the presence of insert by double digestion with XhoI and ClaI restriction enzymes. This intermediate vector was named as 5' *PbS10*-pBC-GFP-hDHFR.

3.2.3.3 Cloning of 3' CDS region of *PbS10*

PCR amplified and purified 3' CDS part and 5' *PbS10*-pBC-GFP-hDHFR intermediate vector were kept for double digestion with AscI and NotI restriction enzymes (Thermo scientific) for 1 h. After digestion, insert and vector were purified and concentration was measured. Ligation was performed at 22 °C for 3-5 hours. Nearly 10 µL of the ligation mixture was used for transforming XL-1 Blue MRF competent cells and positive clones were preliminarily confirmed by colony PCR and re confirmed by double digestion with AscI and NotI restriction enzymes. Sequencing was done for both 5' and 3' inserts that were cloned into the pBC-GFP-hDHFR vector resulting in *PbS10* gene disruption construct. This construct was purified in large scale by Sureprep plasmid MAXI kit (Genetix, Cat No# NP-15162) and was subjected to restriction digestion with XhoI and AscI enzymes to release targeting cassette containing GFP-hDHFR flanked on either ends with 5' and 3' CDS regions of *PbS10*. The restriction digestion products were resolved in 1% agarose gel and the product was extracted by

DNA clean up and gel extraction kit (Fermentas, Cat No#K0831) and concentration was measured with Nanodrop 2000. The purified targeting cassette used for disrupting the *PbS10* locus.

3.2.4 Transfection of *PbS10* gene disruption construct into schizonts and selection of transfected parasites

Electroporation, drug selection and limiting dilution was done as described earlier in the materials and methods of chapter 2 [2]. Briefly, electroporation of *PbS10* gene disruption construct was done using the Amaxa nucleofector kit (Lonza). For electroporation, 90 μ L of mouse T cell nucleofector solution was mixed with 20 μ L of supplement to prepare nucleofector solution. The nucleofector solution was mixed with 10 μ g of purified *PbS10* gene disruption construct. This mixture was then added to the pelleted nearly 5×10^7 schizonts and gently transferred into nucleofector cuvette and placed in Amaxa nucleofector device. Electroporation was done using U033 program. Following electroporation, 100 μ L of schizont culture media was added immediately into the cuvette and the contents were immediately injected intravenously into mice. Twenty four hours post transfection, caudal blood smears were made from mice and were Giemsa stained. Recombinant parasites were selected by allowing mice to obtain orally administered pyrimethamine, that was prepared by dissolving 7 mg drug in 1ml of DMSO and made up to 100 ml in sterile water following adjustment to pH 4.0. After 5-7 days, the non-transfected parasites were cleared and transfected population emerged gradually. When parasitemia reached to 3-5%, 2-3 μ L blood was collected from the tail vein and observed under fluorescence microscope for presence of GFP parasite. After confirming the presence of GFP parasites in the blood, approximately 500 μ L infected blood was collected in freezing medium containing 100 U of 1X heparin. The freezing medium was composed of 9 parts Alsever's solution (Sigma, Cat no# A3551) and 1 part glycerol (Invitrogen, Cat No# 15514011). One part blood and 2 parts freezing media were mixed gently and nearly 250-300 μ L was aliquoted into cryo vials (Corning, Cat No# CLS430658) and stored at -80 $^{\circ}$ C in a freezing container (Nalgene, Cat# 5100) which cools gradually at 1 $^{\circ}$ C per 1 min and the samples were shifted to liquid nitrogen after 24 h for long term preservation.

3.2.5 Confirming the stable integration of *PbS10* gene disruption construct in endogenous locus

The infected RBCs were lysed in a 0.5% saponin solution, centrifuged at 10,000 rpm for 5 min. The saponin lysis was repeated for 2 times. The pellet was washed with 1X PBS and centrifuged at 10,000 rpm for 5 min. Genomic DNA was isolated from pelleted parasites by

using the DNAsure tissue mini kit (Genetix, Cat No# NP-61305). The integration of *PbS10* gene disruption construct into endogenous locus was confirmed by integration specific PCRs. For 5' integration confirmation, FP3 primer was designed beyond the site of integration and RP3 primer was designed within GFP cassette. For 3' integration confirmation, FP4 primer was designed in hDHFR cassette and RP4 primer was designed from genomic sequence after the site of integration. Following this confirmation, the limiting dilution was done to isolate single clones of the *PbS10* gene disrupted mutant. To obtain the single clone, blood was collected from mice that were having 3-5 % parasitemia and was diluted at 1:10,000. The number of RBCs were counted using hemocytometer. Twenty mice were intravenously injected with approximately 0.5 parasites/mouse. After 7-9 days, parasitemia was analysed and parasite genomic DNA was isolated from mice that became positive for infection. The absence of wild type contamination was confirmed by PCR using primers FP5 and RP5 designed within the *PbS10* ORF that confirmed the disruption of gene with the GFP-hDHFR cassette. Two clones were selected from two independent transfections.

3.2.6 Phenotypic analysis of *PbS10* gene disrupted (GD) mutant in blood stages

Since *PbS10* GD mutants were generated as GFP line, as an appropriate control, we also obtained a WT-GFP control line where a non-essential *p230P* locus was disrupted by integration of GFP-hDHFR cassette [225]. This line was designated as WT GFP. Nearly 10^3 mixed blood stage parasites of both WT GFP or *PbS10* GD mutants were injected into 4-6 week old Swiss albino mice by intravenous route. Parasitemia was monitored daily to assess the asexual growth kinetics of the *PbS10* GD mutants by making Giemsa stained blood smears. Parasitemia was determined by checking 25 random fields under light microscope.

3.2.7 Transmission of *PbS10* GD mutants to *A. stephensii* to study mosquito stages of the parasite

A cage of 250-300 female *A. stephensii* mosquitoes were prepared for transmission of malaria. Approximately 10^6 iRBCs of either WT GFP or *PbS10* GD mutants were injected into Swiss albino mice that were nearly 6 weeks old. Following confirmation of gametocytes in these mice, the *A. stephensii* mosquitoes were allowed to obtain blood meal for 15 min. During this process, the position of the mice was moved for every 4-5 minutes to ensure that a maximum number of mosquitoes obtained blood meal from more than one mice. The same procedure was repeated on the second day. Following 2 feedings, the mosquitoes were maintained at 20°C temperature and 80% humidity for 21 days. On D14 post blood feeding, midguts were dissected and the oocyst infectivity was observed under a fluorescence microscope. On D18 post

infection, the salivary glands of mosquitoes were dissected and were observed for sporozoite loads (Fig 9 H). Both midguts and salivary glands were mechanically disrupted with a plastic pestle, centrifuged at 800 RPM for 3 min at 4 °C and supernatant containing partially purified sporozoites was collected. Sporozoite numbers were counted using hemocytometer. Oocysts, salivary glands and sporozoites were observed under an upright fluorescent microscope (Nikon Eclipse). The images were captured, processed and deconvoluted by NIS software.

3.2.8 Assessment of *in vivo* sporozoite infectivity of *PbS10* GD mutants

To determine pre-patent period (defined as defined as the time required for the appearance of blood stages following infection with sporozoites) of *PbS10* GD mutant sporozoites, 2×10^4 sporozoites were injected each into 5 C57BL/6J mice through intravenously route and parasitemia was monitored from D2 onwards daily for 7 days by examination of Giemsa stained blood smears. Malaria was also transmitted through bite mosquitoes infected with mutant sporozoites to a group of 5 naïve C57BL/6J mice. Approximately 25-30 mosquitoes were used per mouse for transmission. Following 25 min feeding, nearly 80% of the mosquitoes were positive for blood meal as evident by visual inspection. Of all the blood meal positive mosquitoes, nearly 70-75% were positive for salivary gland sporozoite infection as judged by fluorescent microscopy.

3.2.9 Cell traversal assay and cell invasion of *PbS10* GD mutant sporozoites

To a monolayer of HepG2 cells maintained in a 24 well plate, 2×10^4 sporozoites of either WT GFP or *PbS10* GD mutants were added in the presence of dextran conjugated to Texas Red (10,000 MW, Neutral, Invitrogen, Cat No# D1828). The plate was centrifuged at 1500 rpm for 4 min. Cells were incubated to allow sporozoites to invade for 1 h in 37 °C CO₂ incubator. In a control experiment, cells were incubated with the lysates from uninfected salivary glands in the presence of dextran Texas Red. As a negative control, sporozoites that were treated for 30 min with cytochalasin D, and washed were added to cultures in the presence of dextran Texas Red. After 1hr incubation, the cells were washed with PBS for removal of excess dextran and stained with DAPI to visualise for host cell and sporozoite nuclei. From each group, 25 fields were counted under fluorescence microscope for dextran positive cells and graph was plotted.

The *PbS10* GD mutant sporozoites ability to invade host cells was also confirmed by performing sporozoite inside out assay. For this assay, 2×10^4 sporozoites of WT GFP or *PbS10* GD mutant were added to HepG2 cells and incubated for 2h. Cells were fixed and

immunostaining was performed. The extracellular sporozoites were stained with mouse anti-PbCSP (3D11) and were revealed with anti-mouse Alexa Fluor 594 (red). Following this staining, cell were permeabilized with 1:3 acetone methanol (for staining total number of sporozoites) and stained with anti-PbCSP 3D11 primary Ab, revealed with Alexa Fluor 488 (green). Approximately 25 fields were counted for both WT GFP and *PbS10* GD sporozoites under florescence microscope and the percentage of host cell invasion was calculated as (green parasites – red parasites)/green parasites and plotted in the graph.

3.2.10 *In vitro* infectivity of *PbS10* GD mutant salivary gland sporozoites

A 24 well plate (Nunc, Cat No# 142475) was coated with 1X collagen (Sigma, Cat No# C3867-1VL) over night and on following day, 2×10^5 cells were seeded and maintained in complete DMEM (cDMEM) at 37 °C in a CO₂ incubator. After confirming the establishment of a monolayer of HepG2 cells under phase contrast microscope, approximately 2×10^4 sporozoites of WT GFP or *PbS10* GD mutants were added to cultures and the plate was centrifuged at 1500 rpm for 4 min. The culture medium was changed after 3 h and to avoid contamination and the medium was subsequently replenished every 8 h till 65 h time point with cDMEM containing 2X antibiotic and antimycotic medium (Gibco, Cat No# 15240062). At 12 h, 36 h and 62 h cover slips were removed, fixed in 4% formalin solution (Sigma, Cat No# HT5011) and stored in 4 °C till it was taken for immunofluorescence assay. The developing EEFs were stained using a parasitophorous vacuolar membrane specific antibody- UIS4 (rabbit polyclonal) and immunoreactivity was revealed using an anti-rabbit secondary antibody conjugated to Alexa fluor 594.

3.3.2 *PbS10* is expressed in all the life cycle stages of *Plasmodium*

Gene expression analysis of *PbS10* across all the parasite stages as measured following normalization with *Pb18S rRNA* revealed maximal expression in midgut sporozoite stage followed by salivary gland sporozoite stage and meagre expression in liver and blood stages. The high expression of *PbS10* in sporozoite stages is in accordance with earlier published microarray data (Kaiser), it was observed that *PbS10* is upregulated in midgut sporozoites, salivary gland sporozoites and very low amounts (negligible) are observed in liver stages and mixed blood stages (Fig 23).

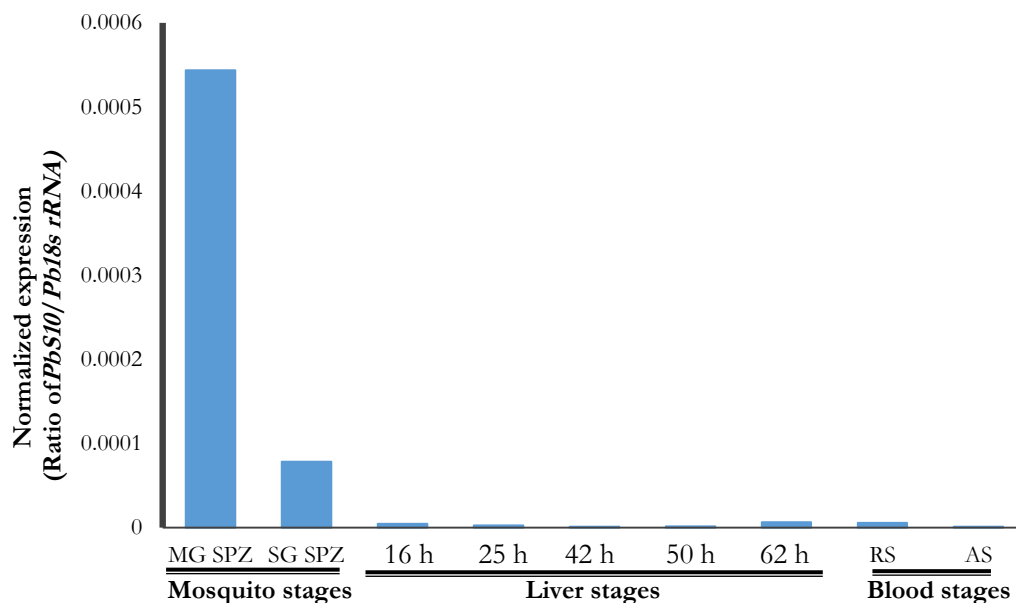


Fig 23: Quantitative real time PCR analysis of *PbS10* across all *Plasmodium* life cycle stages. Analysis of *PbS10* gene expression by qRT-PCR revealed maximum expression in the midgut sporozoites followed by salivary gland sporozoites. *PbS10* absolute transcript numbers were normalized to *Pb18S rRNA* (internal control gene) absolute copy numbers and expressed as a ratio for each of the stage. **Mosquito stages:** MG SPZ; midgut sporozoites (14 days post infection to mosquitoes), SG SPZ; salivary gland sporozoites (18 days post infection). **Liver stages:** 16 h, 25 h, 42 h, 50 h and 62 h of liver stages. **Blood stages:** RS; rings, AS; asexual mixed blood stages.

3.3.3 Successful disruption of *PbS10* locus with GFP-hDHFR cassette by double homologous recombination

The genomic organization of *PbS10* gene locus is shown in Fig 24 A. The targeting construct carrying the 5' and 3' part of the *PbS10* cloned on either ends of GFP-hDHFR cassette is shown in Fig 24 B. Following successful recombination, the endogenous *PbS10* was disrupted resulting in the recombined locus as shown in Fig 24 C. Fig 24 D shows the PCR amplified products of 5' and 3' regions of *PbS10*. Fig 24 E shows the release of the targeting cassette from vector back bone using restriction enzymes Xho1 and Asc1. The adjacent lanes show the release of the respective of 5' and 3' fragments following restriction digestion with Xho1/Cla1 and Not1/Asc1. A diagnostic PCR was set up to confirm correct site specific integration using genomic DNA obtained from drug resistant parasites from two independent transfections. In Fig 24 F, an expected product size of 1231 bp with primer set FP3 and RP3 in clones C1 and C2 indicated correct integration of the GFP-hDHFR cassette at the 5' end of *PbS10*. Also, an expected product size of 1530 bp with primer set FP4 and RP4 in clones C1 and C2 indicated correct integration of the GFP-hDHFR cassette at the 3' end of *PbS10*. Genomic DNA of both clones C1 and C2 did not amplify a PCR product with primer set FP5 and RP5 while WT genomic DNA gave a product of 559 bp confirming the complete absence of WT parasites in clonal populations, C1 and C2 as shown in Fig 24 G. Consistent with the correct integration of the GFP-hDHFR cassette, both clones expressed GFP constitutively, as shown Fig 24 H.

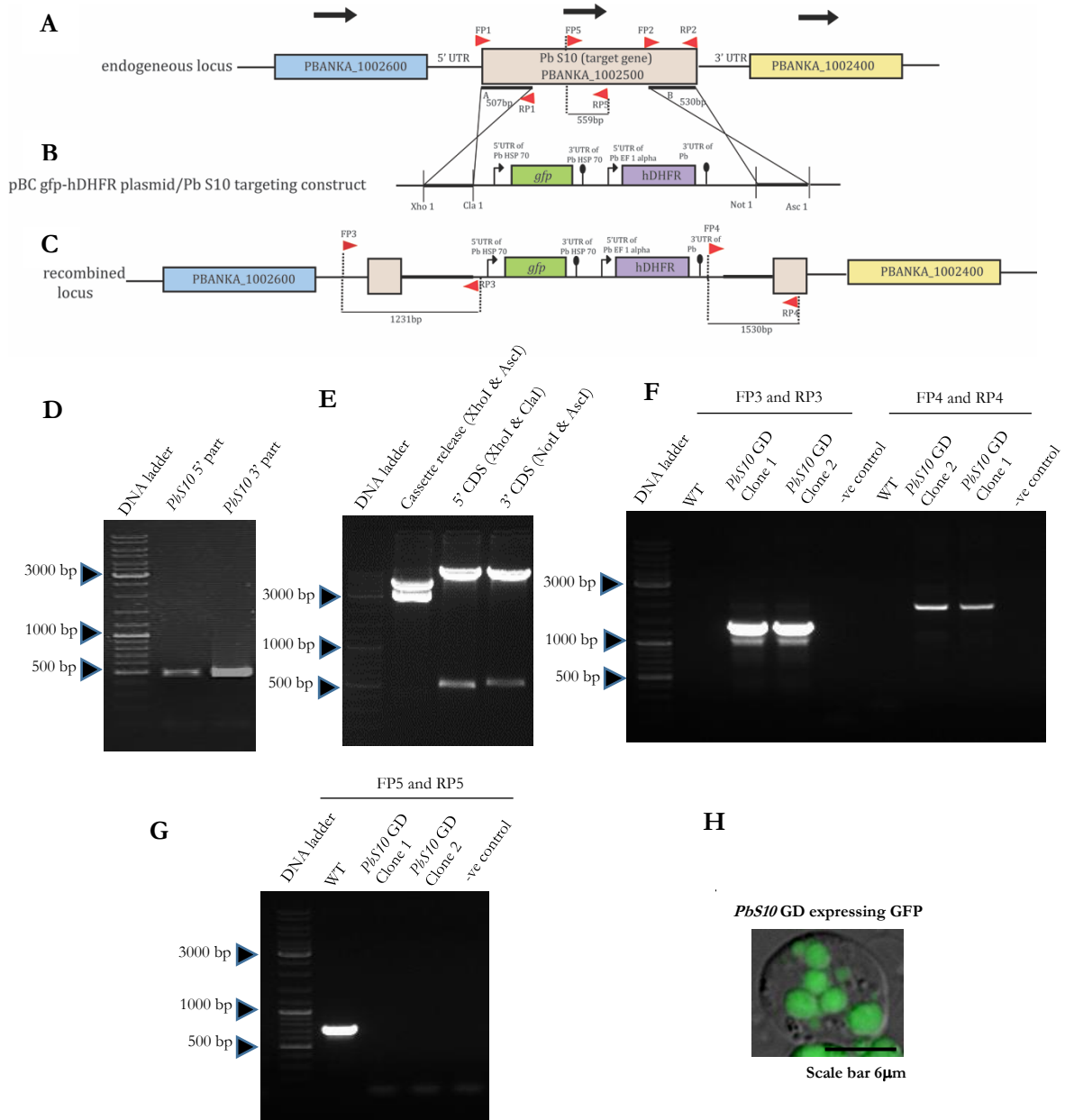


Fig 24: Generation of *PbS10* GD mutant parasites. **A)** Representation of *PbS10* endogenous locus showing *PbS10* ORF, 5' and 3'UTR regions. **B)** Elements of targeting construct showing, 507 bp of 5' CDS part and a 530 bp 3' CDS part of *PbS10* cloned on either ends of pBC-GFP- DHFR vector using XhoI/ClaI and NotI/AscI respectively, GFP reporter and hDHFR drug resistance marker. *PbS10* was linearized with XhoI and AscI, transfected into schizonts to replace the gene. **C)** Representation of endogenous locus after integration of targeting vector into *PbS10* gene by double cross over. **D)** A 1% agarose gel showing PCR amplified 507 bp of 5' and 530 bp 3' CDS parts of *PbS10* with FP1/RP1 and FP2/RP2 primers respectively, **E)** restriction digestion products of 507 bp of 5' CDS part and 530 bp 3' CDS part of *PbS10* following release with XhoI/ClaI and NotI/AscI respectively and construct linearized with XhoI and AscI. **F)** Diagnostic PCR with one primer beyond the site of integration in endogenous locus and the other within the targeting construct. FP3/RP3 primers for 5' integration confirmation and FP4/RP4 primers were used for 3' integration. **G)** Drug resistant parasites were clonal diluted for single clone without wild type contamination and was confirmed by FP5/RP5 primers. **H)** Merged DIC image of infected RBC showing GFP expressing parasite

3.3.4 PbS10 has no role in blood stage propagation

Investigation of asexual blood stage propagation of *PbS10* GD parasites as compared to WT GFP following infection with 1×10^3 iRBC into Swiss albino mice did not show any difference in their rates of propagation. (Fig 25 A). All asexual forms like rings, trophozoites and schizonts as well as sexual gametocyte stages were readily observed in *PbS10* GD mutants. We conclude that PbS10 depletion does not affect the asexual development of parasite in the blood.

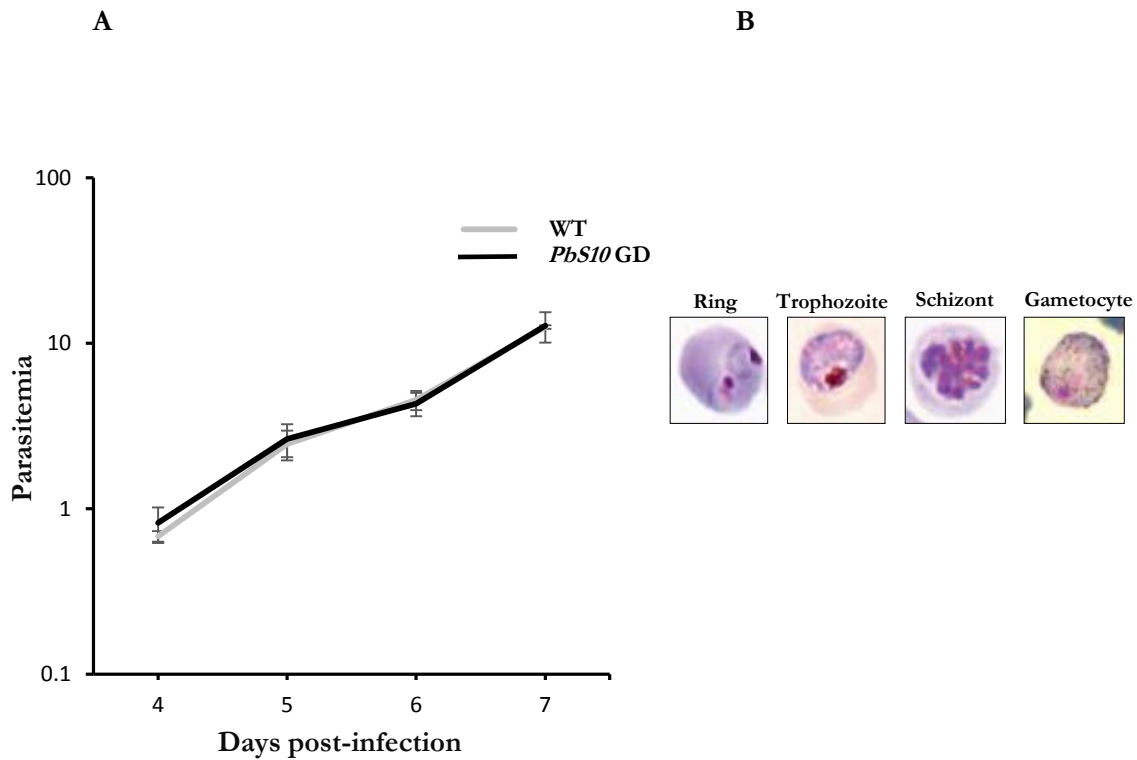


Fig 25: Asexual blood stage propagation of *PbS10* GD mutant parasites: A) One thousand mixed blood stage parasites of both WT GFP and *PbS10* GD mutant parasites were injected into 4–6 weeks old Swiss albino mice through intravenous route. Parasitemia was monitored by observing daily blood smears stained with Giemsa, and found no difference with wild type propagation. **B)** Shown are representative images of rings, trophozoite, schizont and gametocyte obtained from [226].

3.3.5 *PbS10* GD mutants undergo normal development in the mosquito

Following transmission of *PbS10* GD mutants to female *A. stephensi*, the development of the parasite was analysed at D14 by observing the oocyst and the sporulation pattern within it. We noted that the mutants showed similar number of oocyst as WT GFP (Fig 26A and B). Further, there was no difference in the sporulation pattern (Fig 25C) and enumeration of the midgut oocyst sporozoites also showed similar frequency (Fig 26D). On D18–21 post infection, dissected salivary glands contained *PbS10* GD mutant sporozoites whose numbers were similar

to WT GFP sporozoites (Fig 27A and B). Thus PbS10 depletion did not affect the mosquito stages of *Plasmodium*.

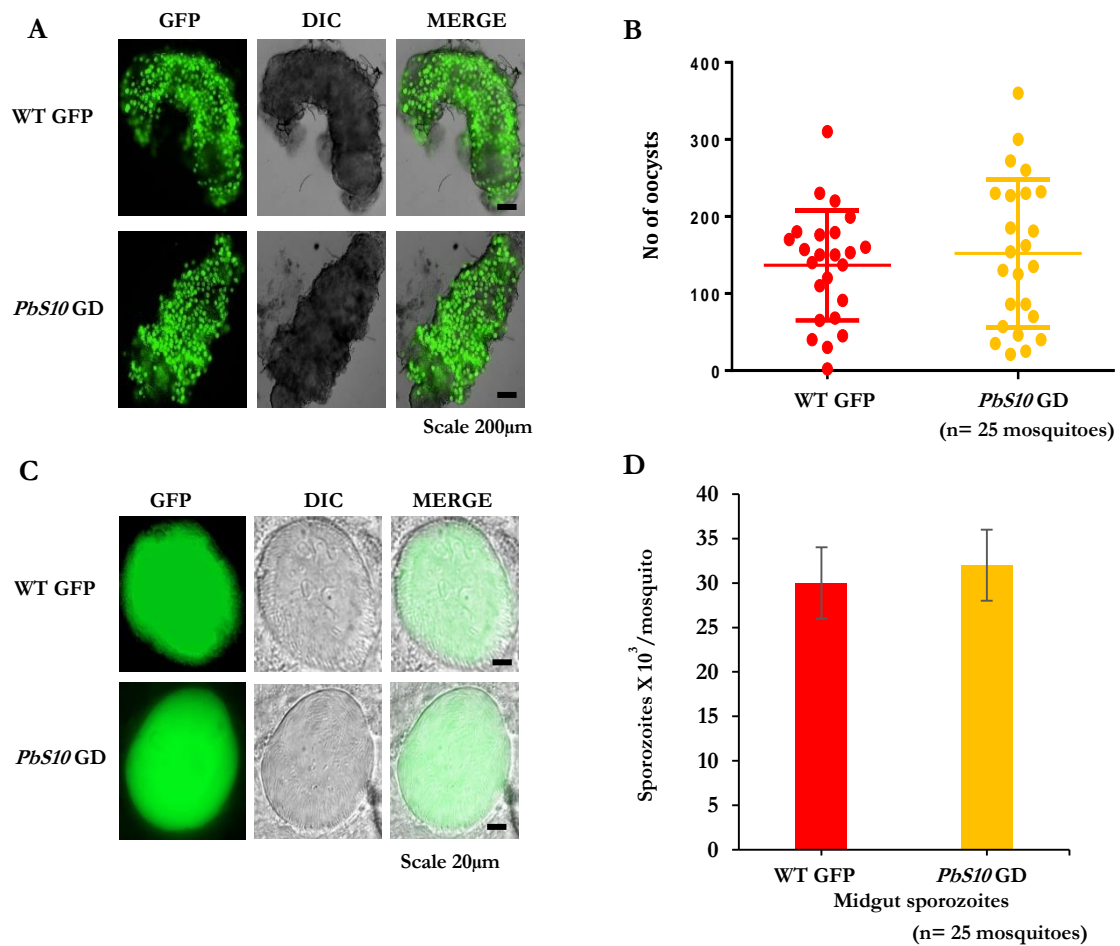


Fig 26: *PbS10* has no role in oocyst infectivity. Mosquitoes were fed on infected mice either with WT GFP or *PbS10* GD mutants harboring gametocytes in the circulation and analysed for oocyst development at day 14 post blood meal. **A)** Dissected midguts of mosquitoes infected with WT GFP and *PbS10* GD mutants at day 14 of post blood meal shows oocysts in similar rates. Individual dissected midgut of WT GFP infected mosquito, *PbS10* GD mutants infected mosquito showing oocysts. **B)** Dot plot showing quantified oocyst numbers in each of 25 mosquitoes for WT GFP and *PbS10* GD mutants infected mosquito. **C)** Individual oocyst from both WT GFP and *PbS10* GD mutants showing sporulation. **D)** Bar graph drawn from average number of midgut sporozoites from 25 infected mosquitoes from WT GFP and *PbS10* GD mutants showing comparable number.

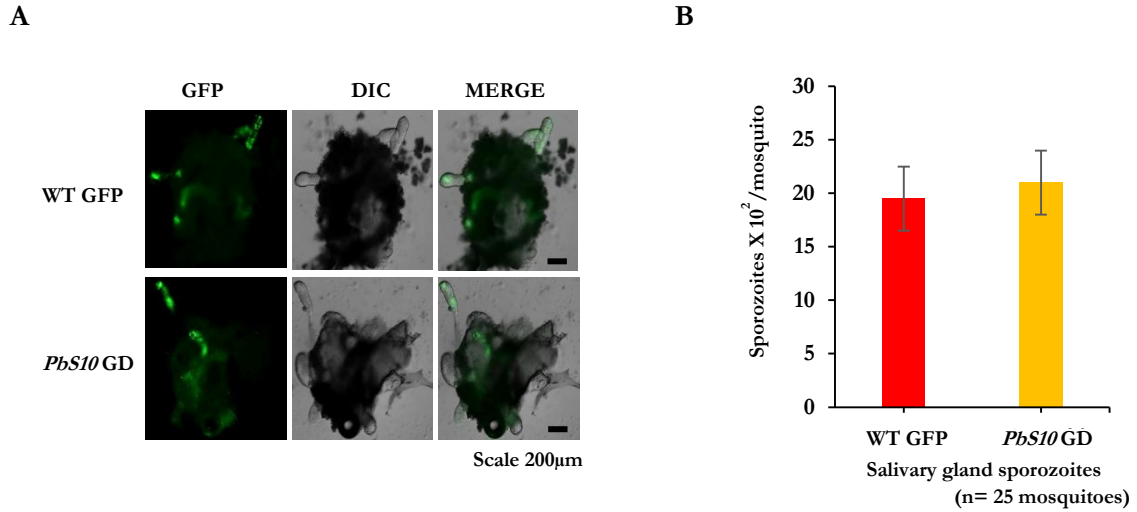


Fig 27: PbS10 depletion does not affect salivary gland sporozoite load. Dissected salivary glands of mosquitoes infected with WT GFP and *PbS10* GD mutants at day 18 of post blood meal shows sporozoites in similar rates. **A)** Individual dissected salivary gland of WT GFP parasites infected mosquito and *PbS10* GD mutants infected mosquito. **B)** Bar graph drawn from average number of salivary gland sporozoites from 25 infected mosquitoes from WT GFP and *PbS10* GD mutants showing comparable number.

3.3.6 *PbS10* GD mutant sporozoites manifested delayed prepatent period

PbS10 GD mutant sporozoites (2×10^4) when induced intravenously (Fig 28) or delivered through mosquito bite (Fig 29) into a group of 3-5 mouse in three to five independent experiments revealed that nearly 80% of the mice were recalcitrant to breakthrough infection as no blood stages were detected until 15 days post infection. However, nearly 20% of mice developed a delayed prepatency period on 9 – 12 days, while WT *Pb* GFP parasites became positive for blood stage infection by D3-3.5 (Table 4&5).

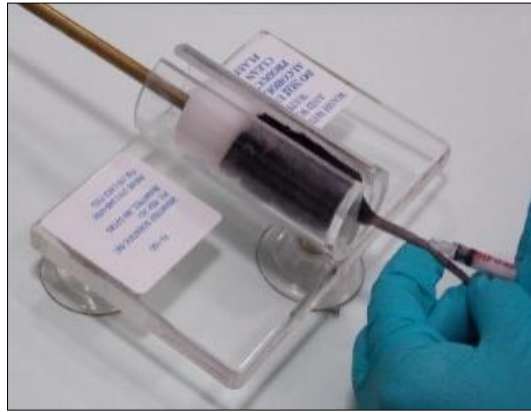


Fig 28: High dose (20,000) of *PbS10* GD mutant sporozoites injected into C57BL6/J through intravenous route mice induced occasional break through infection with delayed prepatent period

Parasite Strain	Expt no.	Number of mice used for intra venous injection (20 K SPZ)	Number of mice positive for blood stage infection	*Pre-patent period
WT	I	3	3/3	D3
	II	3	3/3	D3.5
<i>Pb S10</i> GD mutants	I	3	0/3	ND
	II	5	1♣ /5	D9
	III	5	1♣ /5	D9

Table 4: Following intravenous injection of sporozoites, mice were analysed for parasitemia by observing daily, the Giemsa stained smears for 15 days. Table showing the details about number of experiments, number of mice used for experiment and the pre patent period for each mouse (* Pre patent period: Time after inoculation of sporozoites until detection of single erythrocytic stage by microscopic examination of Giemsa stained blood smears), (♣ Mouse that gave occasional break through following sporozoite inoculation by mosquito bite with 9-12 prepatent period).



Fig 29: Transmission of *PbS10* GD mutant sporozoites to C57BL6/J mice by mosquito bite induced occasional break through infection with delayed prepatent period. Approximately 25 infected mosquitoes harboring either WT GFP or *PbS10* GD mutants were placed in captivity inside a small cage. Anesthetized C57BL6/J mouse were placed over the cage net to facilitate malaria transmission by bite while obtaining a blood meal. All the blood fed mosquitoes were dissected for salivary glands and salivary glands were qualitatively tested for the presence of GFP sporozoites under fluorescence microscope.

Parasite Strain	Expt no.	Number of mice used for bite	Number of mice positive for blood stage infection	*Pre-patent period
WT	I	3	3/3	D3.5
	II	3	3/3	D3.5
<i>Pb S10</i> GD mutants	I	3	0/3	ND
	II	5	1 [♣] /5	D9
	III	5	0/5	ND
	IV	5	1 [♣] /5	D12

Table 5: Following mosquito bite experiment, mice were analysed for parasitemia by observing daily Giemsa stained smears for 15 days. Table showing the details about number of experiments, number of mice used for experiment and number of mice became positive for infection with prepatent period (* Pre patent period: Time after inoculation of sporozoites until detection of single erythrocytic stage by microscopic examination of Giemsa stained blood smears), ([♣] Mouse that gave occasional break through following sporozoite inoculation by mosquito bite with 9-12 prepatent period).

3.3.7 PbS10 is not required for host cell traversal and invasion

The *PbS10* GD mutant sporozoites exhibited cell traversal activity as judged by presence of the dextran labeled cells. The read out of this assay though not quantitative, still implied that host cell activity was not impaired following depletion of PbS10 and that the cell traversal activity was similar to that of WT GFP sporozoites (Fig 30A and B). Quantification of sporozoite infectivity of HepG2 cells by sporozoite inside out assay or double staining method revealed no defect of *PbS10* GD mutant sporozoites in invading cells and establishing infection. Nearly 35% of the sporozoites of either WT GFP or *PbS10* GD mutant sporozoites were invaded. Fig 31 A, B and C show respectively the extracellular sporozoites, the total number of sporozoites, the merge of both A, B, with DAPI. Fig 31D shown percentage infectivity.

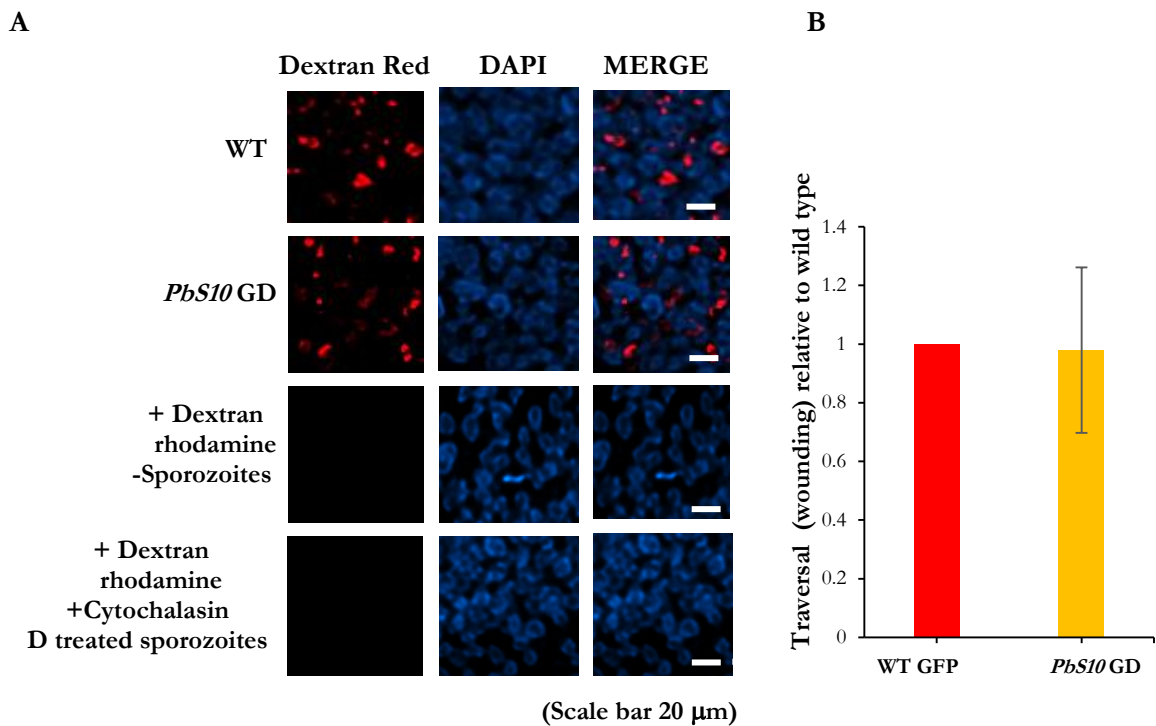


Fig 30: Cell traversal assay. To monolayer of HepG2 cells, sporozoites were added in the presence of dextran Texas red and allowed to traverse through cell for 1h. Following incubation, cells were washed and stained with DAPI for both host and parasite nuclei. **A)** Top panel shows dextran positive cells following traversed by WT GFP sporozoites. Middle panel shows dextran positive cells following incubation with *PbS10* GD mutant sporozoites. Bottom panel shows the absence of dextran positive cells following incubation with lysates from uninfected salivary glands. **B)** 25 field were checked for the number of dextran positive cells and relative number of dextran positive cells in *PbS10* GD mutant sporozoites with that of WT GFP sporozoites was represented in the graph. Graph shows similar cell traversal ability of WT GFP and *PbS10* GD mutant sporozoites.

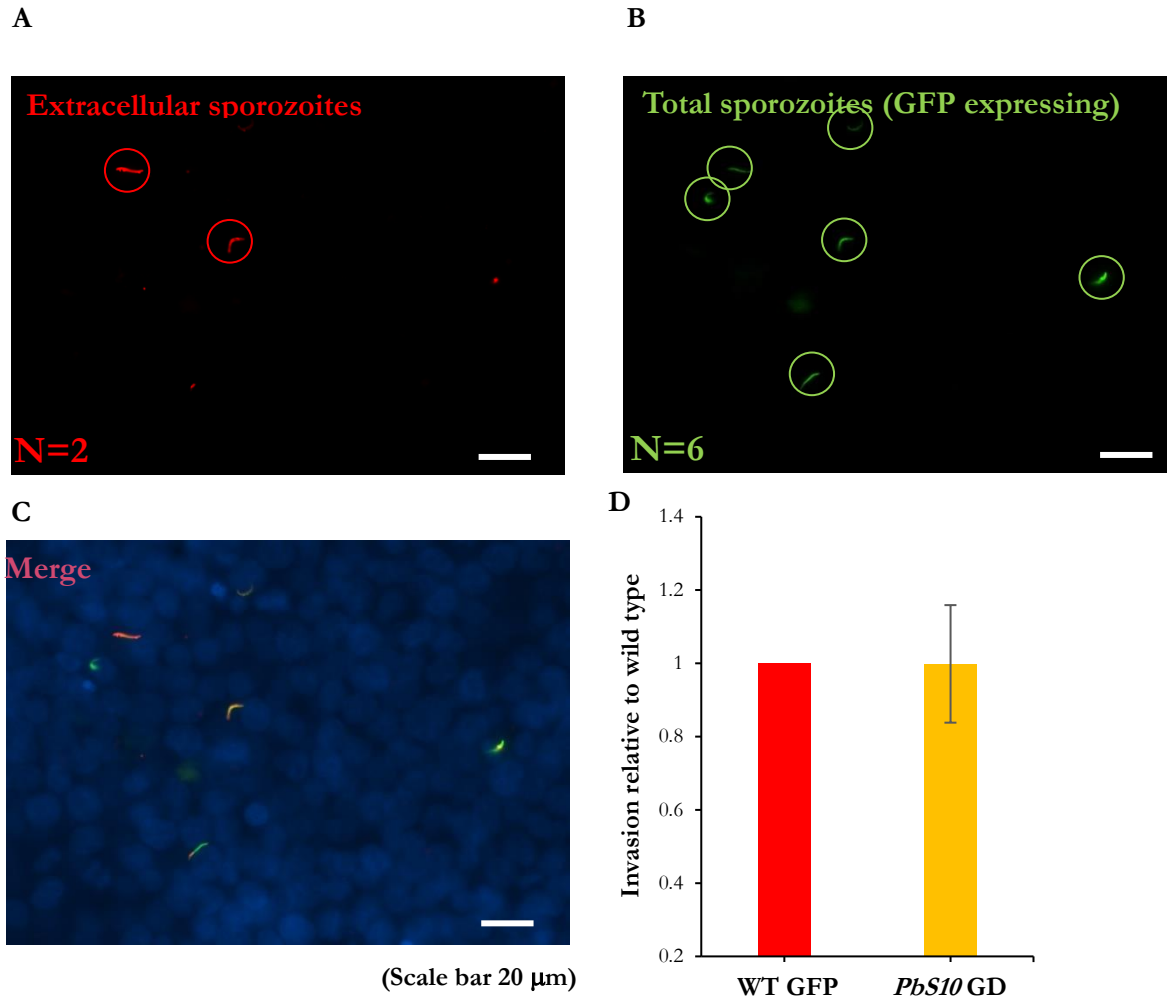


Fig 31: Cell invasion assay by inside out double staining. WT GFP or *PbS10* GD mutant salivary gland sporozoites were incubated with HepG2 cells for 2 h. Following incubation cells were fixed and stained with DAPI to visualize host and parasite nuclei and double immunostaining assay was done to distinguish extracellular and intracellular sporozoites. **A)** Extracellular sporozoites stained for CSP and revealed secondary antibody conjugated to Alexa fluor 594 (red). **B)** Following permeabilization with 1:3 acetone: methanol, total number of sporozoites (having GFP reporter) were stained for CSP and revealed with secondary antibody conjugated to Alexa fluor 488. **C)** Merged image of both extracellular and total sporozoites along with DAPI. **D)** Quantification of percentage infectivity of *PbS10* GD mutant sporozoites and WT GFP sporozoites.

3.3.8 *PbS10* GD mutant sporozoites show early developmental arrest after the invasion

Since there is no defect in host cell traversal and invasion by *PbS10* deleted parasites, further development of sporozoite in the hepatocyte was analysed at 12 h, 36 h and 62 h. Till 12 h post infection, no difference in the growth was observed for WT GFP and *PbS10* GD mutant sporozoites. However, in comparison to 36 h and 62 h time points of WT GFP *PbS10* GD mutants showed a strong growth defect that likely corresponded to arrest at around 12 h (Fig 32). Failure to initiate blood stage infection *in vivo* in the majority of mice implicated a role

of *PbS10* in the liver stage development, a finding that is consistent with the arrest of *PbS10* GD mutants during EEF development.

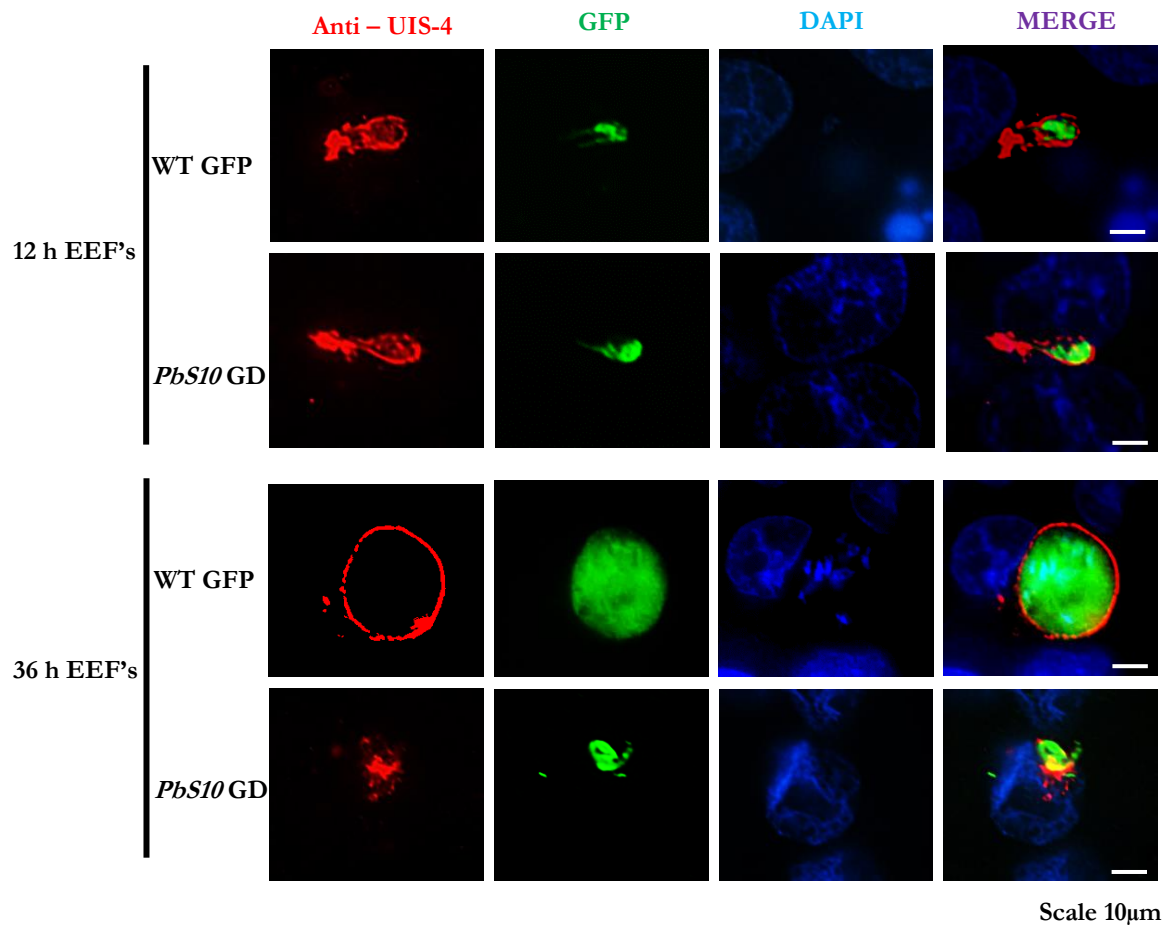


Fig 32: PbS10 is not essential for liver stage development: Nearly 2×10^4 salivary gland sporozoites of either WT GFP or *PbS10* GD mutant sporozoites were added to HepG2 cell cultures. The growth of EEF at 12 h, 36 h and 62 h was revealed by staining with UIS4 (PVM marker) and DAPI was used to stain nuclei of HepG2 cells and EEFs. *PbS10* GD mutant show normal EEF as WT GFP till 12h. *PbS10* GD mutant EEFs failed to grow beyond 12 h and showed growth defect when compared to 36h and 62h WT GFP EEFs.

3.4 Discussion

Transcriptional changes associated with salivary gland sporozoites render them highly infectious to hepatocytes. Therefore, it is very likely that the proteins encoded by these highly expressed transcripts may have important sporozoite specific functions essential for establishment of liver stage infections. Identifying these critical sporozoite genes bears immense potential towards developing attenuated sporozoite that are able to invade hepatocytes but fail to give rise to a breakthrough infections. Infact, a seminal work demonstrated the potential of using sporozoite mutants lacking UIS-3 gene as a whole organism vaccine [36]. Referred to as GAPs (Genetically Attenuated Parasites), these are very powerful antigens capable of inducing sterilising immunity, that is able to resist infection following challenge with infectious sporozoites. Based on the encouraging feasibility to obtain GAPs in rodent models, the human malaria parasite *P. falciparum* was mutated to obtain a triple KO by eliminating the genes, *p36/p52/sap1* [262]. This triple mutant, that is currently in preclinical trials, showed complete arrest in development early after infection of humanised mouse models with no breakthrough infection. Multiple attenuation of parasites seems to be a strategy to make the mutants safer for human subjects. Towards this end, it is highly essential to identify other sporozoite specific genes critical for liver stage development. Working in this direction, several sporozoite specific genes identified in transcriptomic analysis have been knocked out. It is not surprising that these mutants showed varying phenotypes ranging from defect in oocyst egress [245], [246], inability to invade the salivary glands due to compromised gliding [246], [54], [55], [53], failure to infect hepatocytes [248], [56] or lack the ability to breach sinusoidal barriers [22]. Of these mutants, the most interesting ones were those that exhibited a block in the liver stage development, owing to the absence of a desired *S* gene product that is required for normal completion for EEF development like *S3/UIS-4* [35], *S7/UIS-3* [36] and *S22/SAP-1* [57], [58]. The parasites that are stalled in their development within the hepatocytes serves as a whole organism vaccine that expresses a complement of antigens present in sporozoites and liver stages, thus exposing to the immune system to a broad repertoire of antigens.

In pursuit of identifying the functions of yet another uncharacterised gene- the *S10*, we studied its transcriptional profile and also generated a KO to study its phenotype by analysing the mutant in mammalian host as well as *Anopheles* mosquito. Quantification of the transcript abundance across all life cycle stages revealed that *S10* is highly expressed at oocyst sporozoite stage followed by salivary gland sporozoite stages. The need for high expression at these stages justifies for preparing the sporozoite for infection of mammalian host. The mutant exhibited no

defect in asexual blood stages, its ability to infect mosquito, undergo oocyst development, sporulation and reach salivary glands. However, the salivary gland sporozoites when added to HepG2 cells exhibited a block in early liver stage development. This concurred with the inability of these mutants to initiate a break through infection in nearly 80% or above mice, when tested by both intravenous delivery of sporozoites as well as by bite of infected mosquitoes. Our studies unravel the role of *S10* in liver stage development, thus qualifying this gene additionally, for generation of a multiply attenuated parasite. The early arrest of the *S10* may also, be instrumental in generation of CSP specific T cell immunity, as it is a prime target for protective immune responses. Further studies are needed, to unravel the mechanisms that leads to parasite attenuation, and the precise mode of immunity that may be engendered following immunisation of the *S10* mutants.

*Investigation of host long non
coding RNA profiles during
Plasmodium berghei and
Toxoplasma gondii infections*

4.1 Introduction

The human genome encodes nearly 25,000 proteins that represent <2% of human transcriptome and remaining constitutes the non-coding RNA [263]. Based on their length, the noncoding RNAs are subdivided into small non-coding RNAs (sncRNAs) that are shorter than 200 bp and lncRNAs that are longer than 200 bp. The sncRNAs include the microRNAs (miRNAs), short interfering RNAs (siRNAs), small nucleolar RNAs (snoRNAs) and Piwi-interacting RNAs (piRNAs) that have important roles in gene regulation [264], where as the role of lncRNAs have been primarily implicated in development [265], pathogenesis [266], cancer [267] and infections [268]. *Plasmodium* and *Toxoplasma* are obligate intracellular protozoan parasites that successfully establish infection in mammalian cells by the takeover of host cellular machinery [269]. Several lines of evidence link modulation of host non-coding RNA to protozoan infections, in particular, the miRNA [270]. For example, during *Toxoplasma* infection, nearly 14% of host miRNA are altered around 24h infection [270] with miR-146a and miR155 being induced as a host response to infection [271], [272], [273]. During *Leishmania* infection, the parasite burden in the liver is enhanced as a consequence of miR-122 downregulation [274]. Also, several host miRNAs are dramatically altered in macrophages and dendritic cells following infection with *Leishmania* [275], [276]. In *Plasmodium*, infection of hepatocytes with genetically attenuated parasites led to upregulation of miR155 and miR21, and ectopic expression of both these miRNAs circumvented the need for booster immunization dose with GAPs [277]. Some miRNAs like let7 have targets like LR4 and IL6, which are induced following infections with different apicomplexan parasites like *Cryptosporidium*, *Toxoplasma* and *Plasmodium*, likely suggesting some level of conservation in host response against different protozoan infections [270]. In fact, Let-7i that belongs to let-7 miRNA family is involved in innate immune response [278].

Thus, while ample evidence points to the role of host miRNAs in modulating the cellular response to intracellular protozoan parasites, no reports exist on how lncRNAs profiles are altered under similar conditions. We were particularly interested in studying the expression of host disease related lncRNAs during *Plasmodium* and *Toxoplasma* infections due to several interesting considerations. Firstly, in both infections, the effector response of host is by activation of Type I IFN and IFN-gamma pathways [279], [280]. Secondly, infection of *Plasmodium* sporozoites to hepatocytes, though is clinically silent, yet there is evidence for a an inflammatory response [281] while in *Toxoplasma*, infection induces immunopathological responses [282]. However, there are no evidence that bridge these findings to lncRNAs expression, given that they play a major role in modulation of inflammatory gene

expression and pathological response [283]. Third, the known link between some host lncRNAs and signaling pathways like JAK-STAT [284], NF- κ B signaling [285], and activation of such cascades during apicomplexan infections [286], [287], [42], [288] may point to an earlier unappreciated role of lncRNAs in such response. In fact, in infections caused by viruses [289], [290], [291] and intracellular bacteria [292], [293] the lncRNAs have been shown to play a dual role of either mediating clearance of these infectious agents or facilitate the establishment of infection. For example, lncRNA-CMPK2 is involved in anti-viral response and is upregulated in Hepatitis C virus (HCV) infection likely playing a negative regulatory role in the interferon response by JAK-STAT signaling pathway [284]. Negative regulator of antiviral response (NRAV) lncRNA is downregulated in many viral infections including influenza A virus thus facilitating an anti-viral response by histone modifications of interferon-stimulated genes (ISGs) like IFITM3 and MxA [294]. Alternatively, there are evidences for induction of certain lncRNA like CD244 that leads to inhibition of IFN γ and TNF α expression by chromatin modification involving H3K27 trimethylation resulting in inhibiting host defense response and favoring mycobacterium growth [295]. Some lncRNAs are altered upon bacterial lipopolysaccharide (LPS) stimulation and are involved in inflammation and immunity. For example, lincRNA-COX2 is upregulated in LPS stimulation and involved in regulation of immune response genes [296]. More recently, it was shown that down regulation of lncRNA MEG3 is required for elimination of mycobacterium via autophagy, likely involving the mTOR and PI3K and AKT signaling [292]. Thus given the diverse biological role of lncRNAs in regulating innate responses [284], inflammation [283], pathogenesis [266] and autophagy [292], we were interested in expression profiling the disease related lncRNAs following infection with *Plasmodium* and *Toxoplasma*. In the absence of any direct evidence linking lncRNA to *Plasmodium* or *Toxoplasma* associated pathology, we resorted to use a commercial profiler designed for simultaneous expression analysis of 83 human disease associated lncRNAs that were selected based on literature evidence demonstrating lncRNAs modulation during human diseases. Interestingly, 45 of the 83 lncRNAs were also a part of lncRNA-disease association database [297]. The profiler facilitated the identification of a subset of differentially expressed disease associated lncRNAs that were unique to infections caused by Apicomplexan parasites like *Plasmodium* and *Toxoplasma*.

4.2 Materials and Methods

4.2.1 Cell lines, parasite lines, experimental animals and mosquitoes

HepG2 and HFF cells were grown in DMEM (Invitrogen) containing 10% FBS and the cultures were maintained at 37 °C and 5% CO₂. To obtain *P. berghei* sporozoites, BALB/c mice were infected intraperitoneally with asexual blood stages. The parasite propagation in blood was monitored by Giemsa staining of blood smears. All mice that were positive for gametocytes, as judged by Giemsa staining were selected for feeding female *A. stephensi* mosquitoes to initiate *Plasmodium* life cycle. *A. stephensi* mosquitoes were maintained at 80% relative humidity, 28 °C and 12:12 light: dark cycle. *P. berghei* sporozoites were isolated by dissecting salivary glands from infected mosquitoes. The glands were disrupted by using a plastic pestle and sporozoites were partially purified by spinning the sample in eppendorf centrifuge (Model#5415R) at 800 rpm for 3 min at 4 °C. The sporozoite numbers were enumerated using a hemocytometer. Nearly 2X10⁴ sporozoites were added to HepG2 cells and maintained for 24hr. In parallel, HepG2 cells were mock infected by adding lysates prepared from uninfected salivary glands that served as appropriate controls. All experiments involving mice were in accordance with the approved animal handling protocols of the Institutional Animal Ethics Committee at University of Hyderabad (approval no: UH/SLS/IAEC/2014-1/9b and UH/SLS/IAEC/2014-1/9c)

For initiation of *T. gondii* cultures, the cryopreserved parasites (RH strain) were thawed and revived by infecting HFF cells. The tachyzoites were further passaged and maintained in HFF cells. *Toxoplasma* tachyzoites were purified from the 72 h infected culture by lysing the cells using a 26G syringe and the lysate was passed through 5µm syringe filter to remove the cell debris. Purified tachyzoites were counted using hemocytometer. HFF cells were infected with the purified tachyzoites at an MOI of 1:1.

4.2.2 RNA isolation and lncRNA profiling

HepG2 cells infected with *P. berghei* sporozoites and mock infected cells were harvested at 24h post infection for extraction of RNA. HFF cells infected with *T. gondii* parasites and non-infected cells were also harvested after 24h post infection. Total RNA was isolated with Trizol (Invitrogen). Approximately 2µg of RNA was reverse transcribed into cDNA using random hexamer primers and MuLV reverse transcriptase (Applied bio systems). The cDNA samples were diluted and used to profile the expression of host lncRNAs by using disease related long non coding RNA profiler according to manufacturer's instructions (System Biosciences, Cat No # RA920C-1). This profiler plate was pre-coated with primers for 83 disease related lncRNAs

(table 6). After subjecting each of these plates to real time PCR analysis, the Ct values were obtained for each well of the profiler that corresponded to one lncRNA. The difference in the Ct value per well of mock infected versus infected was used to calculate the fold difference by employing the formula $2^{-\Delta\Delta C_t}$.

Plate Array Arrangement												
	1	2	3	4	5	6	7	8	9	10	11	12
A	21A	AAA1	aHIF	AK023948	ANRIL	anti-NOS2A	BACE1AS	BC017743	BC043430	BC200	BCMS	BIC
B	CCND1 ANCR	CMPD	DD3	DGCR5	DISC2	DLG2AS	EGO	GAS5	GOMAFU	H19	H19-AS	HAR1A
C	HAR1B	HOTAIR	HOTAIRM1	HOTTIP	HOXA1AS AA489505	HOXA3AS B1823151	HOXA3AS BE873349	HOXA6AS AK092154	HOXA11AS	HULC	IPW	IGF2AS
D	KRAS ^{P1}	LIPA16	LIT	LOC285194	LUST	LincRNA- VLDLR	LincRNA- SFMBT2	MALAT1	MEG3	MER11C	NEAT1	NCRMS
E	NDM29	PANDA	PAR5	PCAT-1	PCAT-14	PCAT-29	PCAT-32	PCAT-43	PCGEM1	PR-AT2	PRINS	PSF inhibiting RNA
F	PTEN ^{P1}	RMRP	ROR	SAF	SCA8	Sox2OT	SRA	ST7OT1	ST7OT2	ST7OT3	ST7OT4	Telomerase RNA
G	TMEVPG1	TU_0017629	TUG1	UCA1	WT1-AS	Y1	Y3	Y4	Y5	ZEB2NAT	7SK	Negative control
H	7SL scaRNA	5.8S rRNA	U87 scaRNA	U6 smRNA	ACTB	B2M	PGK1	GAPDH	HPRT1	RPL1A	RPL13A	GDC

Table 6: Plate layout with 83 disease related lncRNAs and internal control genes. Internal control genes are highlighted in pink. Genomic DNA Control (GDC) is to test genomic DNA contamination.

4.2.3 RNA knock down by siRNA

Following preliminary analysis of the changes in the expression of lncRNAs, we selected 2 lnc RNAs for reasons justified in the results. The silencing of these 2 lncRNAs was achieved using siRNA. The sequences of siRNAs (Sigma) against the lncRNAs were as follows: NEAT1 siRNA: 5'- GUGAGAAGUUGCUUAGAAACUUUCC-3' (sense), 3'- CACUCUUCAACGAAUCUUUGAAAGG-5' (Anti sense), for UCA1 siRNA: 5'- GUUAAUCCAGGAGACAAAGA-3' (sense), 3'-CAAUUAGGUCCUCUGUUUCU-5' (Anti sense) and control siRNA: 5'-AAUUCUCCGAACGUGUCACGU-3' (Sense) and 3'-UUAAGAGGCUUGCACAGUGCA-5' (Anti sense). The siRNAs were diluted in 100 μ L Opti-Mem (Invitrogen). About 1 μ L of Lipofectamine 2000 was diluted in 100 μ L Opti-Mem and incubated for 5 min. Following this incubation, the diluted siRNAs were mixed with Lipofectamine 2000 (Invitrogen) in the ratio of 1:1 and incubated further for 20 min at room temperature. The mixture was transfected into HepG2 and HFF cells at the final concentration of 100 nM siRNA. Following 24 h, the viability of the cells were analysed by trypan blue exclusion test performed by calculating the number of viable cells (trypan blue negative) divided by the total number of cells within the grids on the hemocytometer. We observed roughly 7-10% death of cells in culture following transfection with mock or target specific siRNAs

suggesting that nearly 90% or more cells in culture were viable. Forty eight hours post transfection, the knockdown efficiency was confirmed using protocols as described earlier [298], [299]. After 48 h, cells were harvested and cDNA was synthesized from isolated RNA. The siRNA mediated silencing of lncRNAs was analyzed using following lnc specific RNAs:

NEAT1 FP: CTTCCTCCCTTTAACTTATCCATTTCAC,

NEAT1 RP: CTCTTCCTCCACCATTACCAACAATAC,

NEAT2 FP: CAGTTAGTTTATCAGTTCTCCCATCCA,

NEAT 2 RP: GTTGTGTGTCGTCACCTTCAACTCT [298],

UCA1 FP: TTTGCCAGCCTCAGCTTAAT, and

UCA1 RP: TTGTCCCCATTTTCCATCAT [300].

4.2.4 Quantitative real time PCR

Following optimized silencing of lncRNAs, the *P. berghei* sporozoites and *T. gondii* tachyzoites were added respectively to HepG2 and HFF cell. The parasite burden in each lncRNA silenced cell line was analyzed by qRT-PCR using parasite specific 18SrRNA. Host cell glyceraldehyde 3-phosphate dehydrogenase (GAPDH) was used as internal control. The difference in parasite burden in control and siRNA treated samples were calculated using the $2^{-\Delta\Delta C_t}$ method.

4.3 Results

4.3.1 Expression profiling of disease related lncRNAs during *P. berghei* and *T. gondii* infection of mammalian cells

We used a qRT-PCR based profiler and investigated the expression of 83 disease related lncRNAs in HepG2 (Fig 33A) and HFF cells (Fig 33B) that support respectively the development of *P. berghei* sporozoites and *Toxoplasma* tachyzoites. From these analyses, we segregated the lncRNAs into 3 categories- 1) up and down regulated during *Plasmodium* infection, 2) up and down regulated during *Toxoplasma* infection and 3) commonly up and down regulated during both *Plasmodium* and *Toxoplasma* infections. In total, we have identified 40 differentially regulated host lncRNAs from both parasite infected cells as shown in Fig 34A. Six lncRNAs were upregulated and 12 were downregulated in *Plasmodium* infection while 18 lncRNAs were upregulated and 12 lncRNAs are downregulated in *Toxoplasma* infection (Fig 34B i-iv). Three lncRNAs NEAT1, UCA1 and DISC2 were commonly upregulated and 4 lncRNAs- KRASP1, PCAT-1, ROR and Y1 were downregulated in *Plasmodium* and *Toxoplasma* infections. Fold difference values with less than 2 and Ct values more than 30 were not considered for comparison.

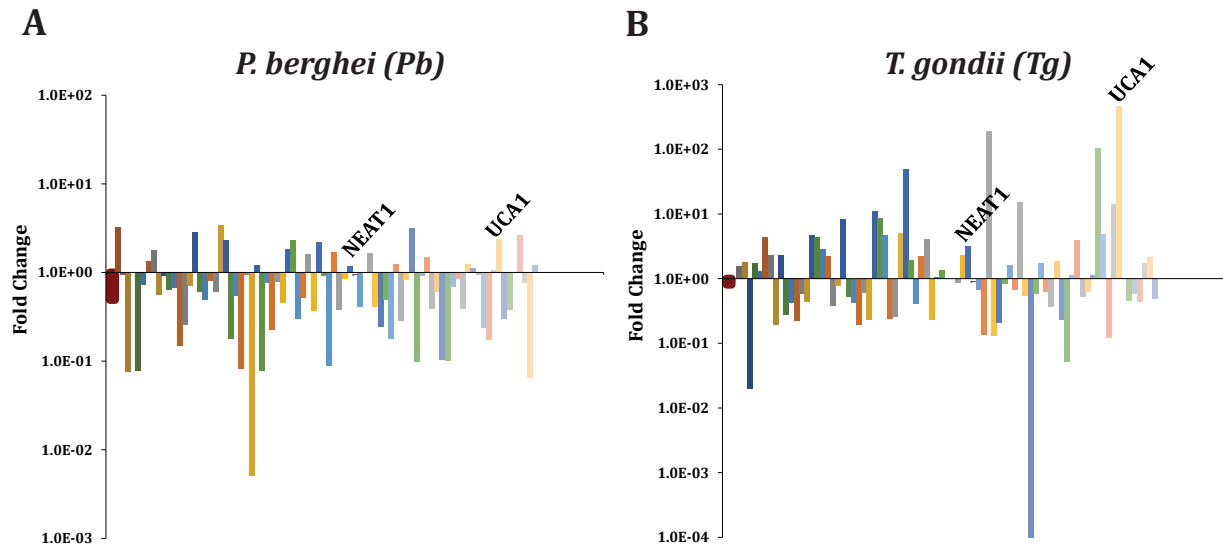
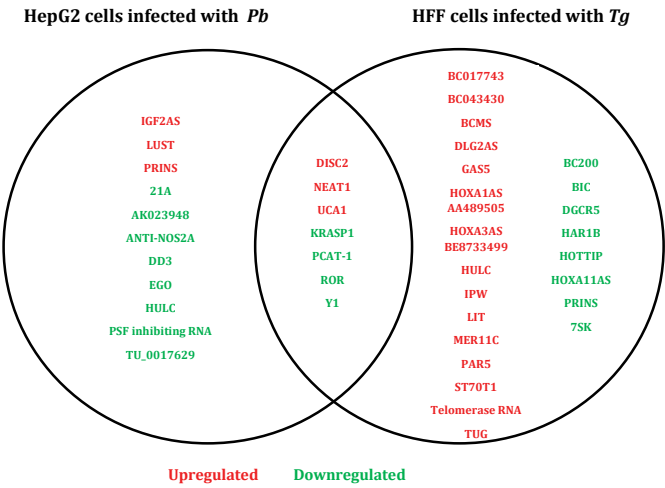


Fig 33: Profiles of differentially expressed 83 disease related long non-coding RNAs. (A) *Plasmodium berghei* (*Pb*) infected HepG2 cells and **(B)** *Toxoplasma gondii* (*Tg*) infected HFF cells.

A



B

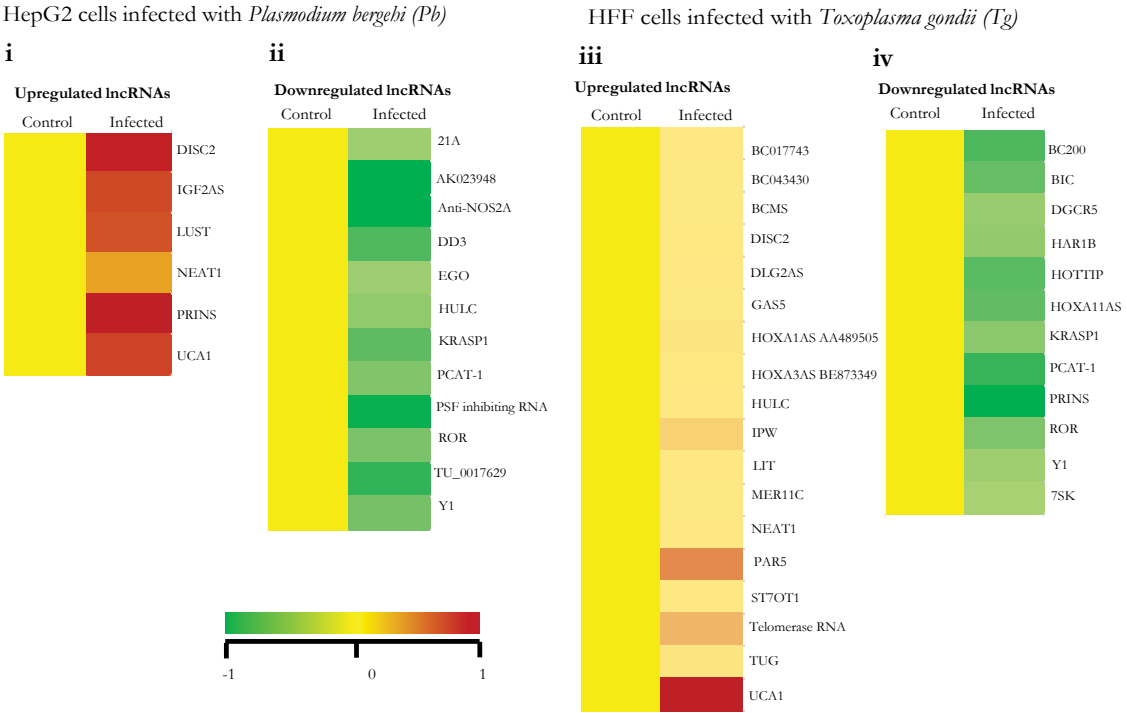


Fig 34: (A) Venn diagram representing the differentially expressed lncRNAs in *Plasmodium* and *Toxoplasma* infection. **(B)** Heat maps showing differential expression of lncRNAs during *Pb* (i & ii) and *Tg* (iii & iv) infections.

4.3.2 qRT-PCR validation of NEAT1 and UCA1 upregulation during *P. berghei* and *T. gondii* infections

Of the 40 differentially expressed lncRNAs out of 83 profiled, we prioritised UCA1 and NEAT1 for further investigation based on few important considerations. Firstly, NEAT1 and UCA1 were upregulated in both the infections likely suggesting the same downstream targets of these lncRNAs may be recruited as cellular response to infection. They may act on similar targets involved in host response to infection. Secondly, both UCA1 and NEAT1 have been implicated in viral infections. UCA1 is upregulated in HBV and HCV infections and promotes cell growth and tumorigenesis [301], [302] whereas NEAT1 is upregulated in Japanese encephalitis virus [303] and HIV infections [304], where it is known to inhibit HIV replication [304].

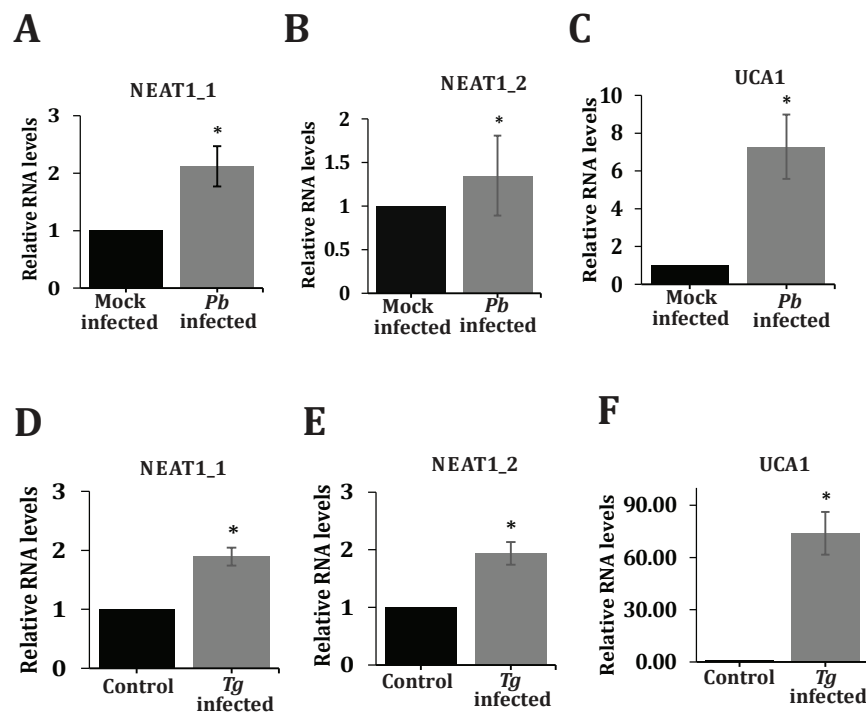


Fig 35: Validation of profiler data for NEAT1 and UCA1 by quantitative real time PCR from *Pb* infected HepG2 cells. **(A)** NEAT_1, **(B)** NEAT1_2 and **(C)** UCA1 and from *Tg* infected HFF cells: **(D)** NEAT_1, **(E)** NEAT1_2 and **(F)** UCA1 transcript levels. Error bars- s.e.m. n=3, *p value <0.05 compared to control.

Therefore induction of UCA1 and NEAT1 in current investigation may point to a conserved paradigm in host responses against different intracellular infectious agents. Upon data analysis, we found that during *Toxoplasma* infection UCA1 and NEAT1 showed respectively 458 fold and 3.12 fold induction. The fold changes were independently validated by qRTPCR using primer specific for UCA1 and two isoforms of NEAT1 (NEAT_1 and NEAT_2). We noted a 73.8, 1.89 and 1.9 fold change respectively for UCA1, NEAT1_1 and NEAT1_2. In *Plasmodium* we noted 2.3 and 1.17 fold induction for UCA1 and NEAT1 in the profiler studies. However, qRTPCR validations revealed 7.2, 2.1 and 1.3 fold induction respectively for UCA1, NEAT1 and NEAT2 (Fig 35A-F).

4.3.3 siRNA mediated silencing of NEAT1 and UCA1 modulates the intracellular parasite burden of *P. berghei* and *T. gondii*

Since UCA1 and NEAT1 are upregulated in parasitic infections, we next investigated the parasite burden in cells that were silenced for both these lncRNAs using specific siRNAs. The efficiency of siRNA mediated silencing for UCA1 and NEAT1 was monitored by qRTPCR in multiple independent experiments. In HepG2 cells, we observed nearly 60% reduction in NEAT1_1 levels (Fig 36A) and nearly 40% reduction in both NEAT1_2 and UCA1 levels (Fig 36B and C). In HFF cells, we observed reduction in the range of 70-80% for NEAT1_1, NEAT1_2 and UCA1 (Fig 36D, E and F). Having optimized significant depletion in expression of these lncRNAs, we next infected these cultures with *P. berghei* sporozoites and *T. gondii* tachyzoites and analyzed their respective burden at 24h by quantifying the parasite specific *18SrRNA* copy number. In NEAT1 silenced cultures, we observed an increase in *Plasmodium* and *Toxoplasma* parasite burden nearly by 2.5 and 1.6 fold respectively. In case of UCA1 silencing we noted an increase in *Toxoplasma* burden by 2 fold and only a slightly inhibition in *Plasmodium* burden (Fig 36G and H).

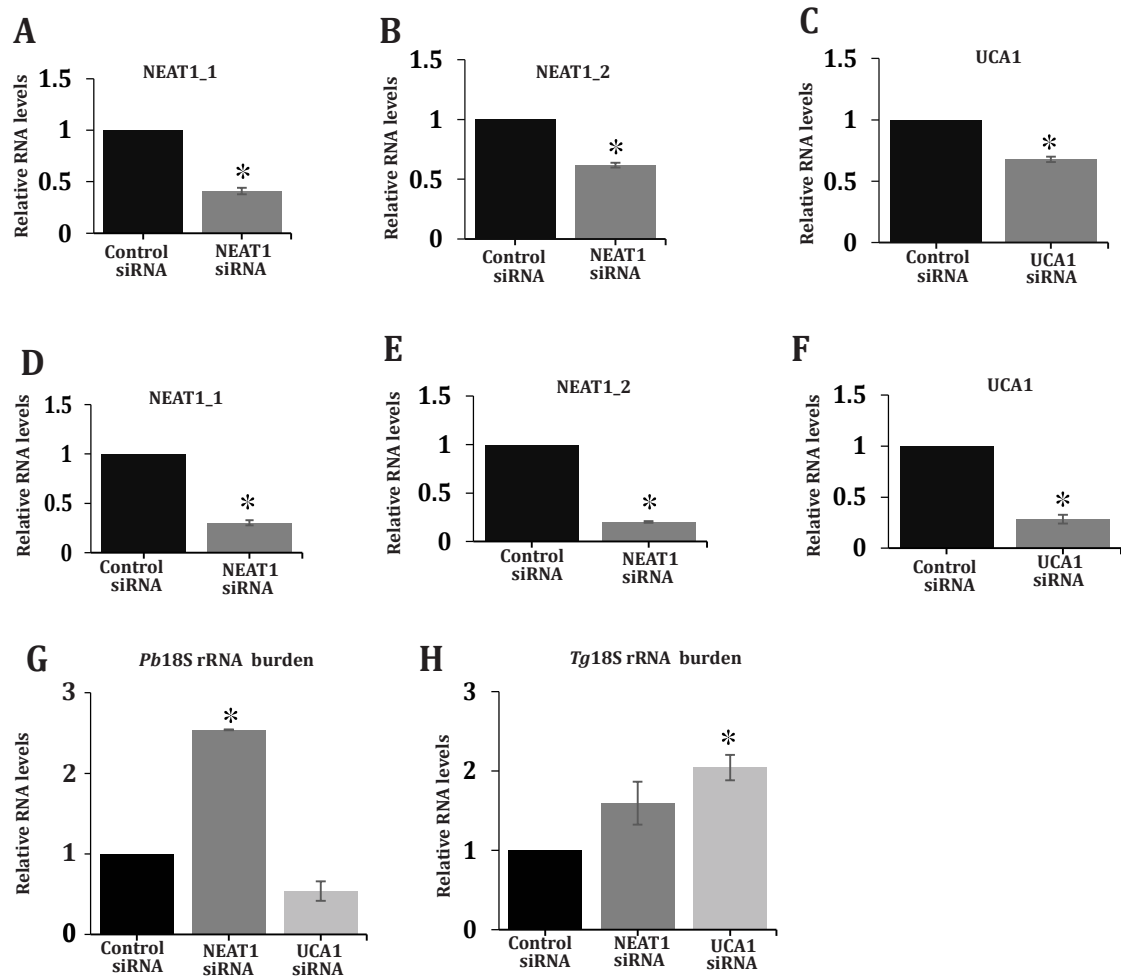


Fig 36: Monitoring the efficiency of siRNA mediated knock-down of NEAT1 and UCA1 in HepG2 and HFF cells by quantitative real time PCR. (A) NEAT_1, (B) NEAT1_2 and (C) UCA1 in HepG2 cells. (D) NEAT_1, (E) NEAT1_2 and (F) UCA1 in HFF cells. Analysis of parasite burden in siRNA silenced cells by quantitative real time PCR. (G) *Plasmodium berghei* (*Pb*) 18SrRNA copy number in HepG2 cell and (H) *Toxoplasma gondii* (*Tg*) 18S rRNA copy number in HFF cells. Error bars - s.e.m. n=3, *p value<0.05 compared with control.

4.4 Discussion

A major limitation in exploring the role of lncRNAs, despite their importance, is the lacuna in understanding the molecular mechanisms that dictate their functions. Thus while both UCA1 and NEAT1 are upregulated during infection by *Plasmodium* and *Toxoplasma*, whether this increased expression is a cellular response to limit infection or promote intracellular development of parasite is speculative. Our data pertaining to better growth of both parasites intracellularly following NEAT1 depletion and its enhanced expression following infection may suggest a role of NEAT1 in an effector response. This finding reiterates its known role in regulation of innate response. In fact, malaria liver stage infection stimulates a robust innate immune response that includes type I interferon(s) (IFN) and IFN- γ [279]. Also, *Toxoplasma* parasites are effectively eliminated by the classical IFN- γ [305] and alternate IFN- β [306] pathway of macrophage activation. In light of these observations, the induction of NEAT1 during both infections is not unexpected. Interestingly, during HIV infections, NEAT1 is upregulated [304] and its binding to the Splicing factor proline/glutamine-rich (SFPQ) facilitates translocation of SFPQ from the IL-8 promoter region to the paraspeckles resulting in activation of IL-8 [307] augmenting antiviral response. While the mechanism as how NEAT1 influences parasite infectivity is not well understood, other line of evidence suggests that knock-down of NEAT1 results in down regulation of nearly 259 immune responsive genes induced by poly IC immunisation [307]. This may possibly mean a role for NEAT1 being involved in feedback regulatory loop of innate responses. Currently, we do not know how the downregulation of both lncRNAs are promoting the growth. Though it is understandable that an overall depletion of NEAT1 may affect the quality of innate responses, more investigations are needed to address as how UCA1 affects the same.

An enormous increase in the levels of UCA1 during *Toxoplasma* infection is intriguing. Modulation of host miRNAs has been linked to brain cancer during *Toxoplasma* infections [308]. Other independent studies reveal induction of UCA1 during glioma and inhibition of cell metastasis by knockdown of UCA1 [309]. During HBV and HCV infections, the virus stimulated upregulation of UCA1 promotes tumorigenesis [301], [302]. Thus by articulating these findings, one possible speculation is that UCA1 induction during *Toxoplasma* may have implications for host cell proliferation that may explain the underlying basis for causing brain cancer. Also, the fact that UCA1 levels during *Plasmodium* infection are not as dramatically altered as in *Toxoplasma* may reflect the unique biology of each parasite. We currently do not know the relevance of UCA1 induction during *Plasmodium* infections. Further

studies are also required to ascertain whether the enhanced burden of *P. berghei* during NEAT1 silencing and *T. gondii* during NEAT1 and UCA1 silencing is due to increased susceptibility of the transfected cells to infection or better growth of both the parasites.

Interestingly, during *Toxoplasma* infection, lncRNAs-HOTTIP and 7SK were down-regulated. HOTTIP was reported to promote histone H3K4me3 (trimethylation) and transcription of genes encoding homeobox A [310] and integrin- α 1 [311]. While the homeobox products are transcription factors that regulate cellular transcription, the integrins constitute a family of signalling receptors exploited by viruses and bacteria to access cells and Integrin α 1 has a role in inflammation [312]. It is speculative if downregulation of HOTTIP may have implications in mitigating the inflammation during *Toxoplasma* infections.

With the rapid expansion of our knowledge on lncRNAs in recent past, an increasing number of new candidates have been linked to infectious diseases [296], [284], [294], [295] not included in the profiler used for current study. Other than NEAT1 and UCA1, our studies identified other important differentially induced lncRNAs like DISC2, PRINS, AK023948, Anti-NOS2A, PSF inhibiting RNA and TU_0017629 in *Plasmodium* and BC200 and PRINS in *Toxoplasma*. The balance of cellular response to infection versus pathology may be crucial in the outcome of a disease that may, in part be governed by altering the expression of disease related lncRNAs. The astonishing levels of UCA1 induction during *Toxoplasma* infection is interesting that merits further investigation. More detailed studies are needed to address the role of other lncRNAs upregulated in either infections. Such information may have important implications in understanding the disease progression and hence devising therapeutic strategies in controlling protozoan infections.

Summary

Summary

The focus of the current study was to investigate the functional role of two *Plasmodium* genes: (i) one that encodes for a metabolic enzyme- *Plasmodium berghei* nicotinamidase (*Pbnic*), that converts nicotinamide into nicotinic acid, appears in the NAD⁺ biosynthetic pathway and (ii) *PbS10* - a gene highly transcribed in sporozoite stages and encodes for a sporozoite secretory antigen. Reverse genetics approach were used for functional characterization of both genes. In addition, we also investigated host disease related long noncoding RNA profiles during *Plasmodium berghei* and *Toxoplasma gondii* infections *in vitro* and showed their involvement in host-pathogen interactions

We attempted a targeted deletion of *nic* in *Plasmodium berghei* (*Pb*) and studied the fate of *Pbnic* deficient parasites during their cyclic passage from mammalian host to the *Anopheles* mosquito. *Pbnic* deleted parasites were able to propagate at similar rates as wild type parasites within erythrocytes. However, they failed to transmit malaria to the mosquito. Data from genetic crosses indicated that *Pbnic* KO are defective in both male and female gamete formation leading to complete absence of ookinete and oocyst stages there upon. To study the role of *Pbnic* at salivary gland sporozoite stage and liver stage, we generated conditional mutant of *Pbnic* using a yeast based FLP/*FRT* site specific recombination system. FlpL, a thermolabile variant of Flp was expressed under oocyst specific promoter that allowed efficient excision of Flirted 3' UTR of *Pbnic* thus leading to its temporal inactivation. The *Pbnic* conditional mutants were able to invade salivary glands and complete exo-erythrocytic development *in vitro*. This observation demonstrates the essentiality of NAD⁺ for sexual reproduction and informs the possibility of developing inhibitors against nicotinamidase as transmission blocking drug.

Plasmodium sporozoites are infective forms of parasite to vertebrate host that invade hepatocytes after inoculation by mosquito bite and develop into liver stages (LS). To enhance infection competence of sporozoites to hepatocytes, few genes are transcriptionally upregulated in sporozoite stage that play an essential role in liver stage development. *Plasmodium* liver stages are clinically silent and produce thousands of merozoites for blood stage infection. These stages are ideal targets for prophylaxis based treatment and vaccine development. *PbS10* was identified in the SSH screen for sporozoite enriched transcripts. Here we show that *PbS10*, a sporozoite secretory protein has a role in liver stage development. Targeted disruption of *PbS10* in rodent malaria parasite *Plasmodium berghei* did not lead to any defect in blood stage propagation, midgut and salivary gland sporozoite colonization, traversal and invasion of hepatocytes, however the mutants revealed severe growth arrest in liver stage development. *PbS10* GD mutants were

highly compromised to establish infection, with only 20% mice becoming positive for blood stage infection after mosquito bite or intravenous inoculation of sporozoites. The mice that became positive for infection showed a delayed pre-patent period of 9-12 days. These findings have important implications in developing liver stage attenuated parasites that can act as whole organism vaccines to induce pre-erythrocytic immunity.

Apart from functional characterization of *Plasmodium* genes, we investigated the expression of 83 disease related lncRNAs in mammalian cell lines following infection with *Plasmodium* and *Toxoplasma*. Our observations revealed varying expression levels of disease related host lncRNAs during both infections. Interestingly 2 lncRNAs- UCA1 and NEAT1 that were commonly upregulated in both infections, were also implicated in viral infections. The siRNA mediated silencing of UCA1 and NEAT1 affected intracellular burden of both parasites. These findings demonstrate the role of lncRNAs in regulating the parasite infectivity in a yet to be deciphered mechanism.

References

1. Cox, F.E., *History of the discovery of the malaria parasites and their vectors*. Parasit Vectors, 2010. **3**(1): p. 5.
2. Janse, C.J., J. Ramesar, and A.P. Waters, *High-efficiency transfection and drug selection of genetically transformed blood stages of the rodent malaria parasite Plasmodium berghei*. Nat Protoc, 2006. **1**(1): p. 346-56.
3. Shortt, H.E. and P.C. Garnham, *Demonstration of a persisting exo-erythrocytic cycle in Plasmodium cynomolgi and its bearing on the production of relapses*. Br Med J, 1948. **1**(4564): p. 1225-8.
4. Miller, L.H. and B. Greenwood, *Malaria--a shadow over Africa*. Science, 2002. **298**(5591): p. 121-2.
5. WHO, *World Malaria Report 2016*. World Health Organization. 2016.
6. Worrall, E., S. Basu, and K. Hanson, *Is malaria a disease of poverty? A review of the literature*. Trop Med Int Health, 2005. **10**(10): p. 1047-59.
7. WHO, *World Malaria Report 2015*. World Health Organization. 2015.
8. Amino, R., et al., *Quantitative imaging of Plasmodium transmission from mosquito to mammal*. Nat Med, 2006. **12**(2): p. 220-4.
9. Su, X., K. Hayton, and T.E. Wellems, *Genetic linkage and association analyses for trait mapping in Plasmodium falciparum*. Nat Rev Genet, 2007. **8**(7): p. 497-506.
10. Salmon, B.L., A. Oksman, and D.E. Goldberg, *Malaria parasite exit from the host erythrocyte: a two-step process requiring extraerythrocytic proteolysis*. Proc Natl Acad Sci U S A, 2001. **98**(1): p. 271-6.
11. Baker, D.A., *Malaria gametocytogenesis*. Mol Biochem Parasitol, 2010. **172**(2): p. 57-65.
12. Medica, D.L. and P. Sinnis, *Quantitative dynamics of Plasmodium yoelii sporozoite transmission by infected anopheline mosquitoes*. Infect Immun, 2005. **73**(7): p. 4363-9.
13. Rosenberg, R., et al., *An estimation of the number of malaria sporozoites ejected by a feeding mosquito*. Trans R Soc Trop Med Hyg, 1990. **84**(2): p. 209-12.
14. Matsuoka, H., et al., *A rodent malaria, Plasmodium berghei, is experimentally transmitted to mice by merely probing of infective mosquito, Anopheles stephensi*. Parasitol Int, 2002. **51**(1): p. 17-23.
15. King, C.A., *Cell surface interaction of the protozoan Gregarina with concanavalin A beads - implications for models of gregarine gliding*. Cell Biol Int Rep, 1981. **5**(3): p. 297-305.
16. Russell, D.G. and R.E. Sinden, *The role of the cytoskeleton in the motility of coccidian sporozoites*. J Cell Sci, 1981. **50**: p. 345-59.
17. Vanderberg, J.P., *Studies on the motility of Plasmodium sporozoites*. J Protozool, 1974. **21**(4): p. 527-37.
18. Pradel, G., S. Garapaty, and U. Frevert, *Proteoglycans mediate malaria sporozoite targeting to the liver*. Mol Microbiol, 2002. **45**(3): p. 637-51.
19. Pradel, G. and U. Frevert, *Malaria sporozoites actively enter and pass through rat Kupffer cells prior to hepatocyte invasion*. Hepatology, 2001. **33**(5): p. 1154-65.
20. Amino, R., et al., *Host cell traversal is important for progression of the malaria parasite through the dermis to the liver*. Cell Host Microbe, 2008. **3**(2): p. 88-96.
21. Ishino, T., et al., *Cell-passage activity is required for the malarial parasite to cross the liver sinusoidal cell layer*. PLoS Biol, 2004. **2**(1): p. E4.
22. Ishino, T., Y. Chinzei, and M. Yuda, *A Plasmodium sporozoite protein with a membrane attack complex domain is required for breaching the liver sinusoidal cell layer prior to hepatocyte infection*. Cell Microbiol, 2005. **7**(2): p. 199-208.
23. Bhanot, P., et al., *A surface phospholipase is involved in the migration of plasmodium sporozoites through cells*. J Biol Chem, 2005. **280**(8): p. 6752-60.
24. Coppi, A., et al., *Heparan sulfate proteoglycans provide a signal to Plasmodium sporozoites to stop migrating and productively invade host cells*. Cell Host Microbe, 2007. **2**(5): p. 316-27.
25. Pinzon-Ortiz, C., et al., *The binding of the circumsporozoite protein to cell surface heparan sulfate proteoglycans is required for plasmodium sporozoite attachment to target cells*. J Biol Chem, 2001. **276**(29): p. 26784-91.
26. Tewari, R., et al., *Function of region I and II adhesive motifs of Plasmodium falciparum circumsporozoite protein in sporozoite motility and infectivity*. J Biol Chem, 2002. **277**(49): p. 47613-8.
27. Ying, P., et al., *The malaria circumsporozoite protein: interaction of the conserved regions I and II-plus with heparin-like oligosaccharides in heparan sulfate*. Exp Parasitol, 1997. **85**(2): p. 168-82.
28. Mota, M.M., et al., *Migration of Plasmodium sporozoites through cells before infection*. Science, 2001. **291**(5501): p. 141-4.
29. Vaughan, A.M., A.S. Aly, and S.H. Kappe, *Malaria parasite pre-erythrocytic stage infection: gliding and hiding*. Cell Host Microbe, 2008. **4**(3): p. 209-18.

30. Hugel, F.U., G. Pradel, and U. Frevert, *Release of malaria circumsporozoite protein into the host cell cytoplasm and interaction with ribosomes*. Mol Biochem Parasitol, 1996. **81**(2): p. 151-70.
31. Gomes, P.S., et al., *Immune Escape Strategies of Malaria Parasites*. Front Microbiol, 2016. **7**: p. 1617.
32. Meis, J.F., et al., *Ultrastructural observations on the infection of rat liver by Plasmodium berghei sporozoites in vivo*. J Protozool, 1983. **30**(2): p. 361-6.
33. Bano, N., et al., *Cellular interactions of Plasmodium liver stage with its host mammalian cell*. Int J Parasitol, 2007. **37**(12): p. 1329-41.
34. Labaied, M., et al., *Plasmodium yoelii sporozoites with simultaneous deletion of P52 and P36 are completely attenuated and confer sterile immunity against infection*. Infect Immun, 2007. **75**(8): p. 3758-68.
35. Mueller, A.K., et al., *Plasmodium liver stage developmental arrest by depletion of a protein at the parasite-host interface*. Proc Natl Acad Sci U S A, 2005. **102**(8): p. 3022-7.
36. Mueller, A.K., et al., *Genetically modified Plasmodium parasites as a protective experimental malaria vaccine*. Nature, 2005. **433**(7022): p. 164-7.
37. Hiller, N.L., et al., *A host-targeting signal in virulence proteins reveals a secretome in malarial infection*. Science, 2004. **306**(5703): p. 1934-7.
38. Marti, M., et al., *Targeting malaria virulence and remodeling proteins to the host erythrocyte*. Science, 2004. **306**(5703): p. 1930-3.
39. Pick, C., et al., *Phylogenomic analyses of malaria parasites and evolution of their exported proteins*. BMC Evol Biol, 2011. **11**: p. 167.
40. Heiber, A., et al., *Identification of new PNEPs indicates a substantial non-PEXEL exportome and underpins common features in Plasmodium falciparum protein export*. PLoS Pathog, 2013. **9**(8): p. e1003546.
41. Kumar, K.A., et al., *The circumsporozoite protein is an immunodominant protective antigen in irradiated sporozoites*. Nature, 2006. **444**(7121): p. 937-40.
42. Singh, A.P., et al., *Plasmodium circumsporozoite protein promotes the development of the liver stages of the parasite*. Cell, 2007. **131**(3): p. 492-504.
43. Frevert, U., et al., *Malaria circumsporozoite protein inhibits protein synthesis in mammalian cells*. EMBO J, 1998. **17**(14): p. 3816-26.
44. Balaji, S., et al., *Discovery of the principal specific transcription factors of Apicomplexa and their implication for the evolution of the AP2-integrase DNA binding domains*. Nucleic Acids Res, 2005. **33**(13): p. 3994-4006.
45. Iwanaga, S., et al., *Identification of an AP2-family protein that is critical for malaria liver stage development*. PLoS One, 2012. **7**(11): p. e47557.
46. Sturm, A., et al., *Manipulation of host hepatocytes by the malaria parasite for delivery into liver sinusoids*. Science, 2006. **313**(5791): p. 1287-90.
47. Baer, K., et al., *Release of hepatic Plasmodium yoelii merozoites into the pulmonary microvasculature*. PLoS Pathog, 2007. **3**(11): p. e171.
48. Schmidt-Christensen, A., et al., *Expression and processing of Plasmodium berghei SERA3 during liver stages*. Cell Microbiol, 2008. **10**(8): p. 1723-34.
49. Tawk, L., et al., *A key role for Plasmodium subtilisin-like SUB1 protease in egress of malaria parasites from host hepatocytes*. J Biol Chem, 2013. **288**(46): p. 33336-46.
50. Ishino, T., et al., *LISP1 is important for the egress of Plasmodium berghei parasites from liver cells*. Cell Microbiol, 2009. **11**(9): p. 1329-39.
51. Matuschewski, K., et al., *Infectivity-associated changes in the transcriptional repertoire of the malaria parasite sporozoite stage*. J Biol Chem, 2002. **277**(44): p. 41948-53.
52. Kaiser, K., et al., *Differential transcriptome profiling identifies Plasmodium genes encoding pre-erythrocytic stage-specific proteins*. Mol Microbiol, 2004. **51**(5): p. 1221-32.
53. Sultan, A.A., et al., *TRAP is necessary for gliding motility and infectivity of plasmodium sporozoites*. Cell, 1997. **90**(3): p. 511-22.
54. Steinbuechel, M. and K. Matuschewski, *Role for the Plasmodium sporozoite-specific transmembrane protein S6 in parasite motility and efficient malaria transmission*. Cell Microbiol, 2009. **11**(2): p. 279-88.
55. Combe, A., et al., *TREP, a novel protein necessary for gliding motility of the malaria sporozoite*. Int J Parasitol, 2009. **39**(4): p. 489-96.
56. Kariu, T., et al., *CeITOS, a novel malarial protein that mediates transmission to mosquito and vertebrate hosts*. Mol Microbiol, 2006. **59**(5): p. 1369-79.
57. Aly, A.S., et al., *Targeted deletion of SAP1 abolishes the expression of infectivity factors necessary for successful malaria parasite liver infection*. Mol Microbiol, 2008. **69**(1): p. 152-63.

58. Silvie, O., K. Goetz, and K. Matuschewski, *A sporozoite asparagine-rich protein controls initiation of Plasmodium liver stage development*. PLoS Pathog, 2008. **4**(6): p. e1000086.
59. Bijker, E.M., et al., *Novel approaches to whole sporozoite vaccination against malaria*. Vaccine, 2015. **33**(52): p. 7462-8.
60. Matuschewski, K., *Hitting malaria before it hurts: attenuated Plasmodium liver stages*. Cell Mol Life Sci, 2007. **64**(23): p. 3007-11.
61. Ward, G.E., et al., *Staurosporine inhibits invasion of erythrocytes by malarial merozoites*. Exp Parasitol, 1994. **79**(3): p. 480-7.
62. Cowman, A.F. and B.S. Crabb, *Invasion of red blood cells by malaria parasites*. Cell, 2006. **124**(4): p. 755-66.
63. Preiser, P., et al., *The apical organelles of malaria merozoites: host cell selection, invasion, host immunity and immune evasion*. Microbes Infect, 2000. **2**(12): p. 1461-77.
64. Miller, L.H., et al., *The resistance factor to Plasmodium vivax in blacks. The Duffy-blood-group genotype, FyFy*. N Engl J Med, 1976. **295**(6): p. 302-4.
65. Sim, B.K., et al., *Receptor and ligand domains for invasion of erythrocytes by Plasmodium falciparum*. Science, 1994. **264**(5167): p. 1941-4.
66. Mitchell, G.H., et al., *Apical membrane antigen 1, a major malaria vaccine candidate, mediates the close attachment of invasive merozoites to host red blood cells*. Infect Immun, 2004. **72**(1): p. 154-8.
67. Lamarque, M., et al., *The RON2-AMA1 interaction is a critical step in moving junction-dependent invasion by apicomplexan parasites*. PLoS Pathog, 2011. **7**(2): p. e1001276.
68. Richard, D., et al., *Interaction between Plasmodium falciparum apical membrane antigen 1 and the rhoptry neck protein complex defines a key step in the erythrocyte invasion process of malaria parasites*. J Biol Chem, 2010. **285**(19): p. 14815-22.
69. Srinivasan, P., et al., *Binding of Plasmodium merozoite proteins RON2 and AMA1 triggers commitment to invasion*. Proc Natl Acad Sci U S A, 2011. **108**(32): p. 13275-80.
70. Aikawa, M., et al., *Erythrocyte entry by malarial parasites. A moving junction between erythrocyte and parasite*. J Cell Biol, 1978. **77**(1): p. 72-82.
71. Pinder, J.C., et al., *Actomyosin motor in the merozoite of the malaria parasite, Plasmodium falciparum: implications for red cell invasion*. J Cell Sci, 1998. **111** (Pt 13): p. 1831-9.
72. Baum, J., et al., *A conserved molecular motor drives cell invasion and gliding motility across malaria life cycle stages and other apicomplexan parasites*. J Biol Chem, 2006. **281**(8): p. 5197-208.
73. Goldberg, D.E. and A.F. Cowman, *Moving in and renovating: exporting proteins from Plasmodium into host erythrocytes*. Nat Rev Microbiol, 2010. **8**(9): p. 617-21.
74. Jewett, T.J. and L.D. Sibley, *Aldolase forms a bridge between cell surface adhesins and the actin cytoskeleton in apicomplexan parasites*. Mol Cell, 2003. **11**(4): p. 885-94.
75. Charpian, S. and J.M. Przyborski, *Protein transport across the parasitophorous vacuole of Plasmodium falciparum: into the great wide open*. Traffic, 2008. **9**(2): p. 157-65.
76. Egan, T.J., *Recent advances in understanding the mechanism of hemozoin (malaria pigment) formation*. J Inorg Biochem, 2008. **102**(5-6): p. 1288-99.
77. Dahl, E.L. and P.J. Rosenthal, *Multiple antibiotics exert delayed effects against the Plasmodium falciparum apicoplast*. Antimicrob Agents Chemother, 2007. **51**(10): p. 3485-90.
78. Scherf, A., J.J. Lopez-Rubio, and L. Riviere, *Antigenic variation in Plasmodium falciparum*. Annu Rev Microbiol, 2008. **62**: p. 445-70.
79. Yeoh, S., et al., *Subcellular discharge of a serine protease mediates release of invasive malaria parasites from host erythrocytes*. Cell, 2007. **131**(6): p. 1072-83.
80. Taylor, L.H. and A.F. Read, *Why so few transmission stages? Reproductive restraint by malaria parasites*. Parasitol Today, 1997. **13**(4): p. 135-40.
81. Chaubey, S., M. Grover, and U. Tatu, *Endoplasmic reticulum stress triggers gametocytogenesis in the malaria parasite*. J Biol Chem, 2014. **289**(24): p. 16662-74.
82. Sinha, A., et al., *A cascade of DNA-binding proteins for sexual commitment and development in Plasmodium*. Nature, 2014. **507**(7491): p. 253-7.
83. Eksi, S., et al., *Plasmodium falciparum gametocyte development 1 (Pfgcd1) and gametocytogenesis early gene identification and commitment to sexual development*. PLoS Pathog, 2012. **8**(10): p. e1002964.
84. Mantel, P.Y., et al., *Malaria-infected erythrocyte-derived microvesicles mediate cellular communication within the parasite population and with the host immune system*. Cell Host Microbe, 2013. **13**(5): p. 521-34.

85. Regev-Rudzki, N., et al., *Cell-cell communication between malaria-infected red blood cells via exosome-like vesicles*. Cell, 2013. **153**(5): p. 1120-33.
86. Duffy, S. and V.M. Avery, *Identification of inhibitors of Plasmodium falciparum gametocyte development*. Malar J, 2013. **12**: p. 408.
87. Billker, O., et al., *Identification of xanthurenic acid as the putative inducer of malaria development in the mosquito*. Nature, 1998. **392**(6673): p. 289-92.
88. Janse, C.J., et al., *DNA synthesis in gametocytes of Plasmodium falciparum*. Parasitology, 1988. **96** (Pt 1): p. 1-7.
89. McRobert, L., et al., *Gametogenesis in malaria parasites is mediated by the cGMP-dependent protein kinase*. PLoS Biol, 2008. **6**(6): p. e139.
90. Billker, O., et al., *Calcium and a calcium-dependent protein kinase regulate gamete formation and mosquito transmission in a malaria parasite*. Cell, 2004. **117**(4): p. 503-14.
91. Tewari, R., et al., *The systematic functional analysis of Plasmodium protein kinases identifies essential regulators of mosquito transmission*. Cell Host Microbe, 2010. **8**(4): p. 377-87.
92. Guttery, D.S., et al., *Genome-wide functional analysis of Plasmodium protein phosphatases reveals key regulators of parasite development and differentiation*. Cell Host Microbe, 2014. **16**(1): p. 128-40.
93. Stitzel, M.L. and G. Seydoux, *Regulation of the oocyte-to-zygote transition*. Science, 2007. **316**(5823): p. 407-8.
94. Mair, G.R., et al., *Regulation of sexual development of Plasmodium by translational repression*. Science, 2006. **313**(5787): p. 667-9.
95. van Dijk, M.R., et al., *Three members of the 6-cys protein family of Plasmodium play a role in gamete fertility*. PLoS Pathog, 2010. **6**(4): p. e1000853.
96. van Dijk, M.R., et al., *A central role for P48/45 in malaria parasite male gamete fertility*. Cell, 2001. **104**(1): p. 153-64.
97. Gerald, N., B. Mahajan, and S. Kumar, *Mitosis in the human malaria parasite Plasmodium falciparum*. Eukaryot Cell, 2011. **10**(4): p. 474-82.
98. Sinden, R.E., *The cell biology of sexual development in plasmodium*. Parasitology, 1983. **86** (Pt 4): p. 7-28.
99. Shimizu, H., et al., *GAK, a regulator of clathrin-mediated membrane traffic, also controls centrosome integrity and chromosome congression*. J Cell Sci, 2009. **122**(Pt 17): p. 3145-52.
100. Reininger, L., et al., *An essential role for the Plasmodium Nrk-2 Nima-related protein kinase in the sexual development of malaria parasites*. J Biol Chem, 2009. **284**(31): p. 20858-68.
101. Reininger, L., et al., *A NIMA-related protein kinase is essential for completion of the sexual cycle of malaria parasites*. J Biol Chem, 2005. **280**(36): p. 31957-64.
102. Yuda, M., et al., *Identification of a transcription factor in the mosquito-invasive stage of malaria parasites*. Mol Microbiol, 2009. **71**(6): p. 1402-14.
103. Huber, M., E. Cabib, and L.H. Miller, *Malaria parasite chitinase and penetration of the mosquito peritrophic membrane*. Proc Natl Acad Sci U S A, 1991. **88**(7): p. 2807-10.
104. Siden-Kiamos, I., et al., *Plasmodium berghei calcium-dependent protein kinase 3 is required for ookinete gliding motility and mosquito midgut invasion*. Mol Microbiol, 2006. **60**(6): p. 1355-63.
105. Patzewitz, E.M., et al., *An ancient protein phosphatase, SHLP1, is critical to microneme development in Plasmodium ookinetes and parasite transmission*. Cell Rep, 2013. **3**(3): p. 622-9.
106. Rosenberg, R. and J. Rungsiwongse, *The number of sporozoites produced by individual malaria oocysts*. Am J Trop Med Hyg, 1991. **45**(5): p. 574-7.
107. Vanderberg, J. and J. Rhodin, *Differentiation of nuclear and cytoplasmic fine structure during sporogonic development of Plasmodium berghei*. J Cell Biol, 1967. **32**(3): p. C7-10.
108. Dorin-Semlat, D., et al., *Disruption of the Pfk7 gene impairs schizogony and sporogony in the human malaria parasite Plasmodium falciparum*. Eukaryot Cell, 2008. **7**(2): p. 279-85.
109. Menard, R., et al., *Circumsporozoite protein is required for development of malaria sporozoites in mosquitoes*. Nature, 1997. **385**(6614): p. 336-40.
110. Wang, Q., H. Fujioka, and V. Nussenzweig, *Exit of Plasmodium sporozoites from oocysts is an active process that involves the circumsporozoite protein*. PLoS Pathog, 2005. **1**(1): p. e9.
111. Mastan, B.S., et al., *Plasmodium berghei plasmepsin VIII is essential for sporozoite gliding motility*. Int J Parasitol, 2017. **47**(5): p. 239-245.
112. Pimenta, P.F., M. Touray, and L. Miller, *The journey of malaria sporozoites in the mosquito salivary gland*. J Eukaryot Microbiol, 1994. **41**(6): p. 608-24.

113. Hillyer, J.F., C. Barreau, and K.D. Vernick, *Efficiency of salivary gland invasion by malaria sporozoites is controlled by rapid sporozoite destruction in the mosquito haemocoel*. Int J Parasitol, 2007. **37**(6): p. 673-81.
114. Mueller, A.K., et al., *Invasion of mosquito salivary glands by malaria parasites: prerequisites and defense strategies*. Int J Parasitol, 2010. **40**(11): p. 1229-35.
115. Yuda, M., et al., *Transcription factor AP2-Sp and its target genes in malarial sporozoites*. Mol Microbiol, 2010. **75**(4): p. 854-63.
116. Morrisette, N.S. and L.D. Sibley, *Cytoskeleton of apicomplexan parasites*. Microbiol Mol Biol Rev, 2002. **66**(1): p. 21-38; table of contents.
117. Aly, A.S., A.M. Vaughan, and S.H. Kappe, *Malaria parasite development in the mosquito and infection of the mammalian host*. Annu Rev Microbiol, 2009. **63**: p. 195-221.
118. Tucker, R.P., *The thrombospondin type 1 repeat superfamily*. Int J Biochem Cell Biol, 2004. **36**(6): p. 969-74.
119. Whittaker, C.A. and R.O. Hynes, *Distribution and evolution of von Willebrand/ integrin A domains: widely dispersed domains with roles in cell adhesion and elsewhere*. Mol Biol Cell, 2002. **13**(10): p. 3369-87.
120. Kappe, S., et al., *Conservation of a gliding motility and cell invasion machinery in Apicomplexan parasites*. J Cell Biol, 1999. **147**(5): p. 937-44.
121. Matuschewski, K., et al., *Plasmodium sporozoite invasion into insect and mammalian cells is directed by the same dual binding system*. EMBO J, 2002. **21**(7): p. 1597-606.
122. Shute, P.G., et al., *A strain of Plasmodium vivax characterized by prolonged incubation: the effect of numbers of sporozoites on the length of the prepatent period*. Trans R Soc Trop Med Hyg, 1976. **70**(5-6): p. 474-81.
123. Garnham, P.C., *Swellengrebel lecture. Hypnozoites and 'relapses' in Plasmodium vivax and in vivax-like malaria*. Trop Geogr Med, 1988. **40**(3): p. 187-95.
124. Kappe, S.H., C.A. Buscaglia, and V. Nussenzweig, *Plasmodium sporozoite molecular cell biology*. Annu Rev Cell Dev Biol, 2004. **20**: p. 29-59.
125. Tarun, A.S., et al., *A combined transcriptome and proteome survey of malaria parasite liver stages*. Proc Natl Acad Sci U S A, 2008. **105**(1): p. 305-10.
126. Cerami, C., et al., *The basolateral domain of the hepatocyte plasma membrane bears receptors for the circumsporozoite protein of Plasmodium falciparum sporozoites*. Cell, 1992. **70**(6): p. 1021-33.
127. Muller, K., K. Matuschewski, and O. Silvie, *The Puf-family RNA-binding protein Puf2 controls sporozoite conversion to liver stages in the malaria parasite*. PLoS One, 2011. **6**(5): p. e19860.
128. Gomes-Santos, C.S., et al., *Transition of Plasmodium sporozoites into liver stage-like forms is regulated by the RNA binding protein Pumilio*. PLoS Pathog, 2011. **7**(5): p. e1002046.
129. Silvie, O., et al., *A role for apical membrane antigen 1 during invasion of hepatocytes by Plasmodium falciparum sporozoites*. J Biol Chem, 2004. **279**(10): p. 9490-6.
130. Kwiatkowski, D.P., *How malaria has affected the human genome and what human genetics can teach us about malaria*. Am J Hum Genet, 2005. **77**(2): p. 171-92.
131. Reyburn, H., et al., *Association of transmission intensity and age with clinical manifestations and case fatality of severe Plasmodium falciparum malaria*. JAMA, 2005. **293**(12): p. 1461-70.
132. Karunaweera, N.D., et al., *The paroxysm of Plasmodium vivax malaria*. Trends Parasitol, 2003. **19**(4): p. 188-93.
133. Langhorne, J., et al., *Immunity to malaria: more questions than answers*. Nat Immunol, 2008. **9**(7): p. 725-32.
134. Miller, L.H., M.F. Good, and G. Milon, *Malaria pathogenesis*. Science, 1994. **264**(5167): p. 1878-83.
135. Fernandez, V. and M. Wahlgren, *Rosetting and autoagglutination in Plasmodium falciparum*. Chem Immunol, 2002. **80**: p. 163-87.
136. Bousema, J.T., et al., *Plasmodium falciparum gametocyte carriage in asymptomatic children in western Kenya*. Malar J, 2004. **3**: p. 18.
137. WHO, *World Malaria Report 1999*. World Health Organization. 1999.
138. Moody, A., *Rapid diagnostic tests for malaria parasites*. Clin Microbiol Rev, 2002. **15**(1): p. 66-78.
139. Kattenberg, J.H., et al., *Systematic review and meta-analysis: rapid diagnostic tests versus placental histology, microscopy and PCR for malaria in pregnant women*. Malar J, 2011. **10**: p. 321.
140. Abba, K., et al., *Rapid diagnostic tests for diagnosing uncomplicated non-falciparum or Plasmodium vivax malaria in endemic countries*. Cochrane Database Syst Rev, 2014(12): p. CD011431.
141. White, N.J., *The role of anti-malarial drugs in eliminating malaria*. Malar J, 2008. **7 Suppl 1**: p. S8.

142. Wells, T.N., J.N. Burrows, and J.K. Baird, *Targeting the hypnozoite reservoir of Plasmodium vivax: the hidden obstacle to malaria elimination*. Trends Parasitol, 2010. **26**(3): p. 145-51.
143. Winzeler, E.A. and M.J. Manary, *Drug resistance genomics of the antimalarial drug artemisinin*. Genome Biol, 2014. **15**(11): p. 544.
144. WHO, *World Malaria Report 2012*. World Health Organization. 2012.
145. Fegan, G.W., et al., *Effect of expanded insecticide-treated bednet coverage on child survival in rural Kenya: a longitudinal study*. Lancet, 2007. **370**(9592): p. 1035-9.
146. Pluess, B., et al., *Indoor residual spraying for preventing malaria*. Cochrane Database Syst Rev, 2010(4): p. CD006657.
147. Hoffman, S.L., et al., *Protection of humans against malaria by immunization with radiation-attenuated Plasmodium falciparum sporozoites*. J Infect Dis, 2002. **185**(8): p. 1155-64.
148. Graves, P. and H. Gelband, *Vaccines for preventing malaria (SPf66)*. Cochrane Database Syst Rev, 2006(2): p. CD005966.
149. Olotu, A., et al., *Circumsporozoite-specific T cell responses in children vaccinated with RTS,S/AS01E and protection against P falciparum clinical malaria*. PLoS One, 2011. **6**(10): p. e25786.
150. Duffy, P.E., et al., *Pre-erythrocytic malaria vaccines: identifying the targets*. Expert Rev Vaccines, 2012. **11**(10): p. 1261-80.
151. Kumar, K.A., et al., *Conserved protective mechanisms in radiation and genetically attenuated uis3(-) and uis4(-) Plasmodium sporozoites*. PLoS One, 2009. **4**(2): p. e4480.
152. Yu, M., et al., *The fatty acid biosynthesis enzyme FabI plays a key role in the development of liver-stage malarial parasites*. Cell Host Microbe, 2008. **4**(6): p. 567-78.
153. Falae, A., et al., *Role of Plasmodium berghei cGMP-dependent protein kinase in late liver stage development*. J Biol Chem, 2010. **285**(5): p. 3282-8.
154. Haussig, J.M., K. Matuschewski, and T.W. Kooij, *Inactivation of a Plasmodium apicoplast protein attenuates formation of liver merozoites*. Mol Microbiol, 2011. **81**(6): p. 1511-25.
155. Bejon, P., et al., *A phase 2b randomised trial of the candidate malaria vaccines FP9 ME-TRAP and MV A ME-TRAP among children in Kenya*. PLoS Clin Trials, 2006. **1**(6): p. e29.
156. Cummings, J.F., et al., *Recombinant Liver Stage Antigen-1 (LSA-1) formulated with AS01 or AS02 is safe, elicits high titer antibody and induces IFN-gamma/IL-2 CD4+ T cells but does not protect against experimental Plasmodium falciparum infection*. Vaccine, 2010. **28**(31): p. 5135-44.
157. Bottius, E., et al., *A novel Plasmodium falciparum sporozoite and liver stage antigen (SALSA) defines major B, T helper, and CTL epitopes*. J Immunol, 1996. **156**(8): p. 2874-84.
158. Fidock, D.A., et al., *Conservation of the Plasmodium falciparum sporozoite surface protein gene, STARP, in field isolates and distinct species of Plasmodium*. Mol Biochem Parasitol, 1994. **67**(2): p. 255-67.
159. Girard, M.P., et al., *A review of human vaccine research and development: malaria*. Vaccine, 2007. **25**(9): p. 1567-80.
160. Saul, A., et al., *A human phase 1 vaccine clinical trial of the Plasmodium falciparum malaria vaccine candidate apical membrane antigen 1 in Montanide ISA720 adjuvant*. Vaccine, 2005. **23**(23): p. 3076-83.
161. Beeson, J.G., J.A. Chan, and F.J. Fowkes, *PfEMP1 as a target of human immunity and a vaccine candidate against malaria*. Expert Rev Vaccines, 2013. **12**(2): p. 105-8.
162. Barr, P.J., et al., *Recombinant Pfs25 protein of Plasmodium falciparum elicits malaria transmission-blocking immunity in experimental animals*. J Exp Med, 1991. **174**(5): p. 1203-8.
163. Gozar, M.M., V.L. Price, and D.C. Kaslow, *Saccharomyces cerevisiae-secreted fusion proteins Pfs25 and Pfs28 elicit potent Plasmodium falciparum transmission-blocking antibodies in mice*. Infect Immun, 1998. **66**(1): p. 59-64.
164. Talaat, K.R., et al., *Safety and Immunogenicity of Pfs25-EPA/Alhydrogel(R), a Transmission Blocking Vaccine against Plasmodium falciparum: An Open Label Study in Malaria Naive Adults*. PLoS One, 2016. **11**(10): p. e0163144.
165. Ockenhouse, C.F., et al., *Phase I/IIa safety, immunogenicity, and efficacy trial of NYVAC-Pf7, a pox-vectored, multiantigen, multistage vaccine candidate for Plasmodium falciparum malaria*. J Infect Dis, 1998. **177**(6): p. 1664-73.
166. Rts, S.C.T.P., *Efficacy and safety of RTS,S/AS01 malaria vaccine with or without a booster dose in infants and children in Africa: final results of a phase 3, individually randomised, controlled trial*. Lancet, 2015. **386**(9988): p. 31-45.
167. Ashley, E.A., et al., *Spread of artemisinin resistance in Plasmodium falciparum malaria*. N Engl J Med, 2014. **371**(5): p. 411-23.

168. Shimp, R.L., Jr., et al., *Development of a Pfs25-EPA malaria transmission blocking vaccine as a chemically conjugated nanoparticle*. Vaccine, 2013. **31**(28): p. 2954-62.
169. Vincke, I.H. and M. Lips, [*Cyclic transmission of Plasmodium berghei*]. Ann Soc Belg Med Trop (1920), 1950. **30**(6): p. 1605-11.
170. Franke-Fayard, B., et al., *Sequestration and tissue accumulation of human malaria parasites: can we learn anything from rodent models of malaria?* PLoS Pathog, 2010. **6**(9): p. e1001032.
171. Otto, T.D., et al., *A comprehensive evaluation of rodent malaria parasite genomes and gene expression*. BMC Biol, 2014. **12**: p. 86.
172. Hall, N., et al., *A comprehensive survey of the Plasmodium life cycle by genomic, transcriptomic, and proteomic analyses*. Science, 2005. **307**(5706): p. 82-6.
173. Crabb, B.S., et al., *Targeted gene disruption shows that knobs enable malaria-infected red cells to cytoadhere under physiological shear stress*. Cell, 1997. **89**(2): p. 287-96.
174. Lobo, C.A., et al., *Disruption of the Pfg27 locus by homologous recombination leads to loss of the sexual phenotype in P. falciparum*. Mol Cell, 1999. **3**(6): p. 793-8.
175. Menard, R. and C. Janse, *Gene targeting in malaria parasites*. Methods, 1997. **13**(2): p. 148-57.
176. Laurentino, E.C., et al., *Experimentally controlled downregulation of the histone chaperone FACT in Plasmodium berghei reveals that it is critical to male gamete fertility*. Cell Microbiol, 2011. **13**(12): p. 1956-74.
177. Carvalho, T.G., et al., *Conditional mutagenesis using site-specific recombination in Plasmodium berghei*. Proc Natl Acad Sci U S A, 2004. **101**(41): p. 14931-6.
178. Natarajan, R., et al., *Fluorescent Plasmodium berghei sporozoites and pre-erythrocytic stages: a new tool to study mosquito and mammalian host interactions with malaria parasites*. Cell Microbiol, 2001. **3**(6): p. 371-9.
179. Sturm, A., et al., *Alteration of the parasite plasma membrane and the parasitophorous vacuole membrane during exo-erythrocytic development of malaria parasites*. Protist, 2009. **160**(1): p. 51-63.
180. Graewe, S., et al., *Going live: a comparative analysis of the suitability of the RFP derivatives RedStar, mCherry and tdTomato for intravital and in vitro live imaging of Plasmodium parasites*. Biotechnol J, 2009. **4**(6): p. 895-902.
181. de Koning-Ward, T.F., et al., *Analysis of stage specificity of promoters in Plasmodium berghei using luciferase as a reporter*. Mol Biochem Parasitol, 1999. **100**(1): p. 141-6.
182. Khan, S.M., et al., *Proteome analysis of separated male and female gametocytes reveals novel sex-specific Plasmodium biology*. Cell, 2005. **121**(5): p. 675-87.
183. Miller, L.H., et al., *Malaria biology and disease pathogenesis: insights for new treatments*. Nat Med, 2013. **19**(2): p. 156-67.
184. Sachs, J. and P. Malaney, *The economic and social burden of malaria*. Nature, 2002. **415**(6872): p. 680-5.
185. Roth, E.F., Jr., et al., *Glutathione stability and oxidative stress in P. falciparum infection in vitro: responses of normal and G6PD deficient cells*. Biochem Biophys Res Commun, 1982. **109**(2): p. 355-62.
186. Roth, E., Jr., *Plasmodium falciparum carbohydrate metabolism: a connection between host cell and parasite*. Blood Cells, 1990. **16**(2-3): p. 453-60; discussion 461-6.
187. Francis, S.E., D.J. Sullivan, Jr., and D.E. Goldberg, *Hemoglobin metabolism in the malaria parasite Plasmodium falciparum*. Annu Rev Microbiol, 1997. **51**: p. 97-123.
188. Ke, H., et al., *The heme biosynthesis pathway is essential for Plasmodium falciparum development in mosquito stage but not in blood stages*. J Biol Chem, 2014. **289**(50): p. 34827-37.
189. Meireles, P., et al., *GLUT1-mediated glucose uptake plays a crucial role during Plasmodium hepatic infection*. Cell Microbiol, 2017. **19**(2).
190. Gardner, M.J., et al., *Genome sequence of the human malaria parasite Plasmodium falciparum*. Nature, 2002. **419**(6906): p. 498-511.
191. Rivero, A. and H.M. Ferguson, *The energetic budget of Anopheles stephensi infected with Plasmodium chabaudi: is energy depletion a mechanism for virulence?* Proc Biol Sci, 2003. **270**(1522): p. 1365-71.
192. Wajcman, H. and F. Galacteros, [*Glucose 6-phosphate dehydrogenase deficiency: a protection against malaria and a risk for hemolytic accidents*]. C R Biol, 2004. **327**(8): p. 711-20.
193. Joet, T., et al., *Validation of the hexose transporter of Plasmodium falciparum as a novel drug target*. Proc Natl Acad Sci U S A, 2003. **100**(13): p. 7476-9.
194. Slavic, K., et al., *Plasmodial sugar transporters as anti-malarial drug targets and comparisons with other protozoa*. Malar J, 2011. **10**: p. 165.

195. van Schalkwyk, D.A., W. Priebe, and K.J. Saliba, *The inhibitory effect of 2-halo derivatives of D-glucose on glycolysis and on the proliferation of the human malaria parasite Plasmodium falciparum*. J Pharmacol Exp Ther, 2008. **327**(2): p. 511-7.
196. Mehta, M., H.M. Sonawar, and S. Sharma, *Glycolysis in Plasmodium falciparum results in modulation of host enzyme activities*. J Vector Borne Dis, 2006. **43**(3): p. 95-103.
197. Liu, J., et al., *Plasmodium falciparum ensures its amino acid supply with multiple acquisition pathways and redundant proteolytic enzyme systems*. Proc Natl Acad Sci U S A, 2006. **103**(23): p. 8840-5.
198. Mitamura, T. and N.M. Palacpac, *Lipid metabolism in Plasmodium falciparum-infected erythrocytes: possible new targets for malaria chemotherapy*. Microbes Infect, 2003. **5**(6): p. 545-52.
199. Ben Mamoun, C., S.T. Prigge, and H. Vial, *Targeting the Lipid Metabolic Pathways for the Treatment of Malaria*. Drug Dev Res, 2010. **71**(1): p. 44-55.
200. Roggero, R., et al., *Unraveling the mode of action of the antimalarial choline analog G25 in Plasmodium falciparum and Saccharomyces cerevisiae*. Antimicrob Agents Chemother, 2004. **48**(8): p. 2816-24.
201. Heath, R.J. and C.O. Rock, *Fatty acid biosynthesis as a target for novel antibacterials*. Curr Opin Investig Drugs, 2004. **5**(2): p. 146-53.
202. Cassera, M.B., et al., *Purine and pyrimidine pathways as targets in Plasmodium falciparum*. Curr Top Med Chem, 2011. **11**(16): p. 2103-15.
203. Yuthavong, Y., et al., *Malarial dihydrofolate reductase as a paradigm for drug development against a resistance-compromised target*. Proc Natl Acad Sci U S A, 2012. **109**(42): p. 16823-8.
204. Hyde, J.E., *Exploring the folate pathway in Plasmodium falciparum*. Acta Trop, 2005. **94**(3): p. 191-206.
205. Ying, W., *NAD⁺/NADH and NADP⁺/NADPH in cellular functions and cell death: regulation and biological consequences*. Antioxid Redox Signal, 2008. **10**(2): p. 179-206.
206. Billington, R.A., et al., *Emerging functions of extracellular pyridine nucleotides*. Mol Med, 2006. **12**(11-12): p. 324-7.
207. Nakamura, M., A. Bhatnagar, and J. Sadoshima, *Overview of pyridine nucleotides review series*. Circ Res, 2012. **111**(5): p. 604-10.
208. Bogan, K.L. and C. Brenner, *Nicotinic acid, nicotinamide, and nicotinamide riboside: a molecular evaluation of NAD⁺ precursor vitamins in human nutrition*. Annu Rev Nutr, 2008. **28**: p. 115-30.
209. Preiss, J. and P. Handler, *Biosynthesis of diphosphopyridine nucleotide. I. Identification of intermediates*. J Biol Chem, 1958. **233**(2): p. 488-92.
210. Preiss, J. and P. Handler, *Biosynthesis of diphosphopyridine nucleotide. II. Enzymatic aspects*. J Biol Chem, 1958. **233**(2): p. 493-500.
211. Sestini, S., et al., *Nicotinamide mononucleotide adenylyltransferase activity in human erythrocytes*. Arch Biochem Biophys, 1993. **302**(1): p. 206-11.
212. Foster, J.W. and A.G. Moat, *Nicotinamide adenine dinucleotide biosynthesis and pyridine nucleotide cycle metabolism in microbial systems*. Microbiol Rev, 1980. **44**(1): p. 83-105.
213. Ginsburg, H. and A.M. Abdel-Haleem, *Malaria Parasite Metabolic Pathways (MPMP) Upgraded with Targeted Chemical Compounds*. Trends Parasitol, 2016. **32**(1): p. 7-9.
214. O'Hara, J.K., et al., *Targeting NAD⁺ metabolism in the human malaria parasite Plasmodium falciparum*. PLoS One, 2014. **9**(4): p. e94061.
215. North, B.J. and E. Verdin, *Sirtuins: Sir2-related NAD-dependent protein deacetylases*. Genome Biol, 2004. **5**(5): p. 224.
216. Sorci, L., et al., *Targeting NAD biosynthesis in bacterial pathogens: Structure-based development of inhibitors of nicotinate mononucleotide adenylyltransferase NadD*. Chem Biol, 2009. **16**(8): p. 849-61.
217. Bozdech, Z., et al., *The transcriptome of the intraerythrocytic developmental cycle of Plasmodium falciparum*. PLoS Biol, 2003. **1**(1): p. E5.
218. Llinas, M., et al., *Comparative whole genome transcriptome analysis of three Plasmodium falciparum strains*. Nucleic Acids Res, 2006. **34**(4): p. 1166-73.
219. Huang, N., et al., *Complexes of bacterial nicotinate mononucleotide adenylyltransferase with inhibitors: implication for structure-based drug design and improvement*. J Med Chem, 2010. **53**(14): p. 5229-39.
220. Bathke, J., et al., *Structural and Functional Characterization of Plasmodium falciparum Nicotinic Acid Mononucleotide Adenylyltransferase*. J Mol Biol, 2016. **428**(24 Pt B): p. 4946-4961.
221. Gazanion, E., et al., *The Leishmania nicotinamidase is essential for NAD⁺ production and parasite proliferation*. Mol Microbiol, 2011. **82**(1): p. 21-38.
222. Gazanion, E., et al., *Leishmania infantum nicotinamidase is required for late-stage development in its natural sand fly vector, Phlebotomus perniciosus*. Int J Parasitol, 2012. **42**(4): p. 323-7.

223. Wang, X., et al., *The Riemerella anatipestifer AS87_01735 Gene Encodes Nicotinamidase PncA, an Important Virulence Factor*. Appl Environ Microbiol, 2016. **82**(19): p. 5815-23.
224. Ghislain, M., E. Talla, and J.M. Francois, *Identification and functional analysis of the Saccharomyces cerevisiae nicotinamidase gene, PNC1*. Yeast, 2002. **19**(3): p. 215-24.
225. Al-Nihmi, F.M., et al., *A Novel and Conserved Plasmodium Sporozoite Membrane Protein SPELD is Required for Maturation of Exo-erythrocytic Forms*. Sci Rep, 2017. **7**: p. 40407.
226. Rathore, S., et al., *A cyanobacterial serine protease of Plasmodium falciparum is targeted to the apicoplast and plays an important role in its growth and development*. Mol Microbiol, 2010. **77**(4): p. 873-90.
227. Lin, S.J. and L. Guarente, *Nicotinamide adenine dinucleotide, a metabolic regulator of transcription, longevity and disease*. Curr Opin Cell Biol, 2003. **15**(2): p. 241-6.
228. Ziegler, M. and M. Niere, *NAD⁺ surfaces again*. Biochem J, 2004. **382**(Pt 3): p. e5-6.
229. Satoh, A., L. Stein, and S. Imai, *The role of mammalian sirtuins in the regulation of metabolism, aging, and longevity*. Handb Exp Pharmacol, 2011. **206**: p. 125-62.
230. Liu, C. and X. Yu, *ADP-ribosyltransferases and poly ADP-ribosylation*. Curr Protein Pept Sci, 2015. **16**(6): p. 491-501.
231. Teng, R., et al., *Metabolite profiling of the intraerythrocytic malaria parasite Plasmodium falciparum by (1)H NMR spectroscopy*. NMR Biomed, 2009. **22**(3): p. 292-302.
232. Ma, B., et al., *High-affinity transporters for NAD⁺ precursors in Candida glabrata are regulated by Hst1 and induced in response to niacin limitation*. Mol Cell Biol, 2009. **29**(15): p. 4067-79.
233. Naotunne, T.S., et al., *Cytokine-mediated inactivation of malarial gametocytes is dependent on the presence of white blood cells and involves reactive nitrogen intermediates*. Immunology, 1993. **78**(4): p. 555-62.
234. Lensen, A.H., et al., *Leukocytes in a Plasmodium falciparum-infected blood meal reduce transmission of malaria to Anopheles mosquitoes*. Infect Immun, 1997. **65**(9): p. 3834-7.
235. Margos, G., et al., *Interaction between host complement and mosquito-midgut-stage Plasmodium berghei*. Infect Immun, 2001. **69**(8): p. 5064-71.
236. Simon, N., et al., *Malaria parasites co-opt human factor H to prevent complement-mediated lysis in the mosquito midgut*. Cell Host Microbe, 2013. **13**(1): p. 29-41.
237. Dillon, R.J. and V.M. Dillon, *The gut bacteria of insects: nonpathogenic interactions*. Annu Rev Entomol, 2004. **49**: p. 71-92.
238. Dong, Y., F. Manfredini, and G. Dimopoulos, *Implication of the mosquito midgut microbiota in the defense against malaria parasites*. PLoS Pathog, 2009. **5**(5): p. e1000423.
239. Merrick, C.J., et al., *Functional analysis of sirtuin genes in multiple Plasmodium falciparum strains*. PLoS One, 2015. **10**(3): p. e0118865.
240. Nagaraj, V.A., et al., *Asparagine requirement in Plasmodium berghei as a target to prevent malaria transmission and liver infections*. Nat Commun, 2015. **6**: p. 8775.
241. Tanaka, T.Q., et al., *Plasmodium dipeptidyl aminopeptidases as malaria transmission-blocking drug targets*. Antimicrob Agents Chemother, 2013. **57**(10): p. 4645-52.
242. Hart, R.J., et al., *Plasmodium AdoMetDC/ODC bifunctional enzyme is essential for male sexual stage development and mosquito transmission*. Biol Open, 2016. **5**(8): p. 1022-9.
243. Langer, R.C., et al., *Monoclonal antibody against the Plasmodium falciparum chitinase, PfCHT1, recognizes a malaria transmission-blocking epitope in Plasmodium gallinaceum ookinetes unrelated to the chitinase PgCHT1*. Infect Immun, 2002. **70**(3): p. 1581-90.
244. Matuschewski, K., *Getting infections: formation and maturation of Plasmodium sporozoites in the Anopheles vector*. Cell Microbiol, 2006. **8**(10): p. 1547-56.
245. Lasonder, E., et al., *Proteomic profiling of Plasmodium sporozoite maturation identifies new proteins essential for parasite development and infectivity*. PLoS Pathog, 2008. **4**(10): p. e1000195.
246. Engelmann, S., O. Silvie, and K. Matuschewski, *Disruption of Plasmodium sporozoite transmission by depletion of sporozoite invasion-associated protein 1*. Eukaryot Cell, 2009. **8**(4): p. 640-8.
247. Harupa, A., et al., *SSP3 is a novel Plasmodium yoelii sporozoite surface protein with a role in gliding motility*. Infect Immun, 2014. **82**(11): p. 4643-53.
248. Labaied, M., N. Camargo, and S.H. Kappe, *Depletion of the Plasmodium berghei thrombospondin-related sporozoite protein reveals a role in host cell entry by sporozoites*. Mol Biochem Parasitol, 2007. **153**(2): p. 158-66.
249. Jacobs-Lorena, V.Y., et al., *A dispensable Plasmodium locus for stable transgene expression*. Mol Biochem Parasitol, 2010. **171**(1): p. 40-4.

250. Nussenzweig, V. and R.S. Nussenzweig, *Circumsporozoite proteins of malaria parasites*. Cell, 1985. **42**(2): p. 401-3.
251. Good, M.F. and D.L. Doolan, *Malaria's journey through the lymph node*. Nat Med, 2007. **13**(9): p. 1023-4.
252. Doolan, D.L., et al., *Identification of Plasmodium falciparum antigens by antigenic analysis of genomic and proteomic data*. Proc Natl Acad Sci U S A, 2003. **100**(17): p. 9952-7.
253. Hafalla, J.C., et al., *Identification of targets of CD8(+) T cell responses to malaria liver stages by genome-wide epitope profiling*. PLoS Pathog, 2013. **9**(5): p. e1003303.
254. Mishra, S., et al., *Identification of non-CSP antigens bearing CD8 epitopes in mice immunized with irradiated sporozoites*. Vaccine, 2011. **29**(43): p. 7335-42.
255. Thathy, V., et al., *Levels of circumsporozoite protein in the Plasmodium oocyst determine sporozoite morphology*. EMBO J, 2002. **21**(7): p. 1586-96.
256. Coppi, A., et al., *The malaria circumsporozoite protein has two functional domains, each with distinct roles as sporozoites journey from mosquito to mammalian host*. J Exp Med, 2011. **208**(2): p. 341-56.
257. Aldrich, C., et al., *Roles of the amino terminal region and repeat region of the Plasmodium berghei circumsporozoite protein in parasite infectivity*. PLoS One, 2012. **7**(2): p. e32524.
258. Ferguson, D.J., et al., *The repeat region of the circumsporozoite protein is critical for sporozoite formation and maturation in Plasmodium*. PLoS One, 2014. **9**(12): p. e113923.
259. Rogers, W.O., et al., *Characterization of Plasmodium falciparum sporozoite surface protein 2*. Proc Natl Acad Sci U S A, 1992. **89**(19): p. 9176-80.
260. Gantt, S., et al., *Antibodies against thrombospondin-related anonymous protein do not inhibit Plasmodium sporozoite infectivity in vivo*. Infect Immun, 2000. **68**(6): p. 3667-73.
261. Kadota, K., et al., *Essential role of membrane-attack protein in malarial transmission to mosquito host*. Proc Natl Acad Sci U S A, 2004. **101**(46): p. 16310-5.
262. Mikolajczak, S.A., et al., *A next-generation genetically attenuated Plasmodium falciparum parasite created by triple gene deletion*. Mol Ther, 2014. **22**(9): p. 1707-15.
263. Stein, L.D., *Human genome: end of the beginning*. Nature, 2004. **431**(7011): p. 915-6.
264. Mo, Y.Y., *MicroRNA regulatory networks and human disease*. Cell Mol Life Sci, 2012. **69**(21): p. 3529-31.
265. Perry, R.B. and I. Ulitsky, *The functions of long noncoding RNAs in development and stem cells*. Development, 2016. **143**(21): p. 3882-3894.
266. Jain, S., et al., *Long non-coding RNA: Functional agent for disease traits*. RNA Biol, 2016: p. 1-14.
267. Schmitt, A.M. and H.Y. Chang, *Long Noncoding RNAs in Cancer Pathways*. Cancer Cell, 2016. **29**(4): p. 452-63.
268. Scaria, V. and A. Pasha, *Long Non-Coding RNAs in Infection Biology*. Front Genet, 2012. **3**: p. 308.
269. Plattner, F. and D. Soldati-Favre, *Hijacking of host cellular functions by the Apicomplexa*. Annu Rev Microbiol, 2008. **62**: p. 471-87.
270. Judice, C.C., et al., *MicroRNAs in the Host-Apicomplexan Parasites Interactions: A Review of Immunopathological Aspects*. Front Cell Infect Microbiol, 2016. **6**: p. 5.
271. Saba, R., D.L. Sorensen, and S.A. Booth, *MicroRNA-146a: A Dominant, Negative Regulator of the Innate Immune Response*. Front Immunol, 2014. **5**: p. 578.
272. Vigorito, E., et al., *miR-155: an ancient regulator of the immune system*. Immunol Rev, 2013. **253**(1): p. 146-57.
273. Cannella, D., et al., *miR-146a and miR-155 delineate a MicroRNA fingerprint associated with Toxoplasma persistence in the host brain*. Cell Rep, 2014. **6**(5): p. 928-37.
274. Ghosh, J., et al., *Leishmania donovani targets Dicer1 to downregulate miR-122, lower serum cholesterol, and facilitate murine liver infection*. Cell Host Microbe, 2013. **13**(3): p. 277-88.
275. Frank, B., et al., *Autophagic digestion of Leishmania major by host macrophages is associated with differential expression of BNIP3, CTSE, and the miRNAs miR-101c, miR-129, and miR-210*. Parasit Vectors, 2015. **8**: p. 404.
276. Geraci, N.S., J.C. Tan, and M.A. McDowell, *Characterization of microRNA expression profiles in Leishmania-infected human phagocytes*. Parasite Immunol, 2015. **37**(1): p. 43-51.
277. Hentzschel, F., et al., *AAV8-mediated in vivo overexpression of miR-155 enhances the protective capacity of genetically attenuated malarial parasites*. Mol Ther, 2014. **22**(12): p. 2130-41.

278. O'Hara, S.P., et al., *NF-kappaB p50-CCAAT/enhancer-binding protein beta (C/EBPbeta)-mediated transcriptional repression of microRNA let-7i following microbial infection*. J Biol Chem, 2010. **285**(1): p. 216-25.
279. Miller, J.L., et al., *Interferon-mediated innate immune responses against malaria parasite liver stages*. Cell Rep, 2014. **7**(2): p. 436-47.
280. Yarovinsky, F., *Innate immunity to Toxoplasma gondii infection*. Nat Rev Immunol, 2014. **14**(2): p. 109-21.
281. Torgler, R., et al., *Sporozoite-mediated hepatocyte wounding limits Plasmodium parasite development via MyD88-mediated NF-kappa B activation and inducible NO synthase expression*. J Immunol, 2008. **180**(6): p. 3990-9.
282. Dupont, C.D., D.A. Christian, and C.A. Hunter, *Immune response and immunopathology during toxoplasmosis*. Semin Immunopathol, 2012. **34**(6): p. 793-813.
283. Carpenter, S. and K.A. Fitzgerald, *Transcription of inflammatory genes: long noncoding RNA and beyond*. J Interferon Cytokine Res, 2015. **35**(2): p. 79-88.
284. Kambara, H., et al., *Negative regulation of the interferon response by an interferon-induced long non-coding RNA*. Nucleic Acids Res, 2014. **42**(16): p. 10668-80.
285. Rapicavoli, N.A., et al., *A mammalian pseudogene lncRNA at the interface of inflammation and anti-inflammatory therapeutics*. Elife, 2013. **2**: p. e00762.
286. Shi, X., et al., *Dynamic balance of pSTAT1 and pSTAT3 in C57BL/6 mice infected with lethal or nonlethal Plasmodium yoelii*. Cell Mol Immunol, 2008. **5**(5): p. 341-8.
287. Schneider, A.G., et al., *Toxoplasma gondii triggers phosphorylation and nuclear translocation of dendritic cell STAT1 while simultaneously blocking IFNgamma-induced STAT1 transcriptional activity*. PLoS One, 2013. **8**(3): p. e60215.
288. Shapira, S., et al., *Initiation and termination of NF-kappaB signaling by the intracellular protozoan parasite Toxoplasma gondii*. J Cell Sci, 2005. **118**(Pt 15): p. 3501-8.
289. Zhang, Q. and K.T. Jeang, *Long non-coding RNAs (lncRNAs) and viral infections*. Biomed Pharmacother, 2013. **3**(1): p. 34-42.
290. Landeras-Bueno, S. and J. Ortin, *Regulation of influenza virus infection by long non-coding RNAs*. Virus Res, 2016. **212**: p. 78-84.
291. Qian, X., et al., *Long non-coding RNA GAS5 inhibited hepatitis C virus replication by binding viral NS3 protein*. Virology, 2016. **492**: p. 155-65.
292. Pawar, K., et al., *Down regulated lncRNA MEG3 eliminates mycobacteria in macrophages via autophagy*. Sci Rep, 2016. **6**: p. 19416.
293. Westermann, A.J., et al., *Dual RNA-seq unveils noncoding RNA functions in host-pathogen interactions*. Nature, 2016. **529**(7587): p. 496-501.
294. Ouyang, J., et al., *NR4V, a long noncoding RNA, modulates antiviral responses through suppression of interferon-stimulated gene transcription*. Cell Host Microbe, 2014. **16**(5): p. 616-26.
295. Wang, Y., et al., *Long noncoding RNA derived from CD244 signaling epigenetically controls CD8+ T-cell immune responses in tuberculosis infection*. Proc Natl Acad Sci U S A, 2015. **112**(29): p. E3883-92.
296. Carpenter, S., et al., *A long noncoding RNA mediates both activation and repression of immune response genes*. Science, 2013. **341**(6147): p. 789-92.
297. Chen, G., et al., *LncRNADisease: a database for long-non-coding RNA-associated diseases*. Nucleic Acids Res, 2013. **41**(Database issue): p. D983-6.
298. Zeng, C., et al., *Inhibition of long non-coding RNA NEAT1 impairs myeloid differentiation in acute promyelocytic leukemia cells*. BMC Cancer, 2014. **14**: p. 693.
299. Li, J.Y., X. Ma, and C.B. Zhang, *Overexpression of long non-coding RNA UCA1 predicts a poor prognosis in patients with esophageal squamous cell carcinoma*. Int J Clin Exp Pathol, 2014. **7**(11): p. 7938-44.
300. Liu, H., et al., *Knockdown of Long Non-Coding RNA UCA1 Increases the Tamoxifen Sensitivity of Breast Cancer Cells through Inhibition of Wnt/beta-Catenin Pathway*. PLoS One, 2016. **11**(12): p. e0168406.
301. Hu, J.J., et al., *HBx-upregulated lncRNA UCA1 promotes cell growth and tumorigenesis by recruiting EZH2 and repressing p27Kip1/CDK2 signaling*. Scientific Reports, 2016. **6**.
302. Kamel, M.M., et al., *Investigation of long noncoding RNAs expression profile as potential serum biomarkers in patients with hepatocellular carcinoma*. Transl Res, 2016. **168**: p. 134-45.
303. Saha, S., S. Murthy, and P.N. Rangarajan, *Identification and characterization of a virus-inducible non-coding RNA in mouse brain*. J Gen Virol, 2006. **87**(Pt 7): p. 1991-5.

-
304. Zhang, Q., et al., *NEAT1 long noncoding RNA and paraspeckle bodies modulate HIV-1 posttranscriptional expression*. MBio, 2013. **4**(1): p. e00596-12.
 305. Andrade, R.M., et al., *CD40 signaling in macrophages induces activity against an intracellular pathogen independently of gamma interferon and reactive nitrogen intermediates*. Infect Immun, 2005. **73**(5): p. 3115-23.
 306. Mahmoud, M.E., et al., *Mechanisms of interferon-beta-induced inhibition of Toxoplasma gondii growth in murine macrophages and embryonic fibroblasts: role of immunity-related GTPase M1*. Cell Microbiol, 2015. **17**(7): p. 1069-83.
 307. Imamura, K., et al., *Long noncoding RNA NEAT1-dependent SFPQ relocation from promoter region to paraspeckle mediates IL8 expression upon immune stimuli*. Mol Cell, 2014. **53**(3): p. 393-406.
 308. Thirugnanam, S., N. Rout, and M. Gnanasekar, *Possible role of Toxoplasma gondii in brain cancer through modulation of host microRNAs*. Infect Agent Cancer, 2013. **8**(1): p. 8.
 309. Chen, H.Y., et al., *Knockdown of long noncoding RNA UCA1 inhibits glioma cell metastasis via reduction of epithelial-mesenchymal transition*. International Journal of Clinical and Experimental Pathology, 2016. **9**(12): p. 12621-12626.
 310. Wang, K.C., et al., *A long noncoding RNA maintains active chromatin to coordinate homeotic gene expression*. Nature, 2011. **472**(7341): p. 120-4.
 311. Kim, D., et al., *Two non-coding RNAs, MicroRNA-101 and HOTTIP contribute cartilage integrity by epigenetic and homeotic regulation of integrin-alpha1*. Cell Signal, 2013. **25**(12): p. 2878-87.
 312. Chen, Y., et al., *CD49a promotes T-cell-mediated hepatitis by driving T helper 1 cytokine and interleukin-17 production*. Immunology, 2014. **141**(3): p. 388-400.
-

Publications

SCIENTIFIC REPORTS

OPEN

A Novel and Conserved *Plasmodium* Sporozoite Membrane Protein SPELD is Required for Maturation of Exo-erythrocytic Forms

Received: 09 August 2016
Accepted: 06 December 2016
Published: 09 January 2017

Faisal Mohammed Abdul Al-Nihmi^{1,*}, Surendra Kumar Kolli^{1,*}, Segireddy Rameswara Reddy^{1,*}, Babu S. Mastan^{1,*}, Jyothi Togiri¹, Mulaka Maruthi¹, Roshni Gupta², Puran Singh Sijwali³, Satish Mishra² & Kota Arun Kumar¹

Plasmodium sporozoites are the infective forms of malaria parasite to vertebrate host and undergo dramatic changes in their transcriptional repertoire during maturation in mosquito salivary glands. We report here the role of a novel and conserved *Plasmodium berghei* protein encoded by *PBANKA_091090* in maturation of Exo-erythrocytic Forms (EEFs) and designate it as Sporozoite surface Protein Essential for Liver stage Development (PbSPELD). *PBANKA_091090* was previously annotated as *PB402615.00.0* and its transcript was recovered at maximal frequency in the Serial Analysis of the Gene Expression (SAGE) of *Plasmodium berghei* salivary gland sporozoites. An orthologue of this transcript was independently identified in *Plasmodium vivax* sporozoite microarrays and was designated as Sporozoite Conserved Orthologous Transcript-2 (*scot-2*). Functional characterization through reverse genetics revealed that PbSPELD is essential for *Plasmodium* liver stage maturation. mCherry transgenic of PbSPELD localized the protein to plasma membrane of sporozoites and early EEFs. Global microarray analysis of *pbspeld* ko revealed EEF attenuation being associated with down regulation of genes central to general transcription, cell cycle, proteasome and cadherin signaling. *pbspeld* mutant EEFs induced pre-erythrocytic immunity with 50% protective efficacy. Our studies have implications for attenuating the human *Plasmodium* liver stages by targeting SPELD locus.

Malaria is an infectious disease caused by a protozoan parasite that belongs to the genus *Plasmodium*. In 2013 alone, the reported mortality associated with malaria was about 854,586 cases¹. Malaria is transmitted to humans by the bite of a female *Anopheles* mosquito that injects sporozoites into the skin of the host². The sporozoites make their way to the liver where they transform into EEFs or liver stages. Following asexual exo-erythrocytic schizogony, the hepatic merozoites are released into the blood stream to initiate an erythrocytic cycle. During this phase, a proportion of parasites undergo differentiation to sexual forms called as gametocytes. When a female *Anopheles* mosquito ingests these gametocytes during the process of obtaining a blood meal, the male and female gametes fuse and result in the formation of a zygote. The zygote transforms into a motile ookinete that breaches the mosquito midgut epithelium and settles on hemocoel side of gut. The end product of sexual reproduction are the oocysts that undergo sporulation and upon rupture, release sporozoites into hemocoel³. The sporozoites migrate to the salivary glands and wait for transmission to humans when the mosquito probes for a blood meal.

High throughput methods of gene expression analysis have offered an insight in understanding the malaria parasite biology and allowed the appreciation of stage specifically regulated gene expression in modulating the infectivity or virulence of parasites^{4–7}. Significant changes occur in the transcriptional repertoire of salivary gland sporozoites rendering them highly infective for hepatocytes⁸. The first comprehensive transcriptomic analysis of sporozoites⁹ opened the possibility of understanding the regulation of *Plasmodium* gene expression in mosquito stages that further led to investigating the differential gene expression between salivary gland sporozoite stages

¹Department of Animal Biology, School of Life Sciences, University of Hyderabad, Hyderabad 500046, India.

²Division of Parasitology, CSIR-Central Drug Research Institute, Lucknow 226031, India. ³CSIR-Centre for Cellular and Molecular Biology, Habsiguda, Uppal Road, Hyderabad 500007, India. *These authors contributed equally to this work. Correspondence and requests for materials should be addressed to S.M. (email: satish.mishra@cdri.res.in) or K.A.K. (email: kaksl@uohyd.ernet.in)

RESEARCH ARTICLE

Modulation of host cell SUMOylation facilitates efficient development of *Plasmodium berghei* and *Toxoplasma gondii*

Mulaka Maruthi¹ | Dipti Singh¹ | Segireddy Rameswara Reddy¹ | Babu S. Mastan¹ |
Satish Mishra² | Kota Arun Kumar¹

¹Department of Animal Biology, School of Life Sciences, University of Hyderabad, Hyderabad, India

²Division of Parasitology, CSIR-Central Drug Research Institute, Lucknow, India

Correspondence

Kota Arun Kumar, Department of Animal Biology, School of Life Sciences, University of Hyderabad, Hyderabad 500046, India. Email: kaks@uohyd.ernet.in

Funding information

Department of Biotechnology (DBT, India), Grant/Award Number: BT/PR2495/BRB/10/950/2011 to KAK; Council for Scientific and Industrial Research (CSIR); Department of Biotechnology (DBT); DBT Ramalingaswami Fellowship, Grant/Award Number: GAP0142

1 | INTRODUCTION

Malaria infection is initiated when sporozoites are introduced in the mammalian host by the bite of a female *Anopheles* mosquito. The sporozoites selectively invade hepatocytes

and develop into exoerythrocytic forms (EEFs) inside a parasitophorous vacuole (Prudencio, Rodriguez, & Mota, 2006). The intrahepatic development of *Plasmodium* is an obligatory step before the onset of disease. Very little is known about the parasite liver stage and their interactions with host cell. Apicomplexan parasites subvert their host cell functions to access essential nutrients and escape from host defense mechanisms. The host processes that are targeted include modulation of gene expression, protein synthesis, membrane trafficking, antigen

Summary

SUMOylation is a reversible post translational modification of proteins that regulates protein stabilization, nucleocytoplasmic transport, and protein–protein interactions. Several viruses and bacteria modulate host SUMOylation machinery for efficient infection. *Plasmodium* sporozoites are infective forms of malaria parasite that invade mammalian hepatocytes and transforms into exoerythrocytic forms (EEFs). Here, we show that during EEF development, the distribution of SUMOylated proteins in host cell nuclei was significantly reduced and expression of the SUMOylation enzymes was downregulated. *Plasmodium* EEFs destabilized the host cytoplasmic protein SMAD4 by inhibiting its SUMOylation. SUMO1 overexpression was detrimental to EEF growth, and insufficiency of the only conjugating enzyme Ubc9/E2 promoted EEF growth. The expression of genes involved in suppression of host cell defense pathways during infection was reversed during SUMO1 overexpression, as revealed by transcriptomic analysis. The inhibition of host cell SUMOylation was also observed during *Toxoplasma* infection. We provide a hitherto unknown mechanism of regulating host gene expression by Apicomplexan parasites through altering host SUMOylation.

KEYWORDS

conjugation enzyme E2, host SUMOylation, *Plasmodium* EEFs, SMAD4, SUMO1, *Toxoplasma*

In addition to ubiquitin, a family of substrates called ubiquitinlike proteins (UBLs) is covalently linked to the target protein and influences diverse biological processes. One such member of UBLs is small ubiquitinlike modifier (SUMO), a 12-kDa polypeptide found ubiquitously in the eukaryotic kingdom. SUMOylation, the covalent linkage of SUMO moiety on Lys residue of the target protein, is mediated by the sequential action of three enzymes: E1-SAE1/SAE2 heterodimer (activating enzyme), E2/Ubc9 (conjugating enzyme), and E3 enzymes (ligating enzymes). SUMOylation is

essential for many cellular functions such as transcription regulation, intracellular transport, maintenance of genome integrity, protein stability, stress responses, and many other biological functions (Zhao, 2007).

Consistent with the indispensable role of SUMOylation in the host cell, the exploitation of host SUMOylation by bacterial pathogens such as *Listeria* (Ribet et al., 2010), *Salmonella* (Verma et al., 2015), *Anaplasma* (Beyer et al., 2015), and many viral pathogens (Boggio & Chiocca, 2006) is well documented. However, there are no reports till date showing the

Anti-plagiarism Certificate

Towards identifying potential drug and vaccine targets for human malaria parasite using rodent Plasmodium berghei model & Investigation of host long non coding RNA profiles during Plasmodium berghei a

ORIGINALITY REPORT

12%

SIMILARITY INDEX

4%

INTERNET SOURCES

10%

PUBLICATIONS

2%

STUDENT PAPERS

PRIMARY SOURCES

- 1

Jessica K. O'Hara, Lewis J. Kerwin, Simon A. Cobbold, Jonathan Tai, Thomas A. Bedell, Paul J. Reider, Manuel Llinás. "Targeting NAD⁺ Metabolism in the Human Malaria Parasite Plasmodium falciparum", PLoS ONE, 2014

Publication

1%
- 2

Mastan, Babu S., Anchala Kumari, Dinesh Gupta, Satish Mishra, and Kota Arun Kumar. "Gene disruption reveals a dispensable role for Plasmepsin VII in the Plasmodium berghei life cycle", Molecular and Biochemical Parasitology, 2014.

Publication

<1%
- 3

www.funakoshi.co.jp

Internet Source

<1%
- 4

Hliscs, Marion(Levashina, Elena A., Lucius, Richard and Matuschewski, Kai). "Functional Characterization of Actin Sequestering Proteins

<1%